

**CARBON DIOXIDE ABSORPTION INTO AQUEOUS
BLENDS OF MONOETHANOLAMINE AND GLYCEROL IN
A PACKED BED COLUMN**

SOMAYEH MIRZAEI

**FACULTY OF ENGINEERING
UNIVERSITY OF MALAYA
KUALA LUMPUR**

2018

**CARBON DIOXIDE ABSORPTION INTO AQUEOUS
BLENDS OF MONOETHANOLAMINE AND
GLYCEROL IN A PACKED BED COLUMN**

SOMAYEH MIRZAEI

**THESIS SUBMITTED IN FULFILMENT OF THE
REQUIREMENTS FOR THE DEGREE OF
DOCTOR OF PHILOSOPHY**

**FACULTY OF ENGINEERING
UNIVERSITY OF MALAYA
KUALA LUMPUR**

2018

UNIVERSITY OF MALAYA
ORIGINAL LITERARY WORK DECLARATION

Name of Candidate: **Somayeh Mirzaei**

Matric No: **KHA130019**

Name of Degree: **Doctor of Philosophy**

Title of Project Paper/Research Report/Dissertation/Thesis (“this Work”):

**CARBON DIOXIDE ABSORPTION INTO AQUEOUS BLENDS OF
MONOETHANOLAMINE AND GLYCEROL IN A PACKED BED COLUMN**

Field of Study: **Purification & Separation Processes**

I do solemnly and sincerely declare that:

- (1) I am the sole author/writer of this Work;
- (2) This Work is original;
- (3) Any use of any work in which copyright exists was done by way of fair dealing and for permitted purposes and any excerpt or extract from, or reference to or reproduction of any copyright work has been disclosed expressly and sufficiently and the title of the Work and its authorship have been acknowledged in this Work;
- (4) I do not have any actual knowledge nor do I ought reasonably to know that the making of this work constitutes an infringement of any copyright work;
- (5) I hereby assign all and every rights in the copyright to this Work to the University of Malaya (“UM”), who henceforth shall be owner of the copyright in this Work and that any reproduction or use in any form or by any means whatsoever is prohibited without the written consent of UM having been first had and obtained;
- (6) I am fully aware that if in the course of making this Work I have infringed any copyright whether intentionally or otherwise, I may be subject to legal action or any other action as may be determined by UM.

Candidate’s Signature

Date:

Subscribed and solemnly declared before,

Witness’s Signature

Date:

Name:

Designation:

CARBON DIOXIDE ABSORPTION INTO AQUEOUS BLENDS OF MONOETHANOLAMINE AND GLYCEROL IN A PACKED BED COLUMN

ABSTRACT

Absorption/stripping process using aqueous amine is a mature technology widely applied for removal of carbon dioxide (CO₂) from natural gas, hydrogen, and other refinery gases, which makes it a suitable option to remove CO₂ from flue gas in coal-fired power plants. The most widely used amine for CO₂ capture from coal fired power plants is monoethanolamine (MEA). The purpose of this work is to investigate glycerol as promoter with MEA solvent to enhance CO₂ capture. Absorption/stripping process with MEA-glycerol blend presents an attractive option for CO₂ capture from the gas mixture of CO₂ and nitrogen (N₂). Absorption process was simulated in Aspen Plus rate-based model using ENRTL-RK thermodynamic model with aqueous mixture of MEA-glycerol. The optimal concentration for CO₂ removal was 10 wt% MEA-10wt% glycerol since, the CO₂ removal efficiency increased from 62.24% for 10 wt% MEA aqueous solution to 64.33% for the mixture of 10 wt% MEA-10 wt% glycerol aqueous solution. Number of absorption/desorption runs (14 runs) were performed in the range of gas flow rate 1.4-3.9 L/min. CO₂ loading analyses confirmed that CO₂ rich loading increases as the gas flow rate rises since, the lowest and highest rich CO₂ loadings for MEA system were 0.0365 and 0.126 mol CO₂/mol MEA at 1.4 and 3.3 L/min, respectively. Moreover, the lowest and highest rich CO₂ loadings increased to 0.0519 and 0.1446 mol CO₂/mol alkalinity for MEA-glycerol system at same conditions. The results suggested that hybrid MEA-glycerol solution showed better CO₂ absorption compared to aqueous MEA solution as glycerol increases the CO₂ absorption capacity for MEA solvent. Five experimental absorption runs using MEA-glycerol solvent were modelled in Aspen Plus using RadFrac columns simulating both absorber and stripper conditions. The highest and lowest deviations between experimental and simulated rich

CO₂ loadings were 9.22% and 0.36% for gas flow rate 2.9 L/min and 1.7 L/min, respectively. Furthermore, with the increase of gas flow rate from 1.4 to 3.9 L/min, an increase in rich streams was observed from 29.46°C to 30.14°C and also reboiler heat duty rose from 98.14 MJ/h to 305.46 MJ/h. Therefore, Aspen Plus predicted the experimental data well, both for the absorber and desorber.

Keywords: CO₂ absorption, glycerol, MEA, packed column

University of Malaya

**PENYERAPAN KARBON DIOKSIDA KE DALAM LARUTAN CAMPURAN
MONOETANOLAMINA DAN GLISEROL DI DALAM TURUS LAPISAN
TERDAPAT
ABSTRAK**

Penyerapan/perlucutan menggunakan akueus amina merupakan teknologi matang yang digunakan secara meluas untuk menyingkirkan karbon dioksida (CO_2) daripada gas asli, hidrogen dan gas penapisan lain, menjadikannya pilihan yang sesuai untuk menyingkirkan CO_2 daripada gas serombong di loji janakuasa arang batu. merupakan Amina yang digunakan secara meluas untuk penangkapan CO_2 di loji janakuasa arang batu adalah monoetanolamina (MEA). Tujuan penyelidikan ini adalah untuk mengkaji gliserol sebagai promoter dengan pelarut MEA untuk meningkatkan penangkapan CO_2 . Proses penyerapan/perlucutan menggunakan campuran MEA-gliserol merupakan pilihan yang menarik untuk penangkapan CO_2 daripada campuran gas CO_2 dan nitrogen (N_2). Proses penyerapan telah disimulasi dalam model Aspen Plus berasaskan kadar menggunakan model termodinamik ENRTL-RK dengan campuran akueus MEA-gliserol. Kepekatan optimum untuk penyingkiran CO_2 adalah 10 wt% MEA-10 wt% gliserol kerana kecekapan penyingkiran CO_2 meningkat daripada 62.24% untuk 10 wt% larutan akueus MEA kepada 64.33% untuk campuran larutan akueus 10 wt% MEA-10 wt% gliserol. 14 ujikaji proses penyerapan/perlucutan telah dilaksanakan dalam anggaran kadar aliran gas 1.4-3.9 L/min. Analisis beban CO_2 menunjukkan beban kaya CO_2 bertambah apabila aliran gas meningkat, di mana beban CO_2 yang paling rendah dan paling tinggi untuk MEA sistem adalah 0.0365 and 0.126 mol CO_2 /mol MEA dengan 1.4 dan 3.3 L/min kadar aliran gas. Manakala, nilai ini meningkat kepada 0.0519 dan 0.1446 mol CO_2 /mol kealkalian untuk sistem MEA-gliserol pada keadaan yang sama. Hasil kajian ini mencadangkan bahawa larutan hybrid MEA-gliserol menunjukkan penyerapan CO_2 yang lebih baik berbanding dengan larutan akueus MEA

kerana gliserol meningkatkan kapasiti penyerapan CO₂ untuk pelarut MEA. Lima ujikaji bagi proses penyerapan menggunakan pelarut MEA-gliserol dimodelkan di Aspen Plus menggunakan turus RadFrac kedua-duanya penyerap dan pelucut disimulasi. Peratus sisihan tertinggi dan terendah antara ujikaji makmal dan simulasi beban kaya CO₂ adalah sebanyak 9.22% dan 0.36% untuk 2.9 dan 1.7 L/min kadar aliran gas, masing-masing. Selain itu, dengan meningkatkan kadar aliran gas daripada 1.4 kepada 3.9 L/min, peningkatan aliran kaya dapat diperhatikan daripada 29.46°C kepada 30.14°C dan tugas haba pengulang didih meningkat daripada 98.14 MJ/h kepada 305.46 MJ/h. Oleh itu, Aspen Plus didapati dapat meramal data ujikaji makmal dengan baik bagi kedua-dua penyerap dan penyahserap.

Keywords: penyerapan CO₂, gliserol, MEA, turus terpadat

ACKNOWLEDGEMENTS

I would like to sincerely thank and express my gratitude to my supervisors, Professor Dr. Mohamed Kheireddine Aroua and Associate Professor Dr. Ahmad Shamiri for their constant guidance, support and encouragement throughout my PhD's studies. Their invaluable inputs into my research have been the key to the successful development of this project.

I wish to thank the University of Malaya for providing me financial support, through IPPP and HIR grants, and the opportunity to conduct meaningful research during my studies. I would like to thank all the supporting staff and technicians in the Department of Chemical Engineering. I would also like to thank my colleagues and fellow researchers in our group, who encouraged and supported me during my studies.

My gratitude goes to my family, especially my parents for their unconditional love, patience and continued support, without which the studies and research would not have been possible.

I would like to thank Almighty Allah for giving me ability to undertake and complete my research work.

TABLE OF CONTENTS

Title page.....	i
Original Literary Work Declaration Form	ii
Abstract	iii
Abstrak	v
Acknowledgements	vii
Table of Contents	viii
List of Figures	xiii
List of Tables.....	xvi
List of Symbols and Abbreviations.....	xviii
CHAPTER 1: INTRODUCTION.....	1
1.1 Research background.....	1
1.2 Problem statement	1
1.3 Objectives of the research.....	2
1.4 Outline of the thesis	2
CHAPTER 2: LITERATURE REVIEW.....	5
2.1 Introduction.....	5
2.2 Carbon management strategies	5
2.2.1 Carbon capture and storage (CCS).....	5
2.2.1.1 CO ₂ capture	5
2.2.1.2 CO ₂ transport.....	6
2.2.1.3 CO ₂ storage in geological structures	6
2.2.2 Carbon capture, utilization and storage (CCUS).....	6
2.3 CO ₂ capture by amine-based absorption/stripping	7

2.4	Monoethanolamine as a Solvent for CO ₂ Capture.....	8
2.5	Glycerol as a solvent for CO ₂ capture	9
2.6	Modeling of absorption/stripping process	11
2.7	CO ₂ capture technologies	11
2.7.1	Adsorption	13
2.7.2	Membrane absorption.....	14
2.7.3	Membrane-based separation.....	15
2.7.3.1	Facilitated transport membranes	15
2.7.3.2	Mixed-matrix membranes	16
2.8	CO ₂ solubility in solvents	16
2.8.1	Theory of the solubility parameter	16
2.9	Comparison of different solvents based on solubility	30
2.10	Different solvents for CO ₂ capture	30
2.10.1	CO ₂ capture using ILs	31
2.10.2	Physical solvents	32
2.10.2.1	ILs as physical solvents.....	33
2.10.2.2	Glycerol as a physical solvent.....	34
2.10.2.3	Other physical solvents	35
2.11	Chemical solvents.....	36
2.11.1	Amines as chemical solvents.....	37
2.11.2	Amines as promoters	37
2.11.3	Mixed amines	39
2.11.4	PZ as a chemical solvent	39
2.11.5	Carbonate-based systems	40
2.11.5.1	CO ₂ capture with K ₂ CO ₃	40
2.11.5.2	CO ₂ capture with sodium carbonate.....	43

2.11.6	Enzyme-based systems.....	44
2.11.7	ILs as chemical solvents.....	44
2.11.8	NH ₃ -based systems.....	46
2.11.8.1	Comparison of NH ₃ and MEA systems.....	48
2.12	Simulation studies.....	63
2.12.1	Simulation using a rate-based model.....	64
2.13	Summary.....	67
CHAPTER 3: MATERIALS AND METHODS		69
3.1	Introduction.....	69
3.2	Simulation of CO ₂ absorption process using MEA, glycerol and MEA-glycerol aqueous solutions.....	71
3.2.1	Methodology	71
3.2.2	Modeling	71
3.2.2.1	Flow models	72
3.2.2.2	Film resistance methods	72
3.2.2.3	Thermodynamic and transport property models	72
3.2.3	Chemical reactions in the model	74
3.2.4	Process flow diagram of the CO ₂ absorption/desorption unit	77
3.2.5	CO ₂ -MEA system.....	80
3.2.6	CO ₂ -glycerol system.....	81
3.2.7	CO ₂ - MEA- glycerol system	82
3.3	Experimental study of CO ₂ absorption in a packed column.....	84
3.3.1	Materials	84
3.3.2	Pilot scale absorption/desorption unit description.....	84
3.3.2.1	Assembly of pilot scale absorption/desorption unit	87
3.3.3	Solution preparation	90

3.3.4	Operation	91
3.3.5	Experimental Procedure	92
3.3.6	Solvent titration	94
3.3.6.1	Amine titration	94
3.3.6.2	Mixed MEA-glycerol titration	94
3.3.7	CO ₂ loading analysis	95
3.4	Validation of simulation study with experimental work	97
3.4.1	Simulation using a rate-based model.....	97
3.4.1.1	Absorber simulation	98
3.4.1.2	Stripper simulation	101
CHAPTER 4: RESULTS AND DISCUSSION		103
4.1	Simulation of CO ₂ absorption process using MEA, glycerol and MEA-glycerol aqueous solutions.....	103
4.1.1	Validation of rate-based modeling	103
4.1.1.1	Base case simulation (CO ₂ -MEA).....	103
4.1.1.2	Glycerol solvent (CO ₂ -glycerol)	109
4.1.1.3	Glycerol promoter in MEA process (CO ₂ -glycerol-MEA).....	113
4.1.2	The Comparison of ENRTL-RK and ELECNRTL thermodynamic models	
	122	
4.2	Experimental study of CO ₂ absorption in a packed column.....	124
4.3	Validation of simulation study with experimental work	133
4.3.1	Absorber simulation	133
4.3.2	Stripper simulation	142
CHAPTER 5: CONCLUSIONS AND RECOMMENDATIONS		148
5.1	Conclusions	148

5.2 Recommendations.....	149
REFERENCES.....	150
LIST OF PUBLICATION AND PAPER PRESENTED.....	170
APPENDIX	173

University of Malaya

LIST OF FIGURES

Figure 2.1: Typical absorption/desorption process for post-combustion CO ₂ capture.....	8
Figure 3.1: Methodology flow chart	70
Figure 3.2: Process flow diagram of the absorption/desorption process	79
Figure 3.3: Locations of temperature sensors in the absorption column	80
Figure 3.4: Absorption-desorption unit.....	86
Figure 3.5: a) simple schematic of the CO ₂ absorption/desorption pilot scale unit in....	89
Figure 3.6: Typical titration graph for the determination of total alkalinity of mixed MEA-glycerol solution.....	95
Figure 3.7: Process flow diagram of the absorption process	100
Figure 3.8: Process flow diagram of the desorption process	101
Figure 4.1: Liquid temperature profile for the absorber	107
Figure 4.2: Temperature profiles for the liquid phase in the CO ₂ -MEA system with the mixed flow model	108
Figure 4.3: Temperature profiles for the liquid phase in the CO ₂ -MEA system with different film resistances	108
Figure 4.4: Temperature distribution along the stripper	109
Figure 4.5: CO ₂ concentration in the liquid phase along the absorption column for glycerol solvent.....	110
Figure 4.6: CO ₂ concentration in the vapor phase along the absorption column for glycerol solvent.....	111
Figure 4.7: CO ₂ removal efficiency for different glycerol concentrations in water	111
Figure 4.8: H ₂ O mole fraction in the vapor phase along the absorber for different glycerol concentrations in water	112
Figure 4.9: Liquid temperature profiles along the absorber for different glycerol concentrations in water	113
Figure 4.10: Liquid temperature profiles along absorber for MEA, glycerol, and glycerol-MEA solutions	114

Figure 4.11: Comparison of CO ₂ mole fractions in the liquid phase along the absorber for MEA, glycerol, and their mixtures	115
Figure 4.12: Comparison of CO ₂ mole fractions in the vapor phase along the absorber	116
Figure 4.13: Comparison of H ₂ O mole fractions in the vapor phase along the absorber	116
Figure 4.14: Comparison of apparent CO ₂ mole fractions in rich stream to the stripper	117
Figure 4.15: Comparison of apparent CO ₂ mole fraction along the stripper	118
Figure 4.16: Comparison of CO ₂ removal percentage for various concentrations of MEA/ glycerol solution.....	119
Figure 4.17: CO ₂ loading along the absorption column.....	120
Figure 4.18: Comparison of reboiler heat duty between the present simulation results	120
Figure 4.19: Comparison of temperature profile between MEA solution and glycerol–MEA solution along the absorption column	122
Figure 4.20: Temperature profile along the absorber.....	123
Figure 4.21: CO ₂ loading profile along the absorber	123
Figure 4.22: CO ₂ loading in rich solvents. Experiments with a) aqueous MEA solution b) aqueous mixture of MEA-glycerol solution and c) aqueous glycerol solution	127
Figure 4.23: A comparison of CO ₂ loading in the outlet streams of absorber and stripper columns. Experiment with the mixture of 10 wt% MEA-10 wt% glycerol aqueous solution.....	128
Figure 4.24: A comparison of CO ₂ loading in the outlet streams of absorber and stripper columns. Experiment with 10 wt% MEA aqueous solution	128
Figure 4.25: A comparison of CO ₂ loading in the outlet streams of absorber and stripper columns. Experiment with 10 wt% glycerol aqueous solution.....	129
Figure 4.26: Temperature profile of absorber outlet stream at different CO ₂ loadings. Experiment with 10 wt% MEA aqueous solution.....	130
Figure 4.27: Temperature profile of absorber outlet stream at different CO ₂ loadings. Experiment with the mixture of 10 wt% MEA -10 wt% glycerol aqueous solution	131

Figure 4.28: Temperature profile of absorber outlet stream at different CO ₂ loadings. Experiment with 10 wt% glycerol aqueous solution	131
Figure 4.29: A comparison of temperature profiles of absorber outlet stream at different gas flow rates. Experiments with a) aqueous MEA solution b) aqueous mixture of MEA-glycerol solution c) aqueous glycerol solution	132
Figure 4.30: pH Profile at various CO ₂ loadings and same gas flow rates of MEA, MEA-glycerol, and glycerol solutions	133
Figure 4.31: Dependence of the rich CO ₂ loading on L/G ratio	136
Figure 4.32: liquid temperature profiles along the absorber height for different gas flow rates	137
Figure 4.33: liquid temperature profiles along the absorber height for gas flow rates with a)1.4 L/min b)1.7 L/min c)2.9 L/min d)3.3 L/min e)3.9 L/min.....	138
Figure 4.34: CO ₂ mole fraction profiles in liquid phase along the absorber height for CO ₂ -MEA-glycerol system	141
Figure 4.35: CO ₂ loading profiles along the absorber height for CO ₂ -MEA-glycerol system.....	141
Figure 4.36: Dependence of the gas flow rate on reboiler heat duty	144
Figure 4.37: CO ₂ mole fraction profile in liquid phase along the stripper height at different gas flow rates.....	146
Figure 4.38: Dependence of the lean CO ₂ loading on L/G ratio	147

LIST OF TABLES

Table 2.1: Base characteristics of MEA and glycerol.....	10
Table 3.1: Equilibrium constants for reactions 3.1-3.5.....	76
Table 3.2: Kinetic parameters for reactions 3.7-3.10.....	76
Table 3.3: Coefficients for Henry's constants of CO ₂ in H ₂ O, MEA, and glycerol	77
Table 3.4: Packing parameters for columns	78
Table 3.5: Feed conditions for validation	81
Table 3.6: Feed conditions for CO ₂ absorption/desorption using glycerol solvent	82
Table 3.7: Feed conditions for MEA-glycerol process	83
Table 3.8: Characteristics of absorber and stripper.....	85
Table 3.9: Experimental conditions for the CO ₂ absorption in packed column.....	93
Table 3.10: Operating parameters of absorption/desorption unit.....	93
Table 3.11: Experimental conditions for the CO ₂ absorption in packed column.....	98
Table 3.12: Actual operating conditions performed	99
Table 3.13: Characteristics of absorption column.....	99
Table 3.14: Physical characteristics of Raschig rings	100
Table 3.15: Characteristics of desorption column.....	101
Table 3.16: Physical characteristics of Raschig rings	102
Table 3.17: Operating conditions in both experimental and simulation study	102
Table 4.1: Comparison of experimental and simulation data for absorber and stripper.....	105
Table 4.2: Summary of the obtained results for CO ₂ -MEA, CO ₂ -MEA-glycerol and CO ₂ -glycerol systems.....	121
Table 4.3: Operating conditions used in this experimental study with 0.7 L/min solvent flow rate and CO ₂ (15 v%)-N ₂ (85 v%) gas mixture	125

Table 4.4: CO₂ loadings in outlet stream from absorber for CO₂-MEA-glycerol system with 0.7 L/min solvent flow rate and CO₂ (15 v%)-N₂ (85 v%) gas mixture 135

Table 4.5: Rich stream temperature for CO₂-MEA- glycerol system 139

Table 4.6: CO₂ loadings in outlet stream from stripper for CO₂-MEA-glycerol system with 0.7 L/min solvent flow rate and CO₂ (15 v%)-N₂ (85 v%) gas mixture 144

University of Malaya

LIST OF SYMBOLS AND ABBREVIATIONS

LIST OF SYMBOLS

a_e	:	effective interfacial area (ft^2/ft^3)
a_p	:	specific surface of the packing (ft^2/ft^3)
a_t	:	total surface area of packing (m^2/m^3)
a_w	:	wetted surface area of packing (m^2/m^3)
D	:	diffusivity (m^2/h)
D_p	:	nominal size of packing (m)
Fr	:	Froude number
g	:	gravitational constant (m/h^2)
G	:	superficial mass velocity of gas ($\text{kg}/\text{m}^2 \cdot \text{h}$)
k_L	:	liquid-phase mass transfer coefficient (m/h)
k_G	:	gas-phase mass transfer coefficient [$\text{kg}\text{-mol}/\text{m}^2 \cdot \text{h} \cdot \text{atm}$]
L	:	superficial mass velocity of liquid ($\text{kg}/\text{m}^2 \cdot \text{h}$)
R	:	gas constant ($\text{m}^3\text{-atm}/\text{kg}\text{-mol}\cdot\text{K}$)
Re	:	Reynolds number
T	:	absolute temperature (K)
We	:	Weber number
Z	:	height of packing in column (ft)
μ	:	viscosity ($\text{kg}/\text{m}\cdot\text{h}$)
ρ	:	density (kg/m^3)
σ_c	:	critical surface tension of packing material (dynes/cm)
σ	:	surface tension (dynes/cm)

LIST OF ABBREVIATIONS

G : gas

L : liquid

L liter

University of Malaya

CHAPTER 1: INTRODUCTION

1.1 Research background

Carbon dioxide (CO₂) is the major greenhouse gas generated through human activities, particularly from combustion of fossil fuels consumed in transportation vehicles, manufacturing industries, and power generation facilities (Heintz et al., 2008; Lv et al., 2015; Shafeeyan et al., 2015). The reduction in CO₂ emission has gained increased attention of researchers to alleviate global warming issues (F. M. Khan et al., 2011). In recent years, solvent-type processes, which are categorized into chemical, physical, and mixed chemical/physical processes, are employed to remove acid gas from fuel gas (Heintz et al., 2008). In chemical processes, aqueous alkanolamine solutions, (Babamohammadi et al., 2015) such as monoethanolamine (MEA), diethanolamine (DEA) and *N*-methyldiethanolamine (MDEA) are used to separate CO₂ in packed columns (Karpe & Aichele, 2013; F. M. Khan et al., 2011). Physical processes, such as Rectisol, Selexol (Espinal et al., 2013; Mirzaei et al., 2015) and Morphysorb, use chilled methanol, mixture of dimethyl ethers of polyethylene glycol, and *n*-formylmorpholine/*n*-acetylmorpholine as solvents, respectively (Heintz et al., 2008). Sulfinol is another mixed chemical/physical process; this method uses a mixture of sulfolane and aqueous solution of either methyl diethanolamine or diisopropanolamine as solvent (Heintz et al., 2008; Mirzaei et al., 2015).

1.2 Problem statement

Amines undergo thermal degradation in regeneration process and oxidative degradation where oxygen is present in the flue gas stream. Effects of amines degradation include CO₂ loading capacity reduction, foaming, fouling, and increase in viscosity. Moreover, vapour pressure of MEA is relatively high and leads to significant solvent loss through evaporation and also serious environmental drawbacks. To overcome the drawbacks of MEA solvent, researchers have studied the mixture of amines and physical solvents as

chemical solvents are corrosive in nature. Recently, a novel solvent, glycerol has been studied for its application in CO₂ capture. It is nontoxic, stable and liquid at low vapour pressure levels. This compound is available in abundance as a by-product of biodiesel production, thus; it is relatively inexpensive and biodegradable. Glycerol is colorless and odourless. Moreover, it has high boiling point and it is non-volatile at atmospheric pressure. Furthermore, the high viscosity of pure glycerol decreases in glycerol aqueous solutions by increasing the amount of water and temperature. The CO₂ solubility in glycerol is higher than that of CO₂ in water. Therefore, the application of glycerol can reduce the use of harmful chemical solvents with environment friendly solvents.

1.3 Objectives of the research

The aim of this research is to study the application of physical solvent with the purpose of reducing the use of harmful chemical solvents. Therefore, the suitability of glycerol for separating CO₂ from gas mixture of CO₂ (15 v%) and N₂ (85 v%) is investigated. This aim is precisely achieved through the following specific objectives:

1. To evaluate the absorption performance of the MEA, glycerol and different combinations of MEA and glycerol in order to form the best combination for efficient CO₂ absorption using Aspen Plus simulation.
2. To start-up the pilot scale absorption/desorption columns and evaluate experimentally the performance of aqueous mixtures of MEA-glycerol for CO₂ absorption process.
3. To simulate the performance of CO₂ absorption process using aqueous blend of MEA-glycerol and validate simulation results with experimental data.

1.4 Outline of the thesis

This thesis consists of five chapters dealing with different aspects relevant to the topic of the study.

Chapter 1: Introduction

In this chapter research background, problem statement, objectives of work and outline of thesis are described.

Chapter 2: Literature Review

This chapter reviews the history and application of different technologies for CO₂ capture. In addition, good information will be presented about recent studies on CO₂ absorption and detailed physical and chemical solvents on CO₂ absorption are discussed.

Chapter 3: Methodology

Chapter three includes chemicals and materials used in this research. The equipment and experimental setup used in this study are described. New solvent for CO₂ absorption is presented. Also, in this chapter, the equations and methods used to evaluate the CO₂ absorption/desorption process using Aspen Plus simulation are presented.

Chapter 4: Results and Discussion

In this chapter, results and findings of the study were discussed with full details. This chapter is presented in three main sections. The first section is devoted to the modelling of CO₂ absorption process using Aspen Plus v7.3. The second section focuses on the experimental work of CO₂ absorption/stripping using SOLTEQ Absorption-Desorption Unit (Model: BP 51) at University Malaya and the third section discusses on validation of simulation study with experimental work.

Chapter 5: Conclusions and Recommendations

Results and findings in each objective are summarized in this chapter. Furthermore, suggestions are also given for the future work, which are very important and related to this work.

University of Malaya

CHAPTER 2: LITERATURE REVIEW

2.1 Introduction

CO₂ removal methods have been extensively applied in different sections of industry, such as natural gas purification and CO₂ capture from flue gas, with extra emphasis on the latter. Due to international efforts to reduce greenhouse gas discharges, the capture of CO₂ from flue gas has received increasing attention in recent years (Aschenbrenner & Styring, 2010).

Some parameters, such as CO₂ solubility, CO₂ selectivity over N₂, and solvent loss, are very important in selecting a suitable solvent for CO₂ capture. Other parameters, such as toxicity and environmental cost, have to be considered as well, especially when there is solvent degradation and loss caused by evaporation in the process (Aschenbrenner & Styring, 2010).

2.2 Carbon management strategies

2.2.1 Carbon capture and storage (CCS)

CCS refers to a process consisting of the CO₂ separation from industrial and energy-related sources, transport to a storage location and preventing it from entering the atmosphere. Storage should be for at least many hundreds of years to be useful for climate change mitigation. Therefore, CCS involves three stages: CO₂ capture, transport and storage (Araújo and Medeiros 2017).

2.2.1.1 CO₂ capture

Carbon capture is employed to large stationary sources such as industrial plants and power stations, where CO₂ can be separated from the flue gases. There are different capture technologies which are in the development stages. The most developed has been applied in the gas and petroleum industry and has already been used to a few small power plants abroad producing CO₂ for Enhanced Oil Recovery (EOR) or industrial uses (Rubin 2006).

Irons et al. (2007) studied three CO₂ capture technologies for power generation and for the improvement of CO₂ from coal-fired power plants. These three technologies are post-combustion capture, pre-combustion capture, and oxyfuel combustion (Irons et al., 2007; Olajire, 2010). Post-combustion carbon capture is a process that includes the removal of CO₂ from other components of flue gas in the air or generated via the combustion process (Figuerola et al., 2008).

2.2.1.2 CO₂ transport

CO₂ is captured as a gas and its transport needs it to be compressed and/or cooled requiring energy input. Bulk transport can be by pipeline or tanker. For large volumes pipelines are the only practical option but tankers have a role in smaller projects. CO₂ transport by pipeline is an established commercial technology (Rubin 2006).

2.2.1.3 CO₂ storage in geological structures

Under storage conditions in permeable rock, CO₂ is buoyant and moves to the top of the rock layer. If the rock above offers an effective seal CO₂ will trap and store. Another process which is effective in long-term storage in geological structures is permeable rocks which have their pore spaces filled with water in which injected CO₂ may dissolve and/or CO₂ may react chemically with water or minerals in the rock and be immobilized (Rubin 2006).

2.2.2 Carbon capture, utilization and storage (CCUS)

CCUS is consist of methods and technologies to remove CO₂ from the flue gas and atmosphere, followed by recycling the CO₂ for utilization and determining safe and permanent storage options. The plans of carbon utilization and storage can be classified by their environmental consequences, capacity and permanence of storage, and cost of implementation. Any viable system for storing carbon must be (1) effective and stable as long-term storage (2) environmentally benign (3) cost competitive (Zhang, Fan, & Wei, 2013; Al-Saleh, 2012).

Due to their high efficiency over other processes, absorption processes using chemical solvents have been used most often in natural gas purification and in post-combustion CO₂ capture commercially (Tan et al., 2012). Amines are mainly used as chemical absorbents in the CO₂ absorption process (Pires et al., 2011). Industrially, the MEA process is the most effective among different technologies for CO₂ capture from flue gas (Kittel et al., 2009). Basically, CO₂ absorption occurs in a column and allows direct contact among gas flows comprising CO₂ and liquid solvents. In recent years, different kinds of column internal system have been developed for use in the gas treatment process. Tower packing, including random and structured packing, is the most common system that is used to remove CO₂ from gas streams. Structured packing, with its regular geometric structures, is usually recommended due to its excellent performance with mass transfer in lower pressure drops (Aroonwilas & Tontiwachwuthikul, 2000).

2.3 CO₂ capture by amine-based absorption/stripping

Aqueous absorption/stripping using an amine is currently the only technology that is developed for commercial applications to capture of CO₂ from flue gas. Alkanolamines such as MEA, DEA, and MDEA have been traditionally investigated for this application. Other amines such as: 2-amino-2-methyl-1-propanol (AMP) and piperazine (PZ) have been studied as well. Among all amines, MEA is so far the benchmark solvent for post-combustion application (Wang, 2013).

A typical absorption/desorption system comprises of two columns (Figure 2.1). CO₂ is first absorbed from flue gas comprising 10-12% CO₂ by using solvent in the absorber column operated at 40-60°C and atmospheric pressure. CO₂ absorption into the solvent can be physically and chemically. The rich solvent-containing CO₂ leaves the absorber, is heated by reboiler in the stripper column, operating at 100-120°C and 1.5-2 atm to release CO₂. The released CO₂ is subsequently compressed for transport and storage. The hot lean (regenerated) solvent leaves the stripper and is cooled by the cold rich

solvent in a across heat exchanger and subsequently, the lean solvent is cooled to 40°C and is finally recycled to the absorber column (Ziaii Fashami, 2012).

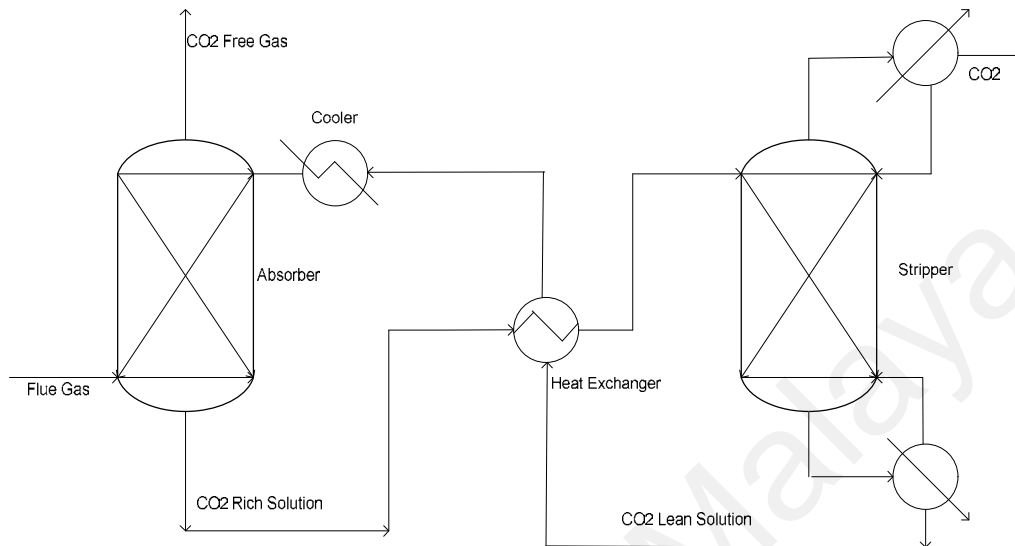


Figure 2.1: Typical absorption/desorption process for post-combustion CO₂ capture. (Karpe & Aichele, 2013; Puxty et al., 2009; Sønderby et al., 2013).

2.4 Monoethanolamine as a Solvent for CO₂ Capture

The current industry standard is the application of 30 wt% MEA aqueous solution for CO₂ absorption/desorption process. MEA is inexpensive compared to other amines and it is soluble in water at all concentrations. It has a high absorbing capacity on a mass basis and high reactivity. MEA reacts quickly with CO₂. However, MEA degrades at high temperature and in the presence of oxygen. It is also corrosive, leading to an increase in operation costs. Many other solvents are being employed in CO₂ capture, having both advantages and disadvantages compared to MEA. Notwithstanding newer solvents, MEA is still the most widely used amine for CO₂ capture (Dugas, 2006).

2.5 Glycerol as a solvent for CO₂ capture

Another alternative for CO₂ capture is physical absorption with less energy intensive regeneration of solvent. Physical absorption is effective for flue gas stream with high CO₂ partial pressure, typically more than 15 vol% (Wang et al., 2011). Recently, the researchers on CO₂ capture focus on enhancing performance by hybrid solutions, which are formed by blending chemical and physical solvents.

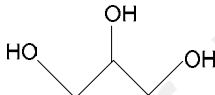
Glycerol is the main by-product biodiesel (Leoneti et al., 2012). In general, 10 kg of glycerol is generated as a by-product of every 100 kg of biodiesel produced (Chi et al., 2007), or, according to (Karinen & Krause, 2006), the production of biodiesel generates approximately 10% of glycerol by volume. Therefore, it is necessary to find alternative applications for this excess glycerol (Adhikari et al., 2008).

The addition of glycerol in MEA and methanol mixture improves the absorption capacity and lowers the regeneration energy compared to aqueous MEA solution. However, the cyclic absorption capacity decreases after the glycerol is added (Jie et al., 2016). The addition of glycerol into ammonia solution reduces the vaporization and improves CO₂ absorption characteristic (Seo et al., 2012). Glycerol has the maximum molar solubility for CO₂ and the highest solubility for nitrogen (N₂) rather than polyethylene glycol (PEG) 300, PEG 600, or poly(ethylenimine) (Aschenbrenner & Styring, 2010; Mirzaei et al., 2015).

Glycerol, a physical solvent used for CO₂ capture, is stable, non-toxic, and liquid at low vapor pressure levels (Aschenbrenner & Styring, 2010). This compound is biodegradable, sweet tasting, colorless, odorless, clear, and viscous liquid. Glycerol exhibits high boiling point (290 °C) and is non-volatile under atmospheric pressure (Safaei et al., 2012). The viscosity of pure glycerol is high but decreases in glycerol aqueous solution with increasing amount of water and temperature (Takamura et al., 2012; Chen et al., 1999). For example, the viscosity of glycerol solution with 30 wt%

water at 20°C is almost 1.59% compared to that of pure glycerol (Chen et al., 1999). Glycerol is safe for living organisms (Morrison, 2000) and is considered an eco-friendly solvent. Therefore, glycerol was selected in this research for blending with MEA for post-combustion CO₂ capture from CO₂-N₂ gas mixture. This technique aims to reduce the use of harmful chemical solvents with environment friendly solvents. Table 2.1 compares the base characteristics of MEA and glycerol.

Table 2.1: Base characteristics of MEA and glycerol

Solvent	Glycerol	MEA (Padurean et al., 2011)
Molecular structure		
Formula	C ₃ H ₈ O ₃ (Pagliaro & Rossi, 2010)	C ₂ H ₇ NO
Molecular weight	92.09(Pagliaro & Rossi, 2010)	61.09
Melting point(°C)	18.2(Pagliaro & Rossi, 2010)	10.00
Boiling point(°C)	290(Pagliaro & Rossi, 2010)	170.00
pH	neutral to litmus(Baker)	12.10
Toxicity (oral LD ₅₀ rate)(mg/kg)	12600.00 (Robertson, 2002)	1720.00
Vapor pressure (mmHg@20°C)	7.15×10 ⁻⁵ (Cammenga et al., 1977)	0.36
Viscosity(cP@20°C)	1412(Segur & Oberstar, 1951)	24.10

2.6 Modeling of absorption/stripping process

Extensive experimental data have been collected in the past twenty years on the CO₂-MEA-H₂O system. The currently most used model for this system is the electrolyte NRTL. The purpose of this work is improvement of CO₂ absorption using a mixture of MEA-glycerol solution in a packed column. Most of the studies on glycerol and hybrid solution system have been performed under laboratory scale and based on our knowledge, there is no reported CO₂ absorption simulation study using glycerol in the open literature. Aspen Plus is a suitable tool for the design of CO₂ removal processes with lower costs. It also provides tools to perform analyses of this mixed solvent. For this reason, it was chosen as platform for this process.

2.7 CO₂ capture technologies

Different technologies have been applied for the removal of CO₂ from flue gas in industries such as the petroleum, chemical, and traditional fossil fuel-fired power industries. These technologies include chemical absorption, physical adsorption, cryogenic methods, membrane separation, and biological fixation (Choi et al., 2009; Li et al., 2011). Figure 2.2 indicates the different technical options for CO₂ capture from flue gas. These options appear under the headings: absorption, adsorption, membranes, cryogenic, and microalgal.

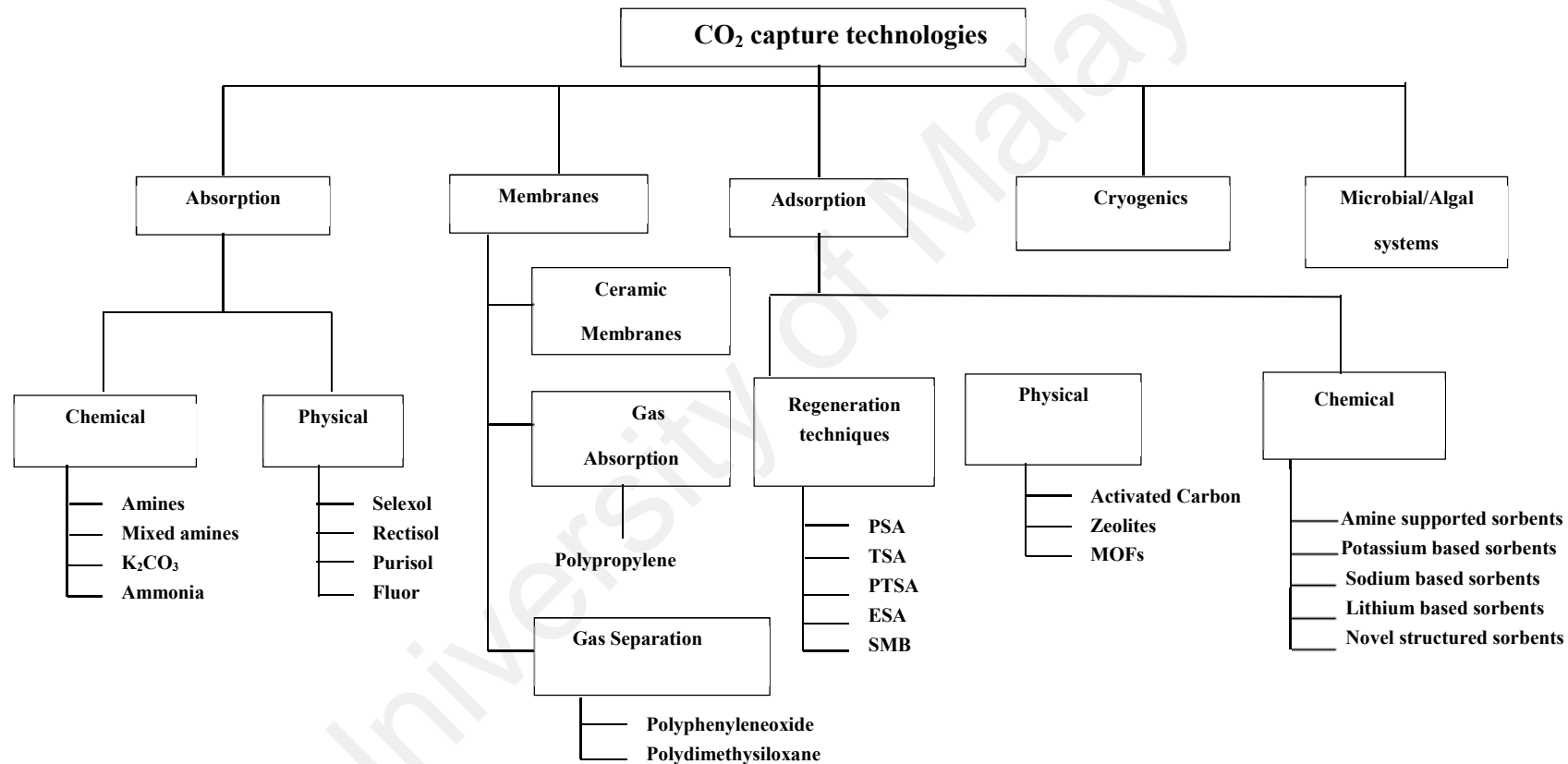


Figure 2.2: CO₂ capture technologies. Reprinted with permission from (Rao & Rubin, 2002).

Copyright © 2002. American Chemical Society

The absorption process is a physical/chemical process in which atoms, molecules, or ions are solved in the bulk phase. In the absorption process, molecules are absorbed by the volume and not by the surface. The absorption process is a common process in the chemical industry and is used for the treatment of industrial gas streams, including acid gases, such as H₂S, NO_x, and CO₂ (Pires et al., 2011). Some of the solvents used for absorption are Selexol, Rectisol, fluorinated solvents (physical solvents), and ammonia (NH₃) solutions as well as amines, such as MEA (chemical solvents) (Hasib-ur-Rahman et al., 2010; Wappel et al., 2010).

2.7.1 Adsorption

In the adsorption process, molecules contained in liquid or gaseous mixtures are absorbed on the surface of the solid adsorbent (Kaithwas et al., 2012; Pires et al., 2011; Wang et al., 2011). There are different regeneration techniques that can be used to regenerate the adsorbent: (1) vacuum swing adsorption (Chou & Chen, 2004) and pressure swing adsorption (PSA; (Wang et al., 2011; Zhao et al., 2007), (2) temperature swing adsorption (TSA; (Wang et al., 2011; Zhao et al., 2007), (3) electric swing adsorption, (4) simulated moving bed, and (5) purge displacement (Li et al., 2011).

In the last few years, the adsorption of CO₂ into progressive sorbents, such as zeolites (Wang et al., 2011) and metal-organic frameworks (MOFs; (Li et al., 2011)), activated carbon, and alumina, has become an intensely researched topic (Wang et al., 2011). Riemer et al. (1994) compared two methods of PSA and TSA and showed that PSA is better than TSA because of less energy requirement (Shafeeyan et al., 2014) and greater regeneration rate (Riemer et al., 1994).

According to the studies of Siriwardane et al. (2001), the PSA and TSA methods are suitable for CO₂ removal from high-pressure flue gas. They reported molecular sieve 13X, 4A, and activated carbon as potential adsorbents for CO₂ in the PSA process (Siriwardane et al., 2001), whereas Gomes and Yee (2002) reported that zeolite 13X

was a suitable adsorbent for CO₂ capture from flue gas. They used the PSA technique for CO₂ removal and found that the nitrogen gas recovered increased from 30 to 90% in this method (Gomes & Yee, 2002). One of the advantages of adsorption in CO₂ separation is that sorbents can be reused many times (Satyapal et al., 2001). The adsorption process requires lower energy and prevents the shortcomings of the absorption process (Drage et al., 2009). On the contrary, there are some major disadvantages in the adsorption process. First, CO₂ concentration in flue gas is approximately 15% for most power plants, but the adsorption system cannot control CO₂ concentrations of more than 0.04–1.5% (Aaron & Tsouris, 2005). Moreover, most available adsorbents have low selectivity, so for flue gas treatment a high concentration of CO₂ is necessary (Wang et al., 2011). The adsorption quality can be determined using the attributes of the adsorbed particles, such as molecular size, molecular weight, and polarity, and the adsorbent surface, such as polarity, pore size, and spacing (Kaithwas et al., 2012). When the purpose of adsorption is CO₂ selectively, gases that have a smaller size than CO₂ can diffuse into the pores. N₂ has this ability. Therefore, the efficiency of the process in CO₂ separation decreases for each sequence. Furthermore, adsorption happens slowly (Aaron & Tsouris, 2005).

2.7.2 Membrane absorption

In gas absorption by membranes, the contact between the gas stream and the liquid solvent will happen through the membrane. The membranes are compact, and they are not sensitive to flooding, entrainment, channeling, or foaming. Therefore, they have some advantages over conventional contacting devices, such as packed columns. However, it should be noted that, for CO₂ transport through a membrane, the pressures on the liquid and gas sides are equal. The performance of the membrane in the separation process is dependent on the CO₂ partial pressure; thus, they are appropriate for CO₂ concentrations of more than 20 vol% (Favre, 2007; Wang et al., 2011). The

membrane gas absorption (MGA) process is a combination of the traditional gas absorption method into liquids and a membrane contactor, in which the membrane contactor provides a significant surface area, independent tunable gas and liquid flow rates, and an energy-efficient device, whereas high selectivity and a high mass-transfer driving force can be provided through gas absorption. Alkanolamines, such as MEA, diethanolamine (DEA), and N-methyldiethanolamine (MDEA), are often employed as chemical absorbents in MGA for CO₂ capture (Lu et al., 2014).

2.7.3 Membrane-based separation

In membrane separation, there are differences in the physical and/or chemical interactions between the gases and the membrane material. By modification, components can pass through the membrane according to their size (kinetics) and/or affinity (thermodynamics). Generally, membranes are highly efficient for the separation of CO₂/H₂ in precombustion capture and postcombustion CO₂/N₂ separation (Li et al., 2011).

2.7.3.1 Facilitated transport membranes

Facilitated transport membranes were studied by Kasahara et al. (2012), who prepared amino acid ionic liquid (IL)- based facilitated transport membranes with tetrabutylphosphonium amino acid ILs and with glycine, alanine, proline, and serine as the anion. They used tetrabutylphosphonium because of its high thermal stability. They reported that proline- based membranes have excellent penetrance and the highest CO₂/N₂ selectivity because of their superior water holding capability (Kasahara et al., 2012).

An ultrathin PVAm/PVA blend-facilitated transport membrane cast on a porous polysulfone support was evaluated by Deng et al. (2009) for the separation of CO₂/N₂ mixed gas. They reported a CO₂/N₂ separation factor of up to 174 and a CO₂ permeability of up to 0.58 m³ (STP)/(m² h bar) in their experiment and showed that the

fixed amino groups in the PVAm matrix function as CO₂ carriers to facilitate the transport, whereas the PVA adds mechanical strength. They showed that CO₂ is transported by the facilitated transport mechanism through this membrane (Deng et al., 2009).

2.7.3.2 Mixed-matrix membranes

Filling the pores of mixed-matrix membranes with inorganic particles leads to increased gas separation efficiency of polymeric membranes. It should be noted that the inorganic particles should be well bonded with the polymer to reduce the voids that may lead to the loss of CO₂ selectivity (Khalilpour et al., 2015). Some researchers have employed inorganic fillers, such as zeolites (Bastani et al., 2013; Junaidi et al., 2014; Nik et al., 2011; Sublet et al., 2012), MOFs (Nafisi & Hägg, 2014; Perez et al., 2009), and carbon nanotubes (Ahmad et al., 2014; Aroon et al., 2013; Rajabi et al., 2013). The permeability and selectivity of membrane-based polymers can be enhanced by inorganic fillers (Shahid & Nijmeijer, 2014). The selection of an appropriate solvent is essential for the economic viability of the process. High solubility and high absorption selectivity of CO₂ over N₂ are the main selection criteria (Aschenbrenner & Styring, 2010).

2.8 CO₂ solubility in solvents

2.8.1 Theory of the solubility parameter

The solubility parameter (δ) is defined as the square root of the cohesive energy density, and cohesive energy (E) is the energy required for breaking the interactions between molecules. Equation 2.1 shows the correlation between the Hildebrand solubility parameter and the cohesive energy (E) and molar volume (V_m).

$$\delta = \sqrt{\frac{E}{V_m}} = \left[\frac{\Delta H_{\vartheta} - RT}{V_m} \right]^{0.5} \quad (2.1)$$

ΔH_{ϑ} is the heat of vaporization, and RT is an ideal gas PV term (Hansen, 2007). Hansen proposed that the total heat of vaporization is composed of (atomic) dispersion forces,

(molecular) permanent dipole-permanent dipole forces, and (molecular) hydrogen bonding (electron exchange). Equation 2.2 describes the Hansen solubility parameter, where δ_D , δ_P , and δ_H are related to dispersion, dipole-dipole, and hydrogen bond contributions, respectively (Sistla et al., 2012):

$$\delta^2 = \delta_D^2 + \delta_P^2 + \delta_H^2 \quad (2.2)$$

Solubility depends on temperature and pressure, so temperature swings or pressure swings are important for understanding the absorption-desorption process (Zaman & Lee, 2013). Additionally, partial pressure, temperature, and feed gas are key parameters in the case of solubility (Olajire, 2010).

Experimentally, the solubility parameter can be assessed by direct and indirect methods. Direct methods include determining the vaporization heat by calorimetry or calculating the solubility/miscibility of the compounds in solvents. However, it is difficult to employ direct methods for ILs as solvents, because ILs are thermally stable compounds, with insignificant vapor pressure. The solubility parameter can also be estimated using indirect experimental approaches, such as inverse gas chromatography, via melting temperatures of ILs, by essential viscosity measurements, or by using the activation energy of viscosity (Sistla et al., 2012). Table 2.2 compiles the CO₂ solubility in numerous solvents.

Table 2.2: CO₂ solubility in different solvents

Solvent	Temperature(°C)	Pressure(bar)	Result	Reference
1-butyl-3-methyl-imidazolium chloride ([Bmim]Cl)	30	$P_{CO_2}=1.013$	The chitin/IL and chitosan/IL solutions are capable and reversible fixing systems in CO ₂ capture, and 10 wt% chitosan/IL solution indicates considerable CO ₂ absorption capacity at 8.1 mol% with respect to ionic liquid under mild conditions	(Xie et al., 2006)
[bmim][PF ₆]	10 to 50	up to 13	CO ₂ solubility of this IL is more than organic solvents, such as heptane, cyclohexane, benzene, ethanol, and acetone	(Hasib-ur-Rahman et al., 2010)
1-ethyl-3-methylimidazolium bis(trifluoromethylsulfonyl)imide, [emim][Tf ₂ N]	up to 176.85	60	CO ₂ solubility is 60 mol%, which shows the better efficiency of IL for CO ₂ capture. In the absence of air but in the presence of CO ₂ , the ionic liquid [emim][Tf ₂ N] is thermally stable up to 450 K. The CO ₂ solubility in [emim][Tf ₂ N] is boosted by raising pressure and falling temperature. The CO ₂ solubility is extremely high in the ionic liquid [emim][Tf ₂ N] compared to [emim][PF ₆]	(Schilderman et al., 2007)
[emim][PF ₆]	up to 176.85	60	At 60°C, CO ₂ solubility in the ionic liquid with the [Tf ₂ N] anion is higher, particularly at greater CO ₂ concentrations	(Schilderman et al., 2007)

Table 2.2, Continued: CO₂ solubility in different solvents

Solvent	Temperature(°C)	Pressure(bar)	Result	Reference
1-ethyl-3-methylimidazolium 2-(2-methoxyethoxy)ethylsulfate, [emim][MDEGSO ₄]	30	8.54–67	Solubility increases with pressure rise	(Hasib-ur-Rahman et al., 2010)
1- <i>n</i> -butyl-1-methylpyrrolidinium bis(trifluoromethylsulfonyl)amide ([bmpy][Tf ₂ N])	19.95 to 140.05	108	CO ₂ becomes less soluble in [bmpy][Tf ₂ N] with rising temperature	(Kumelan et al., 2010)
1-ethyl-3-methylimidazolium ethylsulfate [emim][EtSO ₄]	30 to 80	up to 16	This IL is a good solvent for CO ₂ and H ₂ S separation. H ₂ S is more soluble than CO ₂ and its diffusion coefficient is about two orders of magnitude that of CO ₂	(Jalili et al., 2010)

Table 2.2, Continued: CO₂ solubility in different solvents

Solvent	Temperature(°C)	Pressure(bar)	Result	Reference
1-(2-hydroxyethyl)-3-methylimidazolium ([hemim] ⁺) + A: hexafluorophosphate ([PF ₆] ⁻) B: trifluoromethanesulfonate ([OTf] ⁻) C: bis-(trifluoromethyl)sulfonylimide ([Tf ₂ N] ⁻)	30 to 80	up to 13	CO ₂ solubility in [hemim][Tf ₂ N] is the highest and in [hemim][BF ₄] is the lowest. CO ₂ solubility in [hemim] ILs is more than conventional [emim]s comprising the same anions, demonstrating that these solvents are more efficient for CO ₂ sequestration than the emims	(Jalili et al., 2010)
2-[2-hydroxyethyl (methyl) amino] ethanol chloride ([MDEA][Cl])	40 to 60	12.20 to 86.20	Comparing the solubility of CO, H ₂ , N ₂ and O ₂ with that of CO ₂ in [MDEA][Cl], it shows that the solubility of these four gases is much lower than that of CO ₂ , which means [MDEA][Cl] is a good solvent for CO ₂ capture from mixed gases. Solubility of gases improved with the increasing of pressure while it was reduced with increasing temperature	(Zhao et al., 2011)

Table 2.2, Continued: CO₂ solubility in different solvents

Solvent	Temperature(°C)	Pressure(bar)	Result	Reference
N-methyldiethanolamine (MDEA) and guanidinium trifluoromethanesulfonate ([gua] ⁺ [OTf] ⁻)	30.05, 50.05 and 60.05	P_{CO_2} ranging from 5 to 30	The aqueous [gua] ⁺ [OTf] ⁻ ionic liquid has better solubility, up to 1.63 mol CO ₂ /total mol, in comparison to other pure ionic liquids such as [bmim] ⁺ [BF ₄] ⁻ , [emim] ⁺ [OTf] ⁻ and [emim] ⁺ [C ₂ N ₃] ⁻ , which was noted at 323.2 K and 3000 kPa, by adding the [gua] ⁺ [OTf] ⁻ ionic liquid to aqueous MDEA solubility decreases slightly	(Sairi et al., 2011)
Glycerol	25		Glycerol has the maximum molar solubility for CO ₂ and the highest solubility for N ₂ rather than PEG 300, PEG 600, or poly(ethylenimine)	(Aschenbrenner & Styring, 2010)
PEG 200	25		PEG 200 has the highest molar solubility for CO ₂ and the maximum solubility for N ₂ between PEG 300, PEG 600, and poly(ethylenimine)	(Aschenbrenner & Styring, 2010)
Polyethylenimine	25		This solvent among PEG 200, PEG 300, PEG 600, and glycerol is the only solvent that has amine groups with very low absorption because of its great viscosity	(Aschenbrenner & Styring, 2010)

Table 2.2, Continued: CO₂ solubility in different solvents

Solvent	Temperature(°C)	Pressure(bar)	Result	Reference
PEG 300	25		This solvent among PEG 200, PEG 600, glycerol, and poly (ethylenimine) is the best substance that has high CO ₂ solubility and good selectivity over N ₂ . Although MEA has a superior CO ₂ absorption capacity than PEG 300, the advantages of PEG 300 are the greater stability, less solvent loss, and smaller desorption energy compared to MEA	(Aschenbrenner & Styring, 2010)
Deep eutectic mixture of choline chloride (ChCl) and glycerol	30 to70	up to 63	In the case of this solvent, the gas solubility rises with pressure linearly and falls with increasing temperature. The solubility in molality of CO ₂ in DES is comparable with typical CO ₂ solubility in RTILs [Bmim][PF ₆], 1-butyl-3-methylimidazoliumtetrafluoroborate ([Bmim][BF ₄]), 1-butyl-3-methylimidazolium dicyanamide ([Bmim][C ₂ N ₃]), 1-butyl-3-methylimidazolium trifluoromethanesulfonate ([Bmim][triflate]), and N-butylpyridinium tetrafluoroborate ([Bpy][BF ₄])	(Leron & Li, 2013)

Table 2.2, Continued: CO₂ solubility in different solvents

Solvent	Temperature(°C)	Pressure(bar)	Result	Reference
(2-hydroxyethyl)-trimethyl-ammonium (S)-2-pyrrolidine-carboxylic acid salt [Choline][Pro] + polyethylene glycol 200 (PEG200) mixture	35, 50, 65 and 80	up to 1.1	At the same temperature and pressure, the CO ₂ solubility in this mixture decreases with increasing PEG200 content. The reason is that the solubility of CO ₂ in PEG200 is very low. The CO ₂ solubility in [Choline][Pro]/PEG200 increases with increasing pressure of CO ₂ and is more sensitive to pressure at lower pressures	(Li et al., 2008)
Glycerol	40 to 200	up to 350	The glycerol solubility in CO ₂ is in the range of 10 ⁻⁵ in mole fraction, which is very low. In contrast, the glycerol-rich phase dissolved CO ₂ at mole fractions up to 0.13. The CO ₂ solubility in glycerol is higher than that of CO ₂ in water	(Medina-Gonzalez et al., 2013)
1- <i>n</i> -butyl-3-methylimidazolium hexafluorophosphate [bmim][PF ₆] and 1- <i>n</i> -butyl-3-methylimidazolium tetrafluoroborate [bmim][BF ₄]	10 to 75	20	The solubility data have been effectively associated for the first time using a simple cubic EOS	(Shiflett & Yokozeki, 2005)

Table 2.2, Continued: CO₂ solubility in different solvents

Solvent	Temperature(°C)	Pressure(bar)	Result	Reference
1-ethyl-3-methylimidazolium bis[trifluoromethylsulfonyl]imide, [emim][Tf ₂ N]	60	60	For this solvent, CO ₂ solubility is 60 mol%. The fluoroalkyl group improves the CO ₂ solubility, thus making [emim][Tf ₂ N] more efficient for CO ₂ capture	(Schilderman et al., 2007)
2-amino-2-hydroxymethyl-1,3-propanediol (AHPD)	25	P_{CO_2} ranging from 0.0001 to 30	In aqueous solutions of 10 mass% AHPD, the solubility of CO ₂ was better than that in aqueous 10 mass% MEA solutions at pressures higher than 4 kPa and at a temperature of 298.15°K, but the solubility behavior at a pressure lower than 4 kPa was the opposite. The solubility differences between these two solutions increased with CO ₂ partial pressures above the crossover pressure	(Park et al., 2003)
derivatives of imidazoliumbased ILs, (C ₃ mim, C ₄ mim, C ₆ mim, and C ₈ mim) and the octyl derivative is fluorinated (C ₈ F ₁₃ mim)	25	1	CO ₂ solubility is lower in the ionic liquid including PF ₆ ⁻ than in the corresponding liquid with Tf ₂ N ⁻ anion	(Baltus et al., 2004)

Table 2.2, Continued: CO₂ solubility in different solvents

Solvent	Temperature(°C)	Pressure(bar)	Result	Reference
1-ethyl-3-methylimidazolium hexafluorophosphate ([emim][PF ₆]) and 1-butyl-3-methylimidazolium hexafluorophosphate ([bmim][PF ₆])	34.99–92.88	14.90–971	Solubility of the IL is very low in supercritical CO ₂ and CO ₂ is more soluble in [bmim][PF ₆] in comparison to [emim][PF ₆]	(Shariati & Peters, 2004)
1-hexyl-3-methylimidazolium hexafluorophosphate [hmim][PF ₆]	25.16–90.43	6.40–946	CO ₂ has good solubility in [hmim][PF ₆] at lower pressures and also CO ₂ is more soluble in [hmim][PF ₆] compared to [emim][PF ₆]	(Shariati & Peters, 2004)
potassium carbonate–polyethylene glycol (PEG)	25.05 and 50.05	<i>P</i> _{CO₂} ranging from 0.05 to 20	By adding PEG to 5 wt% K ₂ CO ₃ solution the CO ₂ solubility drops at a constant temperature and pressure	(Park et al., 1997)
potassium carbonate with 2-methylpiperazine and piperazine	39.85 and 59.85	up to 7	CO ₂ loading capacities of K ₂ CO ₃ 15 wt%/2-MPZ and PZ 10 wt% solutions are greater than MEA 30 wt% or AMP 30 wt% at the specific pressure of CO ₂ . Furthermore, the CO ₂ loading capacity of K ₂ CO ₃ /2-MPZ is similar to K ₂ CO ₃ /PZ	(Kim et al., 2012)

Table 2.2, Continued: CO₂ solubility in different solvents

Solvent	Temperature(°C)	Pressure(bar)	Result	Reference
potassium glycinate	19.85-77.85	P_{CO_2} up to 0.6	At temperatures ranging from 19.85°C to 49.85°C no difference was observed in the CO ₂ solubility but, by rising temperature to around 77.85 °C, the CO ₂ solubility reduces significantly	(Portugal et al., 2009)
potassium threonate	39.85	P_{CO_2} up to 0.6	Potassium threonate has lower CO ₂ absorption capacity compared to potassium glycinate	(Portugal et al., 2009)
sodium glycinate	30, 40 and 50°C	P_{CO_2} ranging from 0.001 to 2	Reductions in temperature and sodium glycinate concentration lead to increase CO ₂ solubility. Moreover, an increase in partial pressure of CO ₂ increases CO ₂ solubility for the investigated pressure range. The CO ₂ solubility in 10 mass% sodium glycinate solution is higher than aqueous monoethanolamine (MEA), 2-amino-2-ethyl-1,3-propanediol(AEPD), 2-amino-2-methyl-1,3-propanediol(AMPD) and triisopropanolamine (TIPA)	(Song et al., 2006)
30 mass% MEA	30	1.013	The amount of CO ₂ solubility in the mixture of MEA and H ₂ O is 3181.9 kPa.m ³ .kmol ⁻¹	(Li & Lai, 1995)

Table 2.2, Continued: CO₂ solubility in different solvents

Solvent	Temperature(°C)	Pressure(bar)	Result	Reference
30 mass% MDEA	30	1.013	The amount of CO ₂ solubility in the mixture of MDEA and H ₂ O is 3770.6 kPa.m ³ .kmol ⁻¹	(Li & Lai, 1995)
24(mass% MEA) + 6(mass% MDEA)	30	1.013	The amount of CO ₂ solubility in the mixture of MEA and MDEA and H ₂ O is 3269.0 kPa.m ³ .kmol ⁻¹	(Li & Lai, 1995)
6(mass% MEA) + 24(mass% MDEA)	30	1.013	The amount of CO ₂ solubility in the mixture of MEA and MDEA and H ₂ O is 3550.8 kPa.m ³ .kmol ⁻¹	(Li & Lai, 1995)
30 mass% MEA	40	1.013	The amount of CO ₂ solubility in the mixture of MEA and H ₂ O is 3646.6 kPa.m ³ .kmol ⁻¹	(Li & Lai, 1995)
30 mass% MDEA	40	1.013	The amount of CO ₂ solubility in the mixture of MDEA and H ₂ O is 4401.4 kPa.m ³ .kmol ⁻¹	(Li & Lai, 1995)
24(mass% MEA) + 6(mass% MDEA)	40	1.013	The amount of CO ₂ solubility in the mixture of MEA and MDEA and H ₂ O is 3753.2 kPa.m ³ .kmol ⁻¹	(Li & Lai, 1995)
6(mass% MEA) + 24(mass% MDEA)	40	1.013	The amount of CO ₂ solubility in the mixture of MEA and MDEA and H ₂ O is 4221.3 kPa.m ³ .kmol ⁻¹	(Li & Lai, 1995)

Table 2.2, Continued: CO₂ solubility in different solvents

Solvent	Temperature(°C)	Pressure(bar)	Result	Reference
60 mass% DGA	50	59.8	The amount of CO ₂ solubility in the mixture of DGA and H ₂ O is 0.798 (mole ratio in liquid, CO ₂ /DGA)	(Martin et al, 1978)
60 mass% DGA	100	58.4	The amount of CO ₂ solubility in the mixture of DGA and H ₂ O is 0.619 (mole ratio in liquid, CO ₂ /DGA)	(Martin et al., 1978)
3 kmol.m ⁻³ DEA	39.85	1.013	The amount of CO ₂ solubility in the mixture of DEA and H ₂ O is 5465 kPa.m ³ .kmol ⁻¹	(Mandal et al., 2004)
3 kmol.m ⁻³ AMP	39.85	1.013	The amount of CO ₂ solubility in the mixture of AMP and H ₂ O is 4693 kPa.m ³ .kmol ⁻¹	(Mandal et al., 2004)
3 kmol.m ⁻³ MDEA	39.85	1.013	The amount of CO ₂ solubility in the mixture of MDEA and H ₂ O is 4371 kPa.m ³ .kmol ⁻¹	(Mandal et al., 2004)
27(mass% MDEA) + 3(mass% DEA)	39.85	1.013	The amount of CO ₂ solubility in the mixture of MDEA and DEA and H ₂ O is 4406 kPa.m ³ .kmol ⁻¹	(Mandal et al., 2004)

Table 2.2, Continued: CO₂ solubility in different solvents

Solvent	Temperature(°C)	Pressure(bar)	Result	Reference
24(mass% MEA) + 6(mass% AMP)	40	1.013	The amount of CO ₂ solubility in the mixture of MEA and AMP and H ₂ O is 3943.8 kPa.m ³ .kmol ⁻¹	(Li & Lai, 1995)
6(mass% MEA) + 24(mass% AMP)	40	1.013	The amount of CO ₂ solubility in the mixture of MEA and AMP and H ₂ O is 5081.7 kPa.m ³ .kmol ⁻¹	(Li & Lai, 1995)
27(mass% AMP) + 3(mass% DEA)	39.85	1.013	The amount of CO ₂ solubility in the mixture of AMP and DEA and H ₂ O is 5109 kPa.m ³ .kmol ⁻¹	(Mandal et al., 2004)

2.9 Comparison of different solvents based on solubility

Low-cost and nontoxic solvents with low vapor pressure, which have thermal stability, good solubility of CO₂, and selectivity over N₂, are a very important consideration in CO₂ removal from flue gas. Amine solvents are used in many industries for the treatment of acid gases, such as CO₂, H₂S, and sulfur dioxide (SO₂). The absorption of CO₂ by amine solvents happens through chemical reactions and the formation of carbamate (Palmeri et al., 2008). Although amines have suitable CO₂ solubility, they are very corrosive and have low thermal stability. Consequently, amines cannot be reused efficiently, and the stripping process becomes difficult at larger scales. Moreover, a high heat of decomposition with CO₂ will occur in amine processes. Therefore, all these disadvantages make amine processes highly energy demanding (Sistla et al., 2012). Despite all these drawbacks, amine-based absorption, especially the MEA process, is commonly used in postcombustion carbon capture (Zaman & Lee, 2013).

ILs have high CO₂ selectivity over N₂ but, at present, they are too expensive for use in industrial plants. ILs are more expensive than glycerol, but the properties of Glycerol and ILs are similar (Wolfson et al., 2007). It should be noted that the best solvent according to Table 2.2 is polyethylene glycol (PEG) 300 due to its high CO₂ solubility and good selectivity over N₂. Other advantages of this solvent are its high stability, low solvent loss, and low desorption energy.

2.10 Different solvents for CO₂ capture

The chemical and physical properties, as well as the biological nature, of a solvent also play a key role in environmental, economic, safety, and handling matters as well as product isolation (Wolfson et al., 2007). Some parameters, such as lasting stability, low vapor pressure, and excellent thermal stability, are required to prevent the loss of solvent. Furthermore, the cost and environmental impact of a solvent depends on the amount of evaporation and chemical degradation (Aschenbrenner & Styring, 2010).

2.10.1 CO₂ capture using ILs

ILs as organic salts make stable liquids below 100°C, even at room temperature. ILs are capable of achieving high rates of CO₂ capture, because they have several potential advantages compared to other solvents, such as MEA, including having significant thermal stability and only a slight volatility, thus avoiding the loss of absorbents (Liu et al., 2012). ILs can be organized into groups of room-temperature ILs (RTILs), task-specific ILs (TSILs), and supported IL membranes (SILMs) (Hasib-ur-Rahman et al., 2010).

RTILs are composed of organic cations and organic or inorganic anions (Xue et al., 2011). TSILs such as [Amim] [BF₄] and [Amim][DCA] at low pressures (≤ 1 bar) operate similarly to chemical solvents, but at higher pressures their performance is the same as RTILs, such as 1-butyl-3-methylimidazolium tetrafluoroborate ([bmim][BF₄]). Because RTILs are physical solvents, TSILs can absorb CO₂ up to threefold more than RTILs. The combination of SILMs and TSILs can be a superior option for CO₂ capture at elevated temperatures and pressures (Hasib-ur-Rahman et al., 2010).

TSILs are able to separate greater amounts of CO₂ compared to conventional ILs. This is mainly due to reactivity or chemical interactions between CO₂ and alkaline groups (Sairi et al., 2011). The reaction between CO₂ gas and IL can be explained as:



In equation 2.4, P is the product, and the equilibrium transfer of CO₂ gas into the liquid phase is defined by equation 2.3. The reaction rate for equation 2.4 is determined as:

$$r_{\text{CO}_2} = k_2 C_{\text{CO}_2} C_{\text{IL}} \quad (2.5)$$

In equation 2.5, K_2 (cm³/mols), C_{CO_2} (mol/cm), and C_{IL} (mol/cm) are defined as the second-order reaction rate constant, CO₂ concentration, and IL concentration, respectively (Gurkan et al., 2013). In CO₂ absorption by conventional ILs, CO₂ gas

occupies the free space between the ions. Furthermore, in physical absorption, high-pressure operating conditions are necessary, and the absorption capacity is small (Huang & Rüther, 2009). Because ILs can selectively eliminate CO₂ from gaseous flows, researchers have suggested ILs as the basis of more supportable CO₂ capture processes (Pinto et al., 2013).

In summary, the properties of ILs can be adjusted by (1) various mixtures of the anions and the cations and (2) functionalizing the anions and the cations (Xue et al., 2011).

2.10.2 Physical solvents

The physical absorption of acid gases (CO₂+H₂S) is efficient when the acid gases have high partial pressure. Physical absorption has been used commercially for the separation of acid gas from natural gas and CO₂ from syngas (flue gas) in the production of H₂, NH₃, and methanol, but it has not been used in integrated gasification combined-cycle power plants (Zaman & Lee, 2013). Physical absorption is not economical for flue gas streams with CO₂ partial pressures less than 15 vol% because the flue gas pressurization has an important role in the energy requirements of CO₂ absorption process (Wang et al., 2011).

Organic solvents are used as physical solvents for absorbing the acid gas components physically. CO₂ removal through physical absorption depends on the solubility of CO₂ in the solvents (Olajire, 2010). Because there is no stoichiometric limitation for a physical solvent, the absorption capacity of a physical solvent can be more than that of a chemical solvent (Hermann et al., 2005). Therefore, the rate of circulation for a physical solvent may be lower, particularly with a high acid gas partial pressure. Low temperature and high pressure are desirable for absorption in a physical solvent. Because physical solvents demonstrate their best capacity at low temperatures, the cooling of the syngas is essential before CO₂ capture, which is the most important problem with physical solvents (Zaman & Lee, 2013).

2.10.2.1 ILs as physical solvents

RTILs include an organic cation, such as an imidazolium or pyridinium ring with or without substituents, and an organic or inorganic anion, for example, $[\text{BF}_4]$ or bis(trifluoromethylsulfonyl)imide ($[\text{Tf}_2\text{N}]$) (Hasib-ur-Rahman et al., 2010; Xue et al., 2011). Most of the ILs that have been studied with CO_2 physical absorption are imidazolium-based cations, but pyridinium-based ILs are cheaper and more biodegradable, and low pressure levels appear to make them suitable for CO_2 absorption (Docherty et al., 2006).

A study on 1-butyl-3-methylimidazolium hexafluorophosphate ($[\text{bmim}][\text{PF}_6]$) as a solvent showed that CO_2 was extremely soluble in this IL, reaching a mole fraction of 0.6 at 8 MPa (Blanchard et al., 1999; Feng et al., 2010). 1-Ethylpyridiniummethylsulfate ($[\text{C}_2\text{py}][\text{EtSO}_4]$) as an IL is capable of absorbing CO_2 physically at 298.2 K and up to a molar fraction of approximately 0.10 at approximately 1.6 MPa. The combination of 1-ethyl-3-methylimidazolium bis(trifluoromethanesulfonyl)imide $[\text{C}_2\text{mim}][\text{NTf}_2]$ and $[\text{C}_2\text{py}][\text{EtSO}_4]$ has a considerable effect on CO_2 absorption. The absorption capacity of this mixture is higher than the averaged capacities of the pure ILs. However, none of the mixtures of intermediate composition has a higher CO_2 absorption capacity than pure $[\text{C}_2\text{mim}][\text{NTf}_2]$. On the contrary, the combination of $[\text{C}_2\text{mim}][\text{NTf}_2]$ and $[\text{C}_2\text{py}][\text{EtSO}_4]$ in various proportions brings other beneficial enhancements to the absorbing solvent in the form of better-balanced properties (Pinto et al., 2013).

Li et al. (2008) investigated a (2-hydroxyethyl)-trimethylammonium (S)-2-pyrrolidine-carboxylic acid salt ($[\text{Choline}][\text{Pro}]$) and a mixture of $[\text{Choline}][\text{Pro}]/\text{PEG 200}$ for the purpose of CO_2 capture. Their results indicated that the molar ratio of CO_2 to IL was somewhat more than 0.5. Adding PEG 200 to the IL considerably increased the CO_2 absorption, and the molar ratio of CO_2 to IL reached 0.6 (Li et al., 2008).

2.10.2.2 Glycerol as a physical solvent

Glycerol is a biodegradable, nontoxic, and recyclable liquid that shows properties similar to IL, and, as a potential green solvent, can be used in organic syntheses (Wolfson et al., 2007). Kovvali and Sirkar (2002) indicated the low selectivity of CO₂ over N₂ for glycerol, whereas glycerol carbonate has a higher selectivity and is also stable, nonvolatile, and nontoxic (Aschenbrenner & Styring, 2010).

Wolfson et al. (2006) compared the properties of glycerol with water, 1-butyl-1-methylimidazolium hexafluorophosphate ([Bmim][PF₆]), and perfluorohexane (C₆H₁₄), which are IL and fluoruous solvents. They reported that, except for glycerol and water, which are renewable and biodegradable, the other solvents were recyclable. From an environmental point of view, the low vapor pressure of glycerol and [Bmim][PF₆] are considered to be advantages of these solvents. Furthermore, the toxicity of glycerol is less than that of the three organic solvents. In addition, inorganic and organic compounds can be dissolved in glycerol and [Bmim][PF₆] because these solvents are polar. Polar solvents can perform separation by simple extraction because they are immiscible in different hydrophobic solvents due to their polarity. The high viscosity of glycerol and [Bmim][PF₆] is a disadvantage; nevertheless, raising the temperature to more than 50°C decreases their viscosity (Wolfson et al., 2007).

Leo et al. (Leo et al., 2016) investigated density and viscosity of aqueous mixtures of glycerol and N-Methyldiethanolamine (MDEA), glycerol and MEA, glycerol and Piperazine (PZ) as well as glycerol and 1-butyl-3-methylimidazolium dicyanamide ([bmim][DCA]) in the temperature range from 313.15 to 353.15 K at atmospheric pressure. They reported a decreasing trend for both density and viscosity in all mixtures as the temperature increased but, at constant temperature both density and viscosity of the mixtures increased when the glycerol concentration was increased (Leo et al., 2016). The solubility of CO₂ in aqueous solutions 30 wt% MEA mixed with various glycerol

concentrations in pressures ranging from 500–1500 kPa and three various temperatures (313, 323, and 333 K) was studied by Shamiri et al. (Shamiri et al., 2016) They reported that the addition of 5 wt% and 10 wt% glycerol improved the CO₂ solubility of MEA at pressures below 1000 kPa whereas, the solubility of CO₂ reduced at high glycerol concentrations (15 wt% and 20 wt%) (Shamiri et al., 2016).

2.10.2.3 Other physical solvents

The dimethylether of PEG is in a liquid state and has been used as a solvent in the Selexol process for CO₂ and H₂S removal from natural gas (Davison et al., 2001). The best operational temperature for Selexol solvent is up to 175°C, with a minimum temperature of -18°C (Barry & Lili, 2008). In high concentrations, glycol is an effective solvent for CO₂ and H₂S removal (Olajire, 2010).

Glycol carbonate is attractive due to its high CO₂ selectivity; however, it has a relatively low capacity (Kovvali & Sirkar, 2002). Propylene carbonate (C₄H₆O; Fluor solvent) and N-methyl-2-pyrrolidone (NMP; Purisol solvent) are other types of physical solvent for CO₂ removal (Olajire, 2010; Zaman & Lee, 2013). At low temperatures, C₄H₆O possesses a good mass-transfer performance because it does not become too viscous. The operating temperature for this solvent is less than 65°C, with a minimum of -18°C (Barry & Lili, 2008). The NMP solvent is suitable for the selective removal of acid gases from syngas. The absorption operation can be conducted either at an ambient temperature or at a subambient temperature with refrigeration down to approximately -15°C. Selexol, Rectisol, and Purisol solvents are more selective for H₂S over CO₂ and for CO₂ over other components in comparison with the Fluor solvent (Zaman & Lee, 2013). Sulfinol and Amisol are also examples of mixed solvents. Sulfinol is a mixture of sulfolane (2,3,4,5-tetrahydrothiophene1,1-dioxide) as the physical solvent and amines, such as diisopropylamine (DIPA) or MDEA, as chemical solvents, whereas

Amisol is a mixture of methanol (physical solvent) and secondary amine (chemical solvent) (Olajire, 2010; Zaman & Lee, 2013).

ILs have been studied widely in CO₂ capture and can be selected as physical solvents, they are promising solvents, but they are expensive for application at an industrial scale, and it is better that they are replaced with other suitable solvents. Moreover, physical solvents are not suitable for post-combustion capture because physical absorption from flue gas with CO₂ partial pressures less than 15 vol% is not economical, and absorption capacity is low due to lower CO₂ selectivity compared to N₂. Therefore, the mixing of chemical promoters with physical solvents can be used to increase the CO₂ selectivity.

2.11 Chemical solvents

Aroonwilas et al. (2003) reported that chemical solvents are chosen mainly in the separation process, because at low CO₂ partial pressure they have a higher absorption capacity (Aroonwilas et al., 2003).

Several chemical solvents can be used to capture CO₂ by chemical absorption, such as amines, NH₃, and potassium carbonate (K₂CO₃). For the separation of CO₂ from a gas stream, there are several desirable properties for a commercial absorbent, such as high absorption capacity, high absorption rates for CO₂, high thermal and chemical stability, low regeneration energy requirements, low vapor pressure, low molecular weight, low viscosity, and low corrosion rates (Zaman & Lee, 2013).

In chemical absorption, the existing CO₂ in the gas flow reacts with a chemical solvent to produce several intermediate compounds. Consequently, CO₂ is removed from the exhaust flue gas. In general, in the CO₂ absorption process, the solvent solution containing the intermediate compounds is heated with low-pressure steam for recovery, and then the released CO₂ is captured, pressurized, transported, and then stored. In the next step, the recovered solvent, which contains small amounts of dissolved CO₂, is recycled back into the absorption process. The essential factors in using chemical

solvents for a high gas stream flow with low partial pressure of CO₂ are scale, efficiency, stability, and corrosion. A huge amount of solvent is needed, which undergoes significant changes to its condition, thus leading to high capital investments and energy costs (Mamun et al., 2005).

2.11.1 Amines as chemical solvents

MEA, DEA, and MDEA are conventional chemical absorbents (Seo et al., 2012). One efficient technique for CO₂ capture is using aqueous alkanolamine solutions or their mixtures. However, there are several drawbacks for usage of alkanolamines in industrial application: (1) corrosion caused by amine systems limits the amine concentration in the solution and creates additional cost; (2) amines are degraded at high temperatures, particularly in the regeneration process; (3) the presence of O₂ leads to the oxidative degradation of amines; and (4) the volatile nature of alkanolamine causes absorbent loss into the gas stream, and this leads to an increase in the process cost and environmental concerns (Feng et al., 2010).

Among different amine solvents, MDEA has higher thermal stability and CO₂ loading and lower regeneration cost and volatility. On the contrary, MDEA absorbs CO₂ slowly. Thus, in industrial applications, the MDEA aqueous solution is mixed with effective promoters that have fast reactivity, such as MEA, piperazine (PZ), and DEA (Feng et al., 2010).

2.11.2 Amines as promoters

CO₂ capture using the sodium salt of glycine (NaGly), MEA as a promoter for the potassium salt of dimethylglycine (KDiMGly), and PZ as an additive for KDiMGly compared with 30 wt% MEA was investigated by Weiland and Hatcher (2011). They also considered PZ-promoted MDEA in CO₂ capture. The results showed that both regeneration energy and solvent rates in the KDiMGly process with PZ as a promoter

were approximately 20% less than that in the MEA process in the same plant (Weiland & Hatcher, 2011). Kumar et al. (2003) reported that the reaction rate of NaGly (sodium glycinate) with CO₂ depended on its concentration being two to three times that of MEA. They also studied the kinetics of the reaction between CO₂ and the aqueous potassium salt of taurine (2-aminoethansulfonic acid) and glycine (aminoacetic acid) in a concentration range between 100 and 4000 mol/m³ and temperatures of 11.85°C–31.85°C (Kumar et al., 2003).

Weiland and Hatcher (2011) studied a mixture of 40 wt% potassium dimethyl glycinate (KDiMGly) with 5 wt% PZ as the solvent for the removal of CO₂. KDiMGly has a tertiary amino group that is unable to react with CO₂ and form the carbamate. Although KDiMGly may have a very high capacity for CO₂ absorption, the lack of chemical reaction rate indicates that CO₂ will not easily be absorbed into the solution; therefore, using MEA as a fast-reacting amine or using PZ can raise the CO₂ absorption. These researchers found that 85% CO₂ could be recovered with 82 or 83 MW reboiler duty. The purpose of MEA or PZ as a promoter does not alter the inherent capacity of the solvent, but it does improve the CO₂ absorption rate. According to their experiments, PZ reacted with CO₂ almost 10 times faster than with MEA. Furthermore, they used 5 wt% PZ for promoting 45 wt% MDEA. MDEA and KDiMGly have been classified as tertiary amines, so they do not generate carbamates, and their reaction with CO₂ rarely occurs (Weiland & Hatcher, 2011).

In a comparison between 2-amino-2-methyl-1-propanol (AMP) and MEA, according to the stoichiometry of AMP, each mole of CO₂ theoretically reacts with 1 mole of amine. The reaction of each mole hindered amine (AMP) with only 1.5 mole CO₂ is one of the superior characteristics of AMP over MEA (Aroonwilas & Tontiwachwuthikul, 1997). On the contrary, the absorption rate for AMP is lower than MEA and this is one of the limitations of using AMP (Alper, 1990).

2.11.3 Mixed amines

Xiao et al. (2000) reported that a mixture of AMP and MEA possessed high CO₂ absorption capacity, good selectivity, high CO₂ absorption rates, and increased resistance to corrosion and degradation in comparison to conventional amines (Xiao et al., 2000).

Idem et al. (2006) reported a considerable drop in energy needs and a moderate decrease in circulation rates for amine combinations compared to systems with a single amine as solvent with the same total amine concentration. They performed an experiment using 5 kmol/m³ aqueous MEA with a 4:1 molar ratio and MEA/MDEA with 5 kmol/m³ total amine concentration and then compared these two systems. Their results showed that, in a CO₂ capture plant, the heat duty for the MEA/MDEA solution was much less than that for the single MEA solution, so it is more economical to use the MEA/MDEA system. However, this benefit is only acceptable when the solvent chemical stability can be preserved (Idem et al., 2006).

2.11.4 PZ as a chemical solvent

PZ has approximately twice the absorption capacity for CO₂, twice the absorption rate, and approximately 15% lower energy requirements than MEA. Thus, PZ is commonly used as a blend with other amines. The mixtures of MDEA+PZ have been found to produce some of the highest absorption rates and to have more than 15% lower energy requirements. Of all the amines and blends of amines, MDEA+PZ appears to possess the best properties. AMP has more than twice the CO₂ absorption capacity, approximately 44% slower absorption rate, and approximately 10% lower energy requirements for solvent regeneration (Zaman & Lee, 2013).

Concentrated aqueous solutions of PZ are promising solvents in the absorption/stripping process for CO₂ capture. Researchers have reported that, for 8 m PZ, preserved as a liquid solution without precipitation, a CO₂ loading of approximately 0.25 mol CO₂/mol

alkalinity is required at 20°C. Moreover, the solubility of PZ at 20°C is approximately 14 wt% PZ or 1.9 m PZ. Mass-transfer measurements have shown that the CO₂ absorption rate in 8 m PZ is 1.5–3 times that of 7 m MEA. The operating capacity of 8 m PZ is double that of 7 m MEA at 0.90 mol CO₂/kg PZ+H₂O compared to 0.43 mol CO₂/kg MEA+H₂O.

The amount of work for stripping 8 m PZ solution is approximately 10–20% lower than that for 7 m MEA. The rapid CO₂ absorption rate, low degradation rate, and low predicted equivalent work show that 8 m PZ solutions are a desirable option for CO₂ capture in absorption/stripping systems (Freeman et al., 2010). PZ has been studied at the University of Texas, and the results showed that it has faster kinetics, lower thermal degradation, and lower regeneration energy requirements compared to MEA (Rubin et al., 2012).

2.11.5 Carbonate-based systems

2.11.5.1 CO₂ capture with K₂CO₃

The base of carbonate systems is the capability of a soluble carbonate for reacting with CO₂ and forming the bicarbonate. When the bicarbonate is heated, the CO₂ gas is released and it changes to a carbonate. One of the greatest advantages of the carbonate system compared to the amine system is the lower energy consumption in the regeneration stage. MEA has a higher loading capacity of 40% against 30%, and the energy requirement is almost 5% lower than carbonate system (Figuerola et al., 2008).

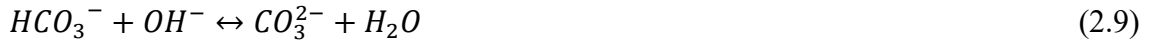
On the contrary, the reaction between CO₂ and K₂CO₃ solution is not fast, which causes a gradual mass transfer in the liquid phase (Savage et al., 1984). Thus, to increase the CO₂ reaction, promoters can be used (Kohl & Nielsen, 1997). The production of K₂CO₃ precipitation and gathering of crystals in unit operations causes important problems (Fosbøl et al., 2013). In contrast, the UNO MK 3 process is a K₂CO₃-precipitating process that has advantages compared to amine-based solvents, such as lower cost of

CO₂ absorption and environmental fewer effects; less regeneration energy requirement; smaller regeneration cycle and column due to lower solvent flow; less corrosion and volatility and low toxicity; the removal of CO₂, SO₂, and NO_x; and the separation of K₂SO₄ and KNO₃ as fertilizer by products (Anderson et al., 2013).

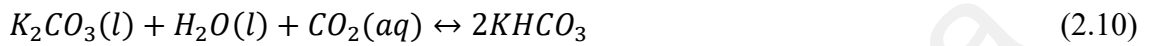
Rubin et al. (2012) investigated CO₂ capture from flue gas using K₂CO₃ solvent. They reported that K₂CO₃ absorbs CO₂ using a low-energy reaction with slow kinetics. The speed of absorption can be increased by mixing K₂CO₃ with different amines (Rubin et al., 2012). Other potential rate promoters include PEG (Park et al., 1997), inorganic acids (Endo et al., 2011; Thee et al., 2012), enzymes such as carbonic anhydrase (Elk et al., 2013; Zhang et al., 2013), amino acids such as glycine, sarcosine, and proline (Thee et al., 2014), and boric acid (Smith et al., 2012). Furthermore, Smith et al. (2015) studied the glycine-promoted precipitating K₂CO₃ solvent in the CO₂ absorption process.

The University of Texas at Austin developed a system using K₂CO₃ with PZ as a promoter. In a K₂CO₃/PZ system comprising 5 molar K₂CO₃ and 2.5 molar PZ, the rate of CO₂ absorption was 10–30% faster than a 30% solution of MEA and had desirable equilibrium characteristics. However, PZ is more expensive than MEA, and the solubility of O₂ in K⁺/PZ solvents is not as good; thus, both PZ and MEA have the same economic impact due to oxidative degradation (Figueroa et al., 2008). Jassim and Rochelle (2006) studied aqueous solvents containing alkanolamines and hot K₂CO₃ solutions for CO₂ absorption from flue gas. Compared to alkanolamines, K₂CO₃ has less toxicity, less degradation of solvent and lower heat requirements for regeneration (Cullinane & Rochelle, 2004; Savage et al., 1980).

The reaction chemistry for aqueous K₂CO₃ solution and CO₂ is shown in the equilibrium reactions 2.6-2.9 (Bohloul et al., 2014):



The reaction of the carbonate formation is prompt; thus, the reaction 2.10 shows the overall reaction between the aqueous K_2CO_3 and CO_2 (Bohloul et al., 2014):



(a) Using promoters in the K_2CO_3 system

Low CO_2 absorption efficiency is the main disadvantage of the K_2CO_3 system. The performance of this process increases through the addition of promoters to the K_2CO_3 solvent or by increasing the packed-column efficiency (Zhao et al., 2011). For a mixture of 0.6 molal PZ and 20 wt% K_2CO_3 as an additive for CO_2 capture, the equilibrium partial pressure was reduced by approximately 85% and the CO_2 absorption rate improved by an order of magnitude (Cullinane & Rochelle, 2004; Kothandaraman, 2010; Smith et al., 2012). The reactions with equilibrium constants for CO_2 absorption in PZ-promoted K_2CO_3 were mentioned by Cullinane and Rochelle (2004). Thee et al. (2012) discovered that the addition of MEA in small quantities boosted the overall CO_2 absorption rate in a K_2CO_3 system by more than one order of magnitude (Thee et al., 2012).

PZ- K_2CO_3 was studied by Cullinane and Rochelle (2005) as a solvent for CO_2 capture, and they reported that K_2CO_3 in solution with PZ exhibited a fast absorption rate comparable to 30 wt% MEA. The absorption heat was lower than in aqueous amine systems, and the temperature for absorption was $25^\circ C$ – $70^\circ C$ (Cullinane & Rochelle, 2005). In comparison with the MEA process, this process required 29–33% less regeneration energy (Davidson, 2007).

2.11.5.2 CO₂ capture with sodium carbonate

Knuutila et al. (2009) used sodium carbonate (Na₂CO₃) as an environment-friendly absorbent for CO₂ capture. Na₂CO₃ absorbs CO₂ and forms sodium bicarbonate (NaHCO₃), but the low solubility of NaHCO₃ limits the total concentration of carbonate. Thus, this low solubility is a drawback for the Na₂CO₃-based liquid systems. In this experiment, CO₂ was captured by the formation of solid bicarbonate, and the formation of slurry increased the capacity of the solvent. One important advantage of this system is that the energy requirement for the regeneration of the solvent is considerably lower than that of the MEA systems (Knuutila et al., 2009).

Reaction 2.11 is the overall reaction for the process that happens in the absorber:



This overall reaction includes reactions 2.12–2.15:



When the concentration of bicarbonate in the liquid phase increases, reaction 2.16 occurs (Knuutila et al., 2009).



K₂CO₃ provides a better rate of absorption than Na₂CO₃ at the same normality. The amount of CO₂ absorption for 2.5 N sodium solutions at 30°C is up to 0.0807 m³ (under standard conditions)/gallon from a flue gas comprising 17% CO₂, but 2.5 N potassium solution will absorb 0.0926 m³. Besides, due to the superior solubility of the potassium salts, the potassium solution is stronger for use in CO₂ capture (Comstock & Dodge, 1937).

2.11.6 Enzyme-based systems

Researchers also studied CO₂ capture using carbonic anhydrase in a hollow fiber-controlled liquid membrane and regeneration at ambient conditions. They reported 90% CO₂ capture at the laboratory scale. Enzyme-based systems absorb and discharge CO₂ similar to mammalian respiratory mechanism. Regeneration under ambient conditions for the carbonic anhydrase system can be an advantage of this process compared to the MEA temperature swing process. Another advantage is a low absorption heat that can decrease the energy penalty for the absorption system (Figuerola et al., 2008).

2.11.7 ILs as chemical solvents

A dual amino-functionalized IL with 1-aminoethyl-2,3-dimethylimidazolium cation and amino acid taurine anion ([aemmim][Tau]) was synthesized by Xue et al. (2011). In this study, the absorption isotherm of CO₂ into [aemmim][Tau] was examined at 303.15 and 323.15 K, and the absorption capacity of CO₂ into [aemmim][Tau] reached 0.9 mol CO₂/mol [aemmim][Tau] at 303.15 K and approximately 1 bar. Absorbed CO₂ can be easily desorbed at higher temperatures or under vacuum; thus, [aemmim][Tau] can be regenerated. These results were reported for a pressure range between 0.2 and 1.0 bar, and they reported that absorption is a chemical process (Xue et al., 2011).

CO₂ capture using dual amino-functionalized phosphonium ILs with amino acid anions was investigated by Zhang et al. (2009), and they reported that the chemical absorption of CO₂ reaches approximately 1 mol of CO₂/mol IL. Zhang et al. (2006) studied a new type of TSIL. They synthesized a tetrabutylphosphonium amino acid by the reaction of tetrabutylphosphonium hydroxide with amino acids (glycine, L-alanine, L-β-alanine, L-serine, and L-lysine). The equilibrium CO₂ absorption capacity was reported 50 mol% of the ILs, and the same amounts of CO₂ absorption were informed for the ILs in the attendance of 1 wt% water (Zhang et al., 2006).

Reversible ILs are a new group of solvents that Georgia Tech Research Corporation is developing. These solvents chemically react with CO₂ to make other ILs that further absorb CO₂ (Rubin et al., 2012).

CO₂ capture in a combination of 4.0 mol/L aqueous MDEA and three types of imidazolium-based ILs, [bmim][BF₄], 1-butyl-3-methylimidazolium acetate ([bmim][Ac]), and 1-butyl-3-methylimidazolium dicyanamide ([bmim][DCA]), with temperatures ranging from 303 to 333 K and CO₂ partial pressure between 100 and 700 kPa, was studied by Ahmady et al. (2011). The influence of ILs on CO₂ loading in aqueous MDEA was defined for a range of 0 to 2 mol/L IL. CO₂ loading in all IL+MDEA mixtures was enhanced with rising partial pressure of CO₂ and dropped with increasing temperature. In addition, all examined ILs decreased the CO₂ loading in aqueous MDEA. They also reported that [bmim][BF₄] has better CO₂ loading in aqueous MDEA than [bmim][Ac] and [bmim][DCA], especially at high CO₂ partial pressure and low temperature (Ahmady et al., 2011).

Zhao et al. (2011) studied the performance of CO₂ capture with a mixture of amines+ILs+H₂O solvents. The volume flows of N₂ and CO₂ were 300 and 100 ml/min, respectively. The capture time was 500 min. The CO₂ absorption ability was investigated at 1.50 MPa and 30°C, and it was found that the 2-[2-hydroxyethyl(methyl)amino] ethanol+2-[2-hydroxyethyl(methyl)amino] ethanol chloride+H₂O+PZ (MCHP) was the best solvent among those investigated (Zhao et al., 2011).

Gurkan et al. (2013) studied the reaction between CO₂ and trihexyl (tetradecyl)phosphonium ([P66614])-based ILs with proline ([Pro]), 2-cyanopyrrolide ([2-CNpyr]), and 3-(trifluoromethyl)pyrazolide ([3-CF₃pyra]) anions. The reaction of [P66614][Pro] with CO₂ was very fast compared to the other two mixtures. They also reported that [Pro]- and [2-CNpyr]-based ILs had higher reaction rates with CO₂ than aqueous amines, such as MEA, whereas [3-CF₃pyra] was similar to MEA. These

reactions took place almost directly at temperatures of more than 50°C. They concluded that ILs can serve as independent solvents and can also be used as activators for aqueous amines or other ILs (Gurkan et al., 2013).

2.11.8 NH₃-based systems

The CO₂ absorption capacity for NH₃ is comparatively high in comparison with most solvents based on its low molecular weight. NH₃ is commercially accessible and is fairly cheap. Moreover, CO₂ absorption based on NH₃ has a low heat of reaction; therefore, the regeneration energy requirements are low, and the corrosion of NH₃ is less than that of MEA (Wang et al., 2011).

The lack of degradation during absorption/regeneration and the potential for regeneration at high pressure are advantages of NH₃-based absorption over amine based systems (Figueroa et al., 2008). The removal of SO_x, NO_x, and mercury from flue gas along with CO₂ capture is another advantage of the NH₃ process compared to conventional amines. Nevertheless, the vapor pressure of NH₃ is much higher, leading to significant solvent losses (Zaman & Lee, 2013). Therefore, Seo et al. (2012) studied the decrease of NH₃ evaporation.

NH₃ liquor (9 wt%) was used by Seo et al. (2012) with various additives, such as ethylene glycol, glycerol, and glycine, to discover its kinetic properties using the blast furnace gas model. High NH₃ concentration can increase the CO₂ absorption efficiency. By evaporating NH₃, the ammonium ions are lost, and this leads to reduced CO₂ absorption because of the lower concentration of the NH₃ solvent. To decrease the NH₃ evaporation, ethylene glycol, glycerol, and glycine, which contain more than one hydroxyl radical, were selected. The most effective additive for reduction in vaporization was glycerol (Seo et al., 2012).

It is very important to remove acid gases, such as SO₂ and NO₂, from flue gas. Concentrations of SO₂ lower than 10 ppm are suggested because these acid gases can

create heat-stable salts with solvents such as MEA and can influence the system functioning (Wang et al., 2011). In the ammonium absorption process, aqueous NH_3 is used as a solvent to absorb the CO_2 ; in fact, this system can control the multicomponents by absorption (Yang et al., 2008). Thus, the MEA process can be substituted with an aqueous NH_3 process to capture all of the SO_2 , NO_x , and CO_2 as well as the HCl and HF that might be in the flue gas. In comparison with the MEA system, the aqueous NH_3 process does not have the problems of the MEA process (Resnik et al., 2004; Yeh et al., 2005), such as degradation problems of SO_2 and O_2 that exist in flue gas (Olajire, 2010). The researchers estimated that the ammonium absorption process saves energy by approximately 60% compared to the MEA process (Yang et al., 2008).

Since the NH_3 process has superior volatility compared to the amine solvents, the chilled NH_3 process (CAP) is used for CO_2 absorption in low temperatures to reduce solvent losses (Wang et al., 2011). Puxty et al. (2010) also reported that, because of the low molecular weight of NH_3 and its high vapor pressure, a low temperature is necessary for the absorption process to reduce NH_3 losses. Darde et al. (2009) investigated the CAP in which the temperature for absorption and desorption were 0–20°C and 100°C–200°C, respectively, and a CO_2 loading between 0.25 and 0.67 mol CO_2 /mol NH_3 and water was reported. The absorption heat of CO_2 by NH_3 was considerably lower than that with amines (Darde et al., 2009).

Most of the research on applying NH_3 in CO_2 capture has been reported by Bai and Yeh (1997) and Yeh and Bai (1999). Under the same test conditions, it was found that the maximum absorption of CO_2 reached 99%, and the CO_2 removal efficiency by NH_3 loading capacity was reported to be 1.20 g CO_2 /g NH_3 . In contrast, the maximum CO_2 absorption performance and the amount of loading capacity by MEA solvent were 94% and 0.409 g CO_2 /g MEA, respectively. In a comparison between the aqueous NH_3

system and the MEA system, the aqueous NH_3 solvent had a high loading capacity. Because this system has a low cost, it can be predicted that the solvent makeup rate and the energy consumption for solvent regeneration are significantly lower than for the MEA process (Olajire, 2010).

Huang et al. (2001) investigated a modified Solvay dual-alkali approach (Huang et al., 2001). The Solvay process uses the dual-alkali approach with NH_3 as the primary alkali. In this process, NH_3 is used as a catalyst for the reaction of CO_2 with sodium chloride for Na_2CO_3 production. Using calcination of limestone, for every 2 moles of CO_2 captured, 1 mole of CO_2 is released. The CO_2 absorption capacity for methylaminoethanol (MAE) is 0.75 mol CO_2 /mol MAE, which is greater than the absorption capacity of MEA solvent (0.5 mol CO_2 /mol MEA). In a reaction between amine and CO_2 , if the reaction product is carbamate, the maximum CO_2 absorption capacity for amine is 0.5 mol CO_2 /mol amine, but if the reaction product is bicarbonate this amount changes to 1.0 (Yang et al., 2008).

Zaman and Lee (2013) investigated CO_2 absorption in NH_3 carbonate at close to 20°C in a process called the Alstom NH_3 process. They reported that low temperature is desirable for this system because it prevents NH_3 loss. The energy requirement for the regeneration of this solvent is considerably lower than that of the conventional MEA process, and this contributes to a lower overall cost of process (Zaman & Lee, 2013).

2.11.8.1 Comparison of NH_3 and MEA systems

Generally, there are several concerns regarding both NH_3 and amine systems: (1) The decomposition of ammonium bicarbonate at 60°C and thus temperatures lower than 60°C are necessary for the absorber. (2) In comparison with MEA, NH_3 has more volatility, which causes NH_3 loss along exit gas (3) NH_3 can be lost through the formation of heat-stable salts, such as ammonium sulfates and nitrates, and by the absorption of HCl and HF . Furthermore, for amine systems: (1) The energy

requirements for CO₂ scrubbing are considerable. (2) The presence of O₂ causes solvent degradation and equipment corrosion. (3) The combination of SO_x and NO_x with amines, and the formation of heat-stable salts, which are nonregenerable. On the contrary, up to 95% of amine scrubbing solvents can be recovered, and the purity of the product can be more than 99 vol%. In contrast, the advantages of the NH₃ process are lower heat of reaction and greater CO₂ transfer capacity than the MEA process (Olajire, 2010).

Puxty et al. (2010) also reported that, for same amounts of CO₂ removal from gas stream based aqueous NH₃ process and MEA process, aqueous NH₃ needs a larger absorber column to provide a higher gas-liquid contact area compared to the MEA process (Puxty et al., 2010). The performance for several chemical solvents is presented in Table 2.3.

The selection of solvent for CO₂ absorption from flue gas plays an important role in many aspects, such as environmental, safety, and economic factors. The key criteria in choosing the solvent are high CO₂ solubility and high CO₂ selectivity over N₂. Moreover, the low energy required for CO₂ desorption is another significant point.

The widely used solvents for CO₂ separation are amines, which can be selected as activators. Amines have selectivity for CO₂ compared to N₂ and they form carbamates by reacting with CO₂, which results in an increase in the absorption capacity. According to Table 2.3 and a comparison between different solvents, PZ can be used in a mixture with other amines to improve the CO₂ capture. The mixture of MDEA+PZ appears to have the most outstanding properties of all the amines and blends of amines. Moreover, aqueous NH₃ seems to have the maximum absorption rate among all the solvents, fairly rapid kinetics, and a considerable reduction in the energy penalty. However, NH₃ vapour pressure is high and a large capital cost might be needed for the reduction of NH₃ losses. The reaction rate of NaGly with CO₂ is two- to threefold that of MEA, so

NaGly can be a good promoter in CO₂ absorption. KDiMGly has been classified as a member of the tertiary amines group and has shown good results in CO₂ absorption with PZ as the additive.

University of Malaya

Table 2.3: A comparison between different chemical solvents

Solvent	Concentration	Absorption capacity(mol CO ₂ /kg amine+water)	Absorption rates(mol/s Pa m ²)	Temperature (°C)	P _{CO₂} (kpa)	Lean loading(mol CO ₂ /mol solvent)	Reaction enthalpy (KJ/mol CO ₂)	Advantage	Disadvantage	Reference
Diisopropylamine (DIPA)	0.58M ¹	0.61(mol CO ₂ /mol amine)	7.63E-3(1/min)	30	10	0.18	-	It is a good solvent for use in the Sulfinol process (Olajire, 2010; Zaman & Lee, 2013)	The rate constant K ₂ (m ³ /mol sec) for DIPA is less than MEA and DEA at the same temperature and concentration	(Singh et al., 2009)
Diisopropylamine (DIPA)	2.81M	0.42(mol CO ₂ /mol amine)	4.45E-3(1/min)	30	10	0.19	-	Cyclic loading (mol CO ₂ /mol amine) is 0.22 while this parameter for 0.58 mol/L is 0.43	Lean loading (mol CO ₂ /mol amine) is 0.19 while this parameter for 0.58 mol/L is 0.18	(Singh et al., 2009)

¹ Mole/L

Table 2.3, Continued: A comparison between different chemical solvents

Solvent	Concentration	Absorption capacity(mol CO ₂ /kg amine+water)	Absorption rates(mol/s Pa m ²)	Temperature (°C)	P _{CO₂} (kpa)	Lean loading(mol CO ₂ /mol solvent)	Reaction enthalpy (KJ/mol CO ₂)	Advantage	Disadvantage	Reference
MEA	7m ²	0.47	4.3 E-7	40	1.5	0.45	82	Doubles the required packing area	Only 50% as fast as 8 m PZ	(Chen & Rochelle, 2011)
MEA/PZ	(1-5)M/(0-1.2)M(Dang & Rochelle, 2001)	Higher than MEA(Zaman & Lee, 2013)	Up to 2.5 times higher than MEA(Dang & Rochelle, 2001)	40 and 60(Dang & Rochelle, 2001)	0.0002-9.55(Dang & Rochelle, 2001)	-	lower than MEA(Dang & Rochelle, 2001)	PZ has approximately twice the absorption capacity for CO ₂ , twice the absorption rate, and around 15% less energy requirements in comparison to MEA. Thus, PZ can be used as a blend with MEA (Zaman & Lee, 2013)	The absorption rate is less than MDEA+PZ and energy requirement is more than MEDA+PZ (Zaman & Lee, 2013)	(Dang & Rochelle, 2001; Zaman & Lee, 2013)

² molality

Table 2.3, Continued: A comparison between different chemical solvents

Solvent	Concentration	Absorption capacity(mol CO ₂ /kg amine+water)	Absorption rates(mol/s Pa m ²)	Temperature (°C)	P _{CO₂} (kpa)	Lean loading(mol CO ₂ /mol solvent)	Reaction enthalpy (KJ/mol CO ₂)	Advantage	Disadvantage	Reference
DEA	3.25M	0.7	Slow kinetics	40	atmospheric	-	76.3	The higher cyclic capacity of DEA for desorption compared to MEA (Galindo et al., 2012) and DEA has a high absorption capacity of 0.7–1 mol CO ₂ /mol DEA within the purification of high-pressure natural gas (Kohl & Nielsen, 1997)	The kinetic for DEA is slower than MEA	(Galindo et al., 2012)
DGA	10m	0.38(10 to 20% less than MEA)	3.6E-7	40	1.5	0.41	81	Since the reaction heat in carbamate production is higher, the heat of CO ₂ absorption for DGA is greater than PZ, PZ/MDEA and AMP	CO ₂ capacity is 10-20% lower than 7 m MEA with 5-15% slower rate	(Chen & Rochelle, 2011)

Table 2.3, Continued: A comparison between different chemical solvents

Solvent	Concentration	Absorption capacity(mol CO ₂ /kg amine+water)	Absorption rates(mol/s Pa m ²)	Temperature (°C)	P _{CO₂} (kpa)	Lean loading(mol CO ₂ /mol solvent)	Reaction enthalpy (KJ/mol CO ₂)	Advantage	Disadvantage	Reference
MEA/MD EA	03/27, 05/25, 07/23 wt%	higher than MEA	Acceptable rates	24.85 -59.85	-	-	Lower than MEA	Heat duty of the MEA/MDEA solution is much less than the MEA solution (Idem et al., 2006)	MEA reacts very quickly with CO ₂ but MEA/MDEA is a slow-reacting mixed-amine system (Aboudheir et al., 2003)	(Ramachandr an et al., 2006)
MDEA/PZ	5m/5m	0.99	8.3E-7	40	1.5	0.21	70	Capacity is 20% better than 8 m PZ and the rate is comparable. 5 m/5 m MDEA/PZ has a rate faster than 7 m/2 m at all temperatures	The heat of CO ₂ absorption for MDEA/PZ is less than all of the primary amines, MEA, DGA, and MAPA	(Chen & Rochelle, 2011)

Table 2.3, Continued: A comparison between different chemical solvents

Solvent	Concentration	Absorption capacity(mol CO ₂ /kg amine+water)	Absorption rates(mol/s Pa m ²)	Temperature(°C)	P_{CO_2} (kpa)	Lean loading(mol CO ₂ /mol solvent)	Reaction enthalpy (KJ/mol CO ₂)	Advantage	Disadvantage	Reference
MDEA/PZ	7m/2m	0.80	6.9E-7	40	1.5	0.13	68	The CO ₂ capacity is similar to 8 m PZ	The CO ₂ absorption rate for MDEA/PZ is 15% slower than 8 m PZ	(Chen & Rochelle, 2011)
PZ	8m	0.79	8.5E-7	40	1.5	0.31	70	PZ increases CO ₂ absorption rate significantly even at lower fractions, and thus the absorption is about 1.5 to 2 times faster than 7 m MEA	Piperazine is more expensive compared to MEA (Figuroa et al., 2008)	(Chen & Rochelle, 2011)

Table 2.3, Continued: A comparison between different chemical solvents

Solvent	Concentration	Absorption capacity(mol CO ₂ /kg amine+water)	Absorption rates(mol/s Pa m ²)	Temperature(°C)	P _{CO₂} (kpa)	Lean loading(mol CO ₂ /mol solvent)	Reaction enthalpy(KJ/mol CO ₂)	Advantage	Disadvantage	Reference
PZ	4.8M	0.17(mol CO ₂ /mol amine)	8.5E-7	40	5	-	-	PZ reacts with CO ₂ almost 10 times faster than MEA(Weiland & Hatcher, 2011)	The CO ₂ capacity of PZ is lower than AMP(X. Chen & Rochelle, 2011)	(Chen et al., 2011; Chen & Rochelle, 2011; Weiland & Hatcher, 2011)
N-methyl PZ	8m	0.83	8.4E-7	40	1.5	0.16	67	The absorption rate is greater than MEA	The absorption rate is slightly lower than PZ	(Chen & Rochelle, 2011)
2-Methyl Piperazine	0.54M	0.87(mol CO ₂ /mol amine)	0.021(L/min)	30	10	-	-	Rich loading is the same PZ but lean loading is more than PZ	Absorption rate and cyclic loading is less than PZ	(Singh et al., 2009)

Table 2.3, Continued: A comparison between different chemical solvents

Solvent	Concentration	Absorption capacity(mol CO ₂ /kg amine+water)	Absorption rates(mol/s Pa m ²)	Temperature(°C)	P _{CO₂} (kpa)	Lean loading(mol CO ₂ /mol solvent)	Reaction enthalpy (KJ/mol CO ₂)	Advantage	Disadvantage	Reference
2-methyl PZ	8m	0.93	5.9E-7	40	1.5	0.27	72	is a reasonably hindered amine and has a somewhat higher CO ₂ capacity than PZ, and it also always has a higher rate than MEA(Chen & Rochelle, 2011)	Absorption rate is less than PZ and N-methyl PZ(Chen et al., 2011)	(Chen et al., 2011; Chen & Rochelle, 2011)
2-MPZ/PZ	4m/4m	0.84	7.1E-7	40	1.5	0.30	70	The rate of the blend is greater than 2-MPZ and it also has a higher CO ₂ capacity compared to PZ	Absorption rate is slightly slower than PZ and CO ₂ capacity is slower than 2-MPZ	(Chen & Rochelle, 2011)

Table 2.3, Continued: A comparison between different chemical solvents

Solvent	Concentration	Absorption capacity(mol CO ₂ /kg amine+water)	Absorption rates(mol/s Pa m ²)	Temperature(°C)	P _{CO₂} (kpa)	Lean loading(mol CO ₂ /mol solvent)	Reaction enthalpy (KJ/mol CO ₂)	Advantage	Disadvantage	Reference
1-Methyl Piperazine	8m	0.83	8.4E-7	40	1.5	0.16	67	8 m 1-MPZ has similar CO ₂ absorption rates as 8 m PZ and greater than 2-MPZ and 2-MPZ/PZ	CO ₂ capacity is less than 2-MPZ and 2-MPZ/PZ	(Chen & Rochelle, 2011)
N-(2-hydroxyethyl)piperazine (HEP)	7.7m	0.68	5.3E-7	40	1.5	0.15	69	The absorption rate is faster than MEA at lean loading and the cyclic CO ₂ capacity is more than MEA	Has smaller rates than PZ, and absorption rate decreases rapidly with P _{CO₂} and becomes a slower solvent than MEA at the rich end	(Chen & Rochelle, 2011)

Table 2.3, Continued: A comparison between different chemical solvents

Solvent	Concentration	Absorption capacity(mol CO ₂ /kg amine+water)	Absorption rates(mol/s Pa m ²)	Temperature(°C)	P _{CO₂} (kpa)	Lean loading(mol CO ₂ /mol solvent)	Reaction enthalpy(KJ/mol CO ₂)	Advantage	Disadvantage	Reference
1-(2-aminoethyl) piperazine (AEP)	6m	0.66	3.5E-7	40	1.5	0.26	72	CO ₂ capacity is higher than MEA	Has smaller rates than PZ and MEA and also CO ₂ capacity is much less than other PZ derivatives	(Chen & Rochelle, 2011)
AMP	4.8m (Chen et al., 2011)	0.96(Chen et al., 2011)	2.4E-7(Chen et al., 2011)	40(Chen et al., 2011)	1.5(Chen et al., 2011)	0.27 (Chen et al., 2011)	73(Chen et al., 2011)	The capacity is twice as great as MEA, but the rate is 45% less (Chen et al., 2011)	Its kinetic reaction with CO ₂ is around 10 times slower than MEA (Alper, 1990; Saha et al., 1995)	(Alper, 1990; Chen et al., 2011; Chen & Rochelle, 2011; Saha et al., 1995)

Table 2.3, Continued: A comparison between different chemical solvents

Solvent	Concentration	Absorption capacity(mol CO ₂ /kg amine+water)	Absorption rates(mol/s Pa m ²)	Temperature(°C)	P _{CO₂} (kpa)	Lean loading(mol CO ₂ /mol solvent)	Reaction enthalpy (KJ/mol CO ₂)	Advantage	Disadvantage	Reference
N-methyl-1,3-propanediamine (MAPA)	8m (Chen et al., 2011)	0.42(Chen & Rochelle, 2011)10 to 20% less than MEA(Zaman & Lee, 2013)	3.1E-7(Chen et al., 2011)	40(Chen et al., 2011)	1.5(Chen et al., 2011)	0.47(Chen et al., 2011)	84(Chen et al., 2011)	MAPA absorbs faster than MEA at lean CO ₂ partial pressure but far slower at the rich end (Chen et al., 2011)	CO ₂ capacity is 10–20% less than MEA with a 5-15% slower rate (Chen et al., 2011)	(Chen et al., 2011; Chen & Rochelle, 2011; Zaman & Lee, 2013)
2-piperidine ethanol (2-PE)	8m	1.23	3.5E-7	40	1.5	0.37	73	Has greater capacity than PZ and MEA	Has slower rate than PZ and MEA	(Chen & Rochelle, 2011)

Table 2.3, Continued: A comparison between different chemical solvents

Solvent	Concentration	Absorption capacity(mol CO ₂ /kg amine+water)	Absorption rates(mol/s Pa m ²)	Temperature(°C)	P _{CO₂} (kpa)	Lean loading(mol CO ₂ /mol solvent)	Reaction enthalpy (KJ/mol CO ₂)	Advantage	Disadvantage	Reference
Aqueous ethylenediamine (EDA)	12m	0.72	2 times slower than MEA	40	0.5 to 5	-	84	EDA can be used at 8 to 12 m, because its viscosity is less than 20 CP in rich solution at 40°C. The working capacity of 12 M EDA is more than 1.5 times that of 7 M MEA. EDA, and MEA have the same CO ₂ absorption heat. At the working value of lean loading, the EDA instability in 12 M EDA is 4 times less than that of 7 M MEA	The absorption rate of CO ₂ into EDA is lower than 50% that of 7 m MEA at rich loading	(Zhou et al., 2010)

Table 2.3, Continued: A comparison between different chemical solvents

Solvent	Concentration	Absorption capacity(mol CO ₂ /kg amine+water)	Absorption rates(mol/s Pa m ²)	Temperature(°C)	P _{CO₂} (kpa)	Lean loading(mol CO ₂ /mol solvent)	Reaction enthalpy (KJ/mol CO ₂)	Advantage	Disadvantage	Reference
Aqueous NH ₃	0.6-6M(Puxty et al., 2010)	1.2(Kevin et al., 2004)	75% (Kevin et al., 2004)	4.85-19.85(Puxty et al., 2010)	0-20(Puxty et al., 2010)	0-8 (Puxty et al., 2010)	Overall mass transfer coefficient 1.5 to 2 times smaller than MEA (Puxty et al., 2010)	The ammonium process saves energy by up to 60% compared to the MEA process (Yang et al., 2008), and it has great absorption capacity, rapid absorption rate, and few corrosion problems (Seo et al., 2011) It has low regeneration temperature (Kim et al., 2009)	Large vapor pressure (Puxty et al., 2010)	-

2.12 Simulation studies

In Aspen Plus (Aspen Technology, Inc., <http://www.aspentech.com>) for the CO₂ absorption process, two approaches are employed in modeling vapor–liquid mass transfer in a section of packed column: the equilibrium-stage and the rate-based approaches (Taylor & Krishna, 1993). For a precise design of CO₂ capture, rate-based modeling can be employed because it is a superior model to simulate CO₂ separation by using physical and chemical solvents. Many studies reported the superiority of the rate-based model over the conventional equilibrium-stage model. Zhang et al. (Ying Zhang et al., 2009) used rate-based and equilibrium-stage models for simulation of CO₂ absorption with aqueous monoethanolamine in a pilot plant. They showed the superiority of the rate-based model over the traditional equilibrium-stage model.

Pandya (Pandya, 1983); Tontiwachwuthikul et al.(Tontiwachwuthikul et al., 1992); Aroonwilas et al.(Aroonwilas et al., 2003b); Liu et al.(Liu et al., 2006); Tobiesen et al.(Tobiesen et al., 2007); Kvamsdal and Rochelle (Kvamsdal & Rochelle, 2008); Faramarzi et al.(Faramarzi et al., 2010); Khan et al. (Khan et al., 2011); Mores et al. (Mores et al., 2012; Mores et al., 2011); (Plaza et al., 2010); (Dugas, 2009); (Dugas, 2006) also have studied the modeling of CO₂ capture with MEA solution in a packed column. All of these studies have focused on the rate-based modeling approach and no study was reported in the literature for equilibrium-stage modeling approach. Alatiqi et al. (Alatiqi et al., 1994) used a rate based model to simulate absorption of CO₂ in MEA, DEA, and AMP solutions by using actual plant data. Therefore, the superiority of rate-based models to the equilibrium-stage models has been confirmed in CO₂ capture process by amine solutions (Afkhamipour & Mofarahi, 2013b; Al-Baghli et al., 2001; Faramarzi et al., 2010; Lawal et al., 2009; Simon et al., 2011; Ying Zhang et al., 2009). Moreover, the RateSep model can be a useful tool for design of CO₂ capture processes, industrial research and development. It has the ability of employing real absorber

configurations and internals, multi-component mass and heat transfer methods, and the actual rigorous kinetic and thermodynamic models. Therefore, rate-based model was used in this study to simulate CO₂ absorption process.

2.12.1 Simulation using a rate-based model

The concept of equilibrium or theoretical stages is used in the equilibrium-stage for modeling columns. Since in the equilibrium stage model heat and mass transfer are kinetically limited processes driven by temperature gradients and chemical potential thus, this model can be insufficient (Henley & Seader, 1981). In contrast, liquid and gas phases in the rate-based model are balanced separately by considering heat and mass fluxes across the interface (Seader, 1989).

The rate-based model has the capability of employing real absorber configurations and internals, multi-component heat and mass transfer methods, and the actual rigorous kinetic and thermodynamic models thus; this model is a great tool for design and scale-up analysis of CO₂ capture with amine solutions. However, this requires a good fundamental for the mass and heat transfer correlations, physical and transport properties, kinetic models. In the rate-based model, both diffusion and reaction occur in the liquid phase, during which mass and heat transfer rate among the contacting phases are calculated. By contrast, phase equilibrium occurs at the gas and liquid interface; the gas phase resistance is determined using an appropriate transfer model. Mass and heat transfer methods can be used in rate-based modeling as well as actual precise kinetic and thermodynamic models (Razi et al., 2013).

In the rate-based model with two-film theory, (Whitman, 1923) liquid film at each stage is discretized into numerous non-homogeneous segments; segments near the liquid bulk phase are thicker than those near the interface (Figure 2.3). Therefore, non-homogeneous discretization can be used to precisely calculate species concentration profiles in the film. The performance of the absorption column was determined through

the combined equations for films, materials, and heat balance at each stage. Multicomponent mass and heat transfer was solved using Maxwell–Stefan theory in the rate-based model (Qi et al., 2013). In this model, liquid and gas phases are balanced separately based on mass and heat transfer rates across the fluid interface (Afkhampour & Mofarahi, 2013a).

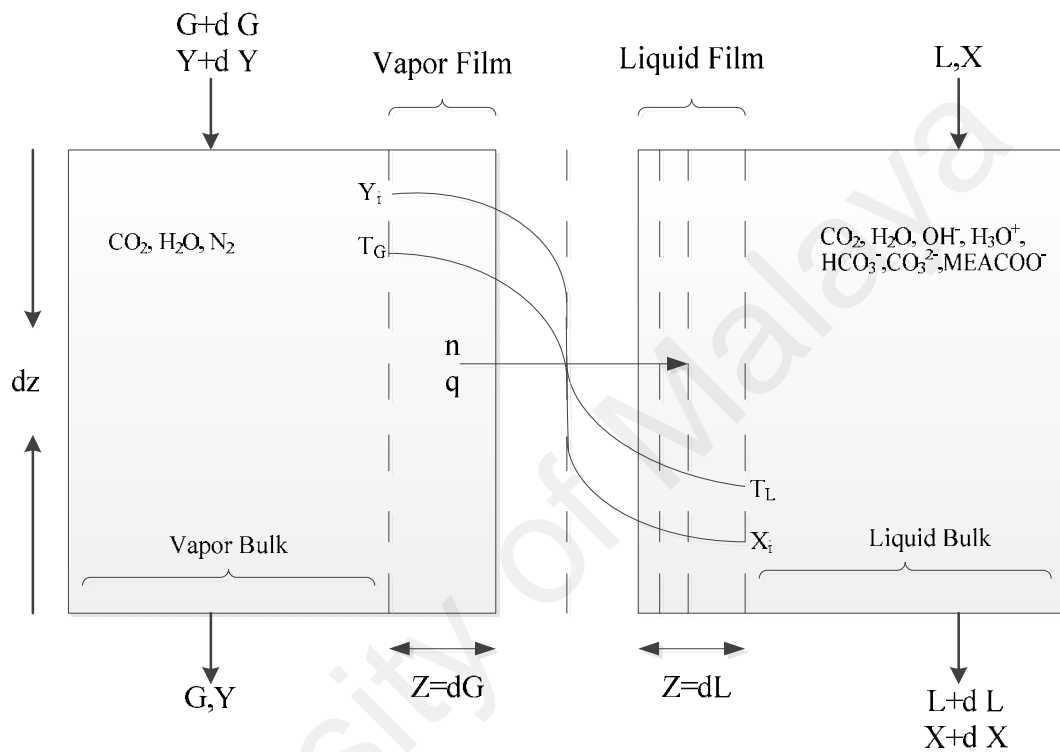


Figure 2.3: Film theory in a rate-based model for each packed segment

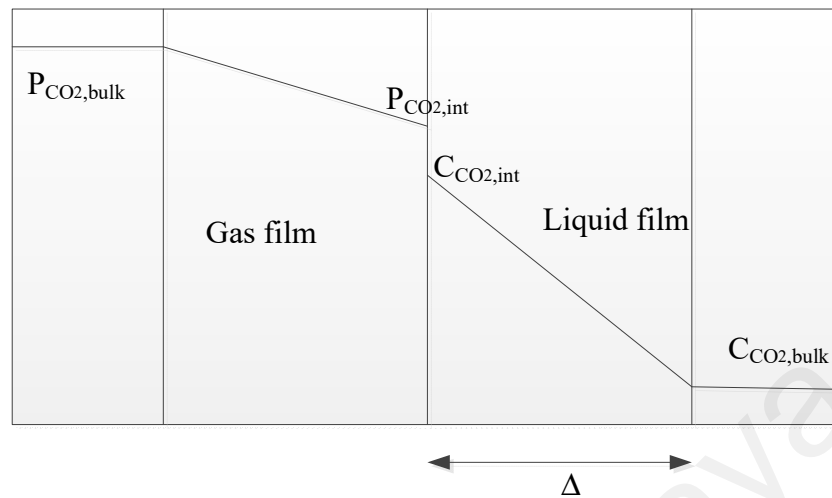


Figure 2.4: Film theory in physical absorption

In the absence of chemical reaction in the system (physical absorption) (Figure 2.4), the concentration profiles were regarded as constant and linear in the bulk and film region, respectively (Freguia, 2002b).

The correlations of individual mass transfer coefficients for packings such as Raschig rings, Berl saddles, and Pall rings were proposed by Bolles and Fair, (Bolles & Fair, 1982) Onda et al., (Onda et al., 1968) and Bravo and Fair (Jose L Bravo & James R Fair, 1982). For example, correlations for structured packings were developed by Bravo et al. (Jose L Bravo et al., 1985). Equations for the wetted surface area (a_w), considering the liquid surface tension, were developed by Onda et al. (Onda et al., 1968).

For the random packings, the correlations related to (Onda et al., 1968), (Billet & Schultes, 1993), and (Hanley & Chen, 2012) are available in the Aspen Plus rate-based model for computing the interfacial area and mass-transfer coefficients. For the structured packings, in addition to (Billet & Schultes, 1993) and (Hanley & Chen, 2012), the models of (Bravo et al., 1992; J. L. Bravo et al., 1985) are also available. Moreover, the model of (Stichlmair et al., 1989) is a holdup method for both random

and structured packings. Table 2.4 illustrates the generalized correlations for mass transfer coefficients and wetted surface area (a_w) of packing, as proposed by Onda et al. (Onda et al., 1968) and Bravo & Fair, (Bravo & Fair, 1982) respectively.

Table 2.4: Proposed correlations for mass transfer coefficients and wetted surface area of packing

Correlations	Reference
$k_L = 0.0051 \left(\frac{L}{a_w \mu_L} \right)^{\frac{2}{3}} \left(\frac{\mu_L}{\rho_L D_L} \right)^{-\frac{1}{2}} \times (a_t D_p)^{0.4} \times \left(\frac{\rho_L}{\mu_L g} \right)^{-\frac{1}{3}}$	(Hiwale et al., 2012; Mirzaei et al., 2015; Onda et al., 1968)
$k_G = 5.23 \left(\frac{G}{a_t \mu_G} \right)^{0.7} \left(\frac{\mu_G}{\rho_G D_G} \right)^{\frac{1}{3}} (a_t D_p)^{-2} \times \frac{a_t D_G}{RT}$	(Mirzaei et al., 2015; Onda et al., 1968; Hiwale et al., 2012)
$\frac{a_w}{a_t} =$ $1 - \exp \left\{ -1.45 \left(\frac{\sigma_c}{\sigma_L} \right)^{0.75} (Re_L)^{0.1} \times (Fr_L)^{-0.05} (We_L)^{0.2} \right\}$	(Mirzaei et al., 2015; Onda et al., 1968; Hiwale et al., 2012)
$\frac{a_e}{a_p} = 19.78 \left(\frac{\rho_G U_G}{\mu_G a_p} \right)^{0.392} \left(\frac{\mu_L U_L^2}{\sigma_L} \right)^{0.392} \left(\frac{\sigma_L}{Z^{0.4}} \right)$	(Bravo & Fair, 1982)

2.13 Summary

Recently, ILs have received much attention in CO₂ capture, but they are toxic and their high price prevents their application on a commercial scale. The most considered chemical for post-combustion capture is MEA because it is very reactive and has an excellent CO₂ removal efficiency. On the contrary, the energy requirement for the MEA process is very high, and amine degradation causes solvent loss and the formation of heat-stable salts in the presence of O₂, NO_x, and SO_x.

PZ increases CO₂ absorption rate even at low fractions, and the CO₂ absorption rate of PZ is superior to MEA. In contrast, PZ is more expensive than MEA. In an aqueous NH₃ system, corrosion problems are less, loading capacity is higher, and the energy requirement for regeneration is less than that of MEA process but, vapor pressure of NH₃ is high.

Vapour pressure of MEA is relatively high and leads to significant solvent loss through evaporation and also serious environmental drawbacks. Amines undergo thermal degradation in regeneration process and oxidative degradation when O₂ presents in the flue gas stream. Replacement of solvent is necessary when the severe degradation of solvent occurs and it increases the cost of operation. Effects of amines degradation include CO₂ loading capacity reduction, foaming, fouling, and increase in viscosity. Moreover, chemical solvents are corrosive, which this problem increases the operating cost. Volatile nature of amines causes significant loss of solvent into the gas stream, leads to serious environmental drawbacks and an increase in the process cost. Solvent regeneration in physical absorption is easier and requires less energy than that in chemical absorption. Therefore, researchers have studied the mixture of amines and physical solvents.

Glycerol as a novel solvent has been studied for CO₂ capture. This compound is available in large amounts as a by-product of biodiesel production thus; it is relatively inexpensive, biodegradable and non-volatile under atmospheric pressure. Glycerol is nontoxic and stable with low vapour pressure. It is colorless, odourless and liquid at low vapour pressure. It has high boiling point. High viscosity of pure glycerol decreases by increasing the amount of water and temperature. The CO₂ solubility in glycerol is higher than that of CO₂ in water. Therefore, the usage of glycerol can reduce the use of harmful chemical solvents with environment friendly solvents.

CHAPTER 3: MATERIALS AND METHODS

3.1 Introduction

This chapter is comprised of three parts with each part incorporating a specific subject of study:

1. Simulation of CO₂ absorption process using MEA, glycerol and MEA-glycerol aqueous solutions.
2. Experimental study of CO₂ absorption in a packed column.
3. Validation of simulation study with experimental work. The detailed methodology of this study is described in Figure 3.1.

University of Malaya

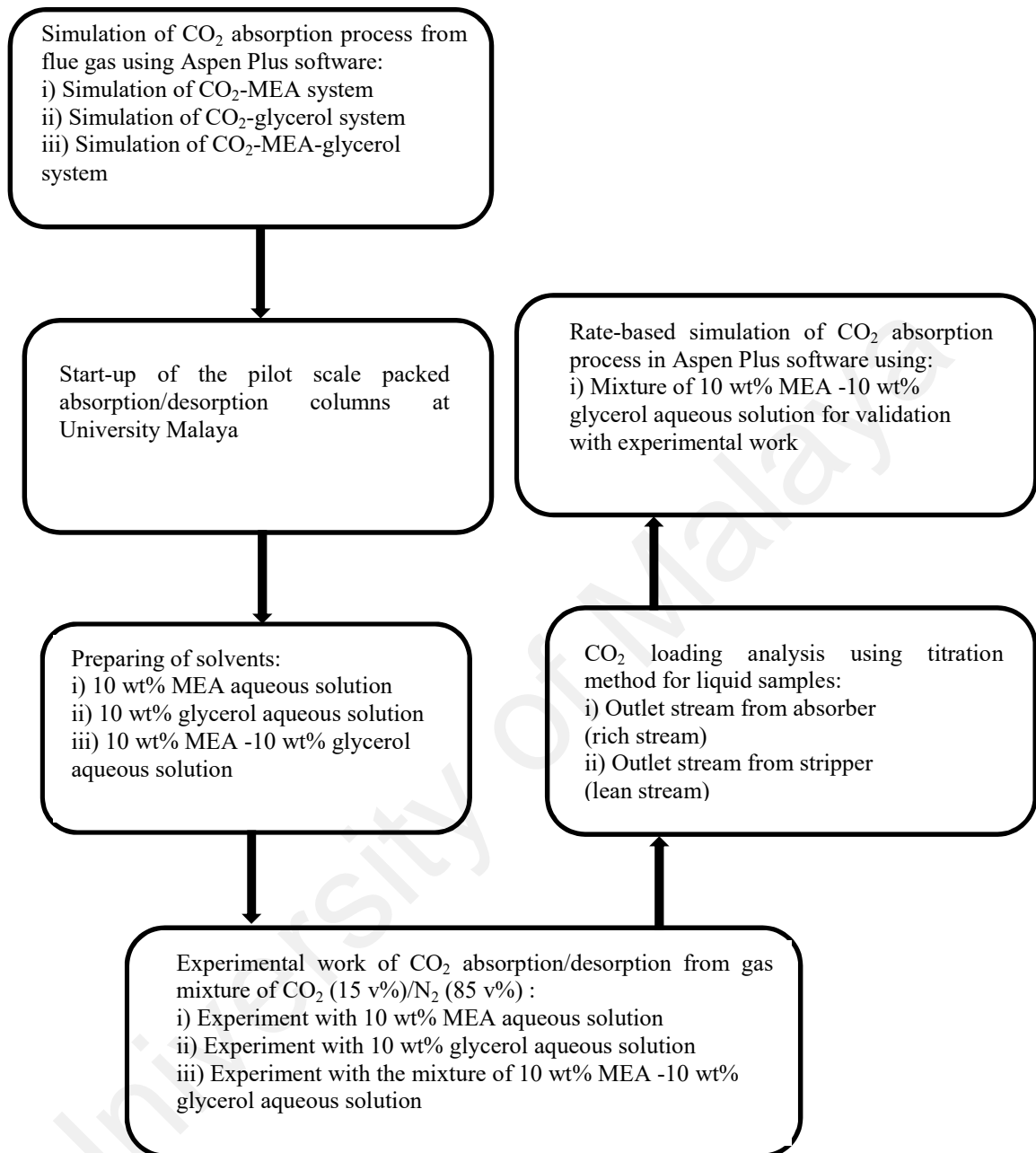


Figure 3.1: Methodology flow chart

3.2 Simulation of CO₂ absorption process using MEA, glycerol and MEA-glycerol aqueous solutions

3.2.1 Methodology

Simulation and modeling studies are used to assess CO₂ absorption and desorption when field experimental data are limited. In this section, CO₂-MEA system, CO₂-glycerol system and CO₂-MEA-glycerol system were simulated using Aspen Plus software in order to achieve the best concentrations of solvents for efficient CO₂ absorption.

The CO₂-MEA system was first simulated in a rate-based model; the system was used as the base case for simulation and validated using the experimental data of Dugas (Ross E Dugas, 2006). Different systems of CO₂-glycerol and CO₂-MEA-glycerol with varied concentrations of glycerol and MEA were simulated and compared. The most effective concentration for the CO₂-MEA-glycerol system was determined using CO₂ removal efficiency. The performance of ENRTL-RK and ELECNRTL, as two thermodynamic models, was also investigated in the system, whereas NRTL-RK thermodynamic model was employed for CO₂-glycerol system.

3.2.2 Modeling

An Aspen Plus model was used for CO₂ removal from flue gas with glycerol as physical solvent. The effect of glycerol as promoter on the amount of CO₂ absorbed was determined. The operating data from the pilot plant at the University of Texas at Austin (Ross E Dugas, 2006) were subjected to Aspen plus process simulator version 7.3 to specify the feed conditions and unit operation specifications for absorber and stripper in the rate-based model. Base case simulation was performed in a non-equilibrium rate-based model, and ENRTL-RK thermodynamic model was used in Aspen Plus software to model the process with MEA solvent. The results were validated against the pilot plant data from the University of Texas at Austin (Ross E Dugas, 2006).

3.2.2.1 Flow models

Four different flow models were specified in a rate-based model to obtain the bulk properties for evaluating mass and energy fluxes and reaction rates. These models include mixed, countercurrent, vplug, and vplug-pavg. In this simulation study, mixed and countercurrent flow models were considered and their results were compared. In the mixed flow model, the bulk properties for each phase should be the same as the passing conditions for the phase leaving that stage; however, in the countercurrent flow model, the bulk properties for each phase are the average of the inlet and outlet properties. Countercurrent flow model yields precise results for packing but is computational and unsteady (Aspen Technology, 2011).

3.2.2.2 Film resistance methods

The rate-based model employs four film resistance options, namely, no film, film, filmrxn, and discrxn for each phase. Film, filmrxn, and discrxn were investigated in this study. Film method defines the diffusion resistance without any reactions in the film in a specific phase (Aspen Technology, 2011). Filmrxn method describes the diffusion resistance with reactions in the film in the phase without film discretization (Ying Zhang et al., 2009; Aspen Technology, 2011). Discrxn method explains diffusion resistance with reactions in the film in a specific phase, and the film is discretized. This method is useful when film reactions dramatically change the composition of the film. Filmrxn or Discrxn methods are used whenever there are reactions involving components in both liquid and vapor phases. In phases and stages without any reaction, Filmrxn and Discrxn are similar to Film (Aspen Technology, 2011).

3.2.2.3 Thermodynamic and transport property models

Electrolyte NRTL model with the Redlich–Kwong (RK) equation of state (ELECNRTL) is a suitable electrolyte system for aqueous and mixed solvents. ENRTL-RK is an improved model of ELECNRTL and can be simplified into NRTL-RK when

no ions exist in the system (Aspen Technology, 2011). In the rate-based model, the liquid and vapor properties were calculated using electrolyte–NRTL method and the RK equation of state, respectively. For the liquid phase, thermodynamic properties such as enthalpy, Gibbs energy, and activity coefficient were calculated using electrolyte–NRTL model. For the vapor phase, fugacity coefficients were estimated using the RK equation of state (Aspen Technology, 2010).

The transport properties of aqueous solvents must be determined to describe mass and heat transfer. Various transport property models can be used to estimate diffusion coefficient, thermal conductivity, surface tension, viscosity, and density of the electrolyte solvent. Nernst–Hartley electrolyte model was used to estimate the diffusion coefficient of a component in the mixture (DLMX). Riedel electrolyte correction model was used to determine liquid mixture thermal conductivity (KLMX). Moreover, Jones–Dole electrolyte and Onsager–Samaras models were employed to specify liquid mixture viscosity (MULMX) and liquid mixture surface tension (SIGLMX), respectively. Furthermore, Clark density model was applied to determine mixture molar volume (VLMX) for electrolyte solutions, and electrolyte NRTL model was applied to determine activity coefficients (GAMMA) (Aspen Technology, 2001b).

Mass transfer coefficients, interfacial areas, heat transfer coefficients, and holdup correlations were obtained from the study of Onda et al., (Onda et al., 1968) Bravo et al., (Bravo et al., 1985; Bravo et al., 1992) Chilton and Colburn,(Chilton & Colburn, 1934) Stichlmair et al., (J. Stichlmair et al., 1989) respectively.

3.2.3 Chemical reactions in the model

Equilibrium reactions 3.1-3.5 (Aspen Technology, 2001a; Nagy & Mizsey, 2013) occur in the liquid phase when the aqueous MEA solution becomes in contact with CO₂ gas. CO₂ then enters into the liquid phase until the equilibrium is stabilized.

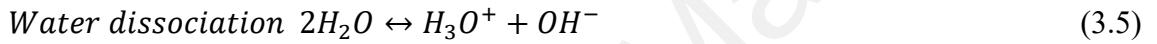
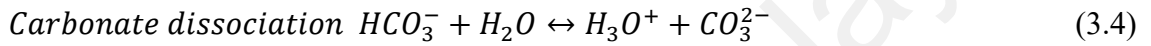
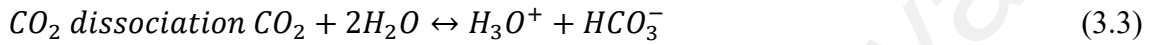
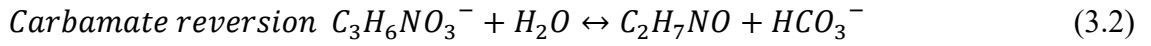
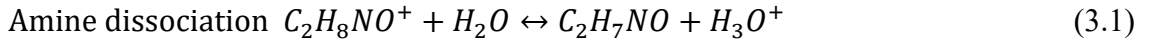
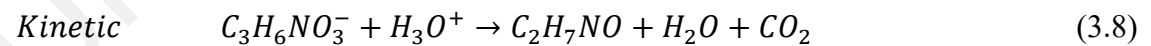
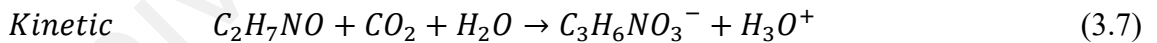


Table 3.1 shows the equilibrium constants obtained using equation 3.6. This equation implies that equilibrium constants are temperature dependent.

$$\ln K_{eq} = A + \frac{B}{T} + C \ln T + DT \quad (3.6)$$

Reactions 3.7-3.10 are the kinetic reactions for the MEA-H₂O-CO₂ system (Q. Zhang et al., 2016).



The power law kinetic expressions were employed for rate-controlled reactions. Equation 3.11, which is temperature dependent, defines the kinetic expression for reactions 3.7-3.10.

$$r = k \left(\frac{T}{T_0}\right)^n \exp \left[\left(\frac{-E}{R}\right) \left(\frac{1}{T} - \frac{1}{T_0}\right) \right] \quad (3.11)$$

where r is the reaction rate, k is the pre-exponential factor, T is the absolute temperature, n is the temperature exponent, E is the activation energy, and R is the gas law constant (Aspen Technology, 2001a). Factors n , k , and E are presented in Table 3.2. Temperature dependence of Henry's constants for carbon dioxide is given by the functional form of equation 3.12 (Y. Liu et al., 1999; Hilliard, 2008; Ostonen et al., 2014). As shown in Table 3.3, H_i is the Henry's constant for CO₂ in H₂O, MEA, and glycerol.

$$\ln H_i = A + \frac{B}{T(K)} + C \ln T(K) + D T(K) + \frac{E}{T(K)^2} \quad (3.12)$$

University of Malaya

Table 3.1: Equilibrium constants for reactions 3.1-3.5

Reaction No.	A	B	C	D	Reference
3-1	2.1211	-8189.38	0	-0.007484	(Austgen et al., 1991; Austgen et al., 1989)
3-2	2.8898	-3635.09	0	0	(Austgen et al., 1991; Austgen et al., 1989)
3-3	231.465	-12092.1	-36.7816	0	(Austgen et al., 1991; Austgen et al., 1989; Y. Liu et al., 1999)
3-4	216.049	-12431.70	-35.4819	0	(Austgen et al., 1991; Austgen et al., 1989; Y. Liu et al., 1999)
3-5	132.899	-13445.9	-22.4773	0	(Austgen et al., 1991; Austgen et al., 1989; Y. Liu et al., 1999)

Table 3.2: Kinetic parameters for reactions 3.7-3.10

Reaction No.	K	E(cal/mol)	n	Reference
3-7	$9.77 \times 10^{+10}$	9855.8	0	(Hikita et al., 1977)
3-8	$3.23 \times 10^{+19}$	15655	0	(Hikita et al., 1977)
3-9	$4.32 \times 10^{+13}$	13249	0	(Pinsent et al., 1956)
3-10	$2.38 \times 10^{+17}$	29451	0	(Pinsent et al., 1956)

Table 3.3: Coefficients for Henry's constants of CO₂ in H₂O, MEA, and glycerol

	A	B	C	D	E	Reference
H _{CO₂-H₂O}	170.7126	-8477.711	-21.95743	0.005781	0.0	(Y. Liu et al., 1999; Hilliard, 2008)
H _{CO₂-MEA}	89.452	-2934.6	-11.592	0.01644	0.0	(Y. Liu et al., 1999)
H _{CO₂-glycerol}	-4.0988	1	2.702	-1×10 ⁻⁵	0.0	(Ostonen et al., 2014)

3.2.4 Process flow diagram of the CO₂ absorption/desorption unit

Figure 3.2 indicates the schematic diagram of absorption/stripping process. A lean solvent is fed into the top of the absorber column and is in counter-current contact with flue gas consisting CO₂. Solvent absorbs CO₂ (CO₂ chemically reacts with amine), and the treated gas leaves the top of the absorption column. The rich solvent containing high CO₂ concentration exits the bottom of the absorption column and is heated before entering the top of the stripper column. At the stripper, the CO₂ rich solvent is then heated to high temperatures to regenerate the solvent and release CO₂ captured. The CO₂ gas leaves the top of the stripper, and the lean solvent (low CO₂ concentration) exits from the bottom of the stripper. Table 3.4 indicates the characteristics of the towers for validation (Dugas, 2006).

Table 3.4: Packing parameters for columns (Dugas, 2006)

Parameter	Absorber	Stripper
Column type	Packed	Packed
Column internal diameter(m)	0.427	0.427
Total packing height(m)	6.1	6.1
Packing type	IMTP#40	FLEXIPAC 1Y
Nominal packing size	0.038	-
Specific area(m ² /m ³)	145	420

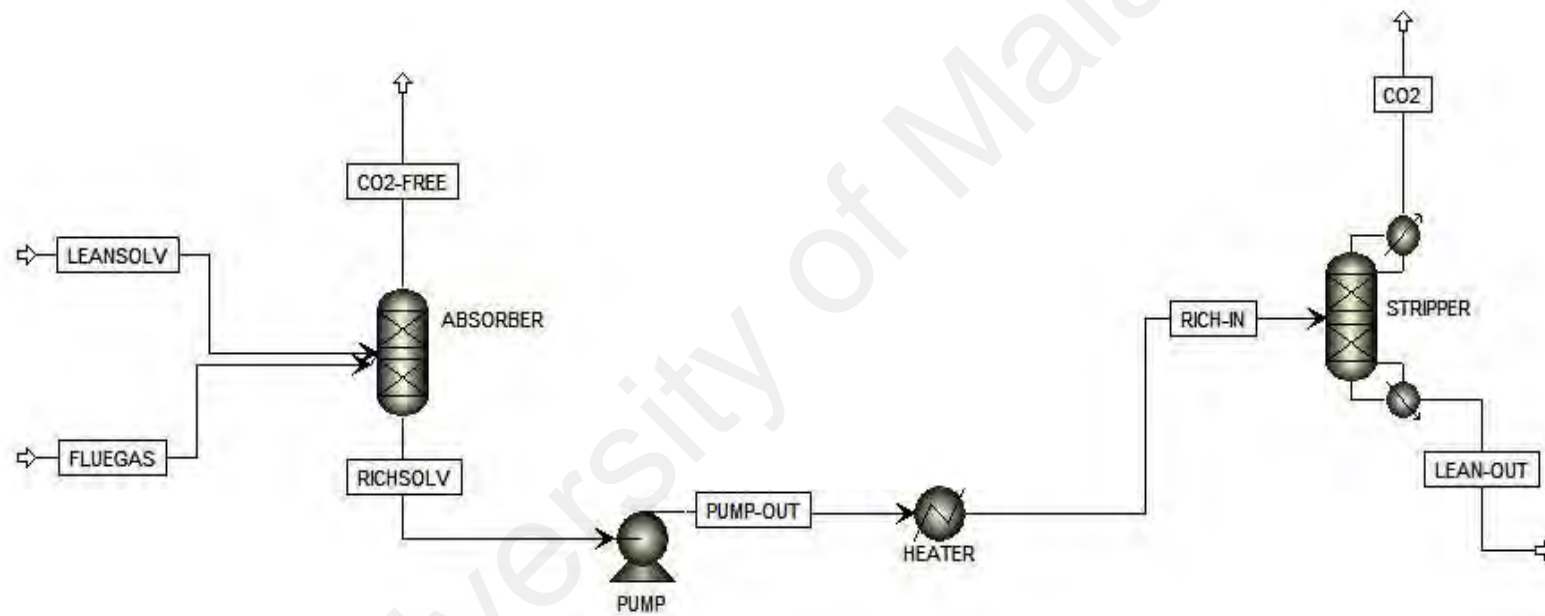


Figure 3.2: Process flow diagram of the absorption/desorption process

3.2.5 CO₂-MEA system

The packed absorber used by Dugas (Ross E Dugas, 2006) comprises seven resistance temperature detectors (RTD). Sensor locations are determined by the height from the bottom of the column. Most of absorber profiles in this part of research are plotted based on these sensor locations. Figure 3.3 illustrates the locations for measuring absorber temperatures (Ross E Dugas, 2006) and Table 3.5 indicates the feed conditions to the absorber.

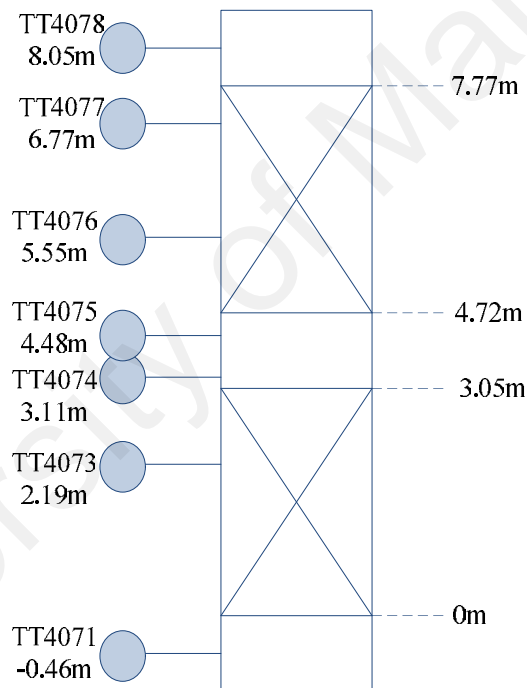


Figure 3.3: Locations of temperature sensors in the absorption column

(Dugas, 2006)

Table 3.5: Feed conditions for validation (Dugas, 2006)

Operating parameter	Flue gas	Lean amine
Temperature (°C)	59.25	40.15
Flow rate (kg/s)	0.158	0.642
Mass fraction		
H ₂ O	0.009	0.633
CO ₂	0.261	0.062
MEA	0	0.305
N ₂	0.681	0
O ₂	0.049	0

3.2.6 CO₂-glycerol system

In glycerol process, packing parameters for columns and the feed conditions for flue gas are the same as MEA process (Tables 3.4 and 3.5). As shown in Table 3.6, the best glycerol concentration for CO₂ absorption/desorption process is determined based on simulation study of the process at different glycerol concentrations (2, 5, 10, 20, 40, 60, 80 and 90 wt%).

Table 3.6: Feed conditions for CO₂ absorption/desorption using glycerol solvent

Operating parameter	Lean solvent							
	1	2	3	4	5	6	7	8
Temperature(°C)	40.15	40.15	40.15	40.15	40.15	40.15	40.15	40.15
Flow rate(kg/s)	0.642	0.642	0.642	0.642	0.642	0.642	0.642	0.642
Mass fraction								
H ₂ O	0.98	0.95	0.9	0.8	0.6	0.4	0.2	0.1
CO ₂	-	-	-	-	-	-	-	-
glycerol	0.02	0.05	0.1	0.2	0.4	0.6	0.8	0.9
N ₂	-	-	-	-	-	-	-	-
O ₂	-	-	-	-	-	-	-	-

3.2.7 CO₂- MEA- glycerol system

CO₂ absorption/desorption process was simulated using the aqueous mixture of MEA-glycerol solution (Table 3.7) based on the obtained optimal concentration of glycerol solvent for CO₂ absorption, to investigate the CO₂ removal efficiency of the mixed solvent and obtain best concentration. Packing parameters and feed conditions for flue gas are shown in the Tables 3.4 and 3.5.

Table 3.7: Feed conditions for MEA-glycerol process

Operating parameter	Lean solvent (1)	Lean solvent(2)	Lean solvent(3)
Temperature(C)	40.15	40.15	40.15
Flow rate(kg/s)	0.642	0.642	0.642
Mass fraction			
H ₂ O	0.83	0.8	0.75
CO ₂	-	-	-
MEA	0.07	0.1	0.15
glycerol	0.1	0.1	0.1
N ₂	-	-	-
O ₂	-	-	-

Glycerol is neutral in litmus test (Table 2.1). For the MEA–glycerol solution, CO₂ loading is defined as moles of CO₂/mole alkalinity. The number of nitrogen atoms on amine determines the alkalinity of the solution (Ross E Dugas, 2007). The number of nitrogen atoms is 1 for MEA. The definition of CO₂ loading is shown below.

$$\text{For glycerol-MEA: CO}_2 \text{ loading} = n_{\text{CO}_2} / [(1) n_{\text{MEA}}] \quad (3.13)$$

$$\text{For MEA: CO}_2 \text{ loading} = \text{mol CO}_2 / \text{mol MEA} \quad (3.14)$$

$$\text{For glycerol: CO}_2 \text{ loading} = \text{mol CO}_2 / \text{mol glycerol} \quad (3.15)$$

3.3 Experimental study of CO₂ absorption in a packed column

3.3.1 Materials

MEA (with a purity >98%) and glycerol (with a purity >99.8%) were supplied by R&M Chemicals and used as purchased without further purification. 0.3M of barium chloride (BaCl₂) solution was prepared by mixing barium chloride dihydrate (BaCl₂·2H₂O) (with a purity >99% obtained from R&M Chemicals) with distilled water. 0.1N sodium hydroxide (NaOH) and 0.1N hydrochloric acid (HCl) were used as received from R&M Chemicals. The distilled water was provided by a Water Still W4L favorit water purification system. This system provides, distilled water produced through a power input by a chromium plated heater housed in a horizontal glass boiler. The CO₂-N₂ gas mixture with the composition of 15 v% CO₂ and 85 v% N₂ was supplied by Linde, special gases centre in Malaysia.

3.3.2 Pilot scale absorption/desorption unit description

An absorption-desorption pilot plant containing two separate but interconnected packed columns was designed, constructed and employed for CO₂ scrubbing and solvent regeneration. The gas and liquid flow counter currently, and the packings serve to provide the contacting and development of interfacial surface through which mass transfer takes place. The unit operates at atmospheric pressure in a continuous operation. It has the following special features; fully instrumented to allow for convenient data collection and analysis. The material of absorber and stripper columns are borosilicate glass and stainless steel which they filled with glass Raschig rings. These glass columns and vessels permit good visual monitoring of the process. Sampling points for composition analysis are provided for liquid streams.

N₂ and CO₂ are mixed before being fed into the bottom of a packed absorption column, while solvent enters from the top of the column through a centrifugal pump. Transfer of CO₂ from gas mixture into solvent occurs when gas and liquid are brought into contact.

The N₂ will exit at the top whereas the CO₂ rich solvent will accumulate at the bottom of the column and overflow into a receiving vessel.

CO₂ now present in the solvent can be stripped in another packed desorption column.

The CO₂ rich solvent is heated before entering the column to decrease the solubility of CO₂ in solvent. The stripper removes CO₂ by increasing the temperature of the solution.

Heat from the solvent emerging at the bottom of the column is recovered in a coil heat exchanger. It is further cooled by cooling water before overflowing into a receiving vessel. Table 3.8 indicates the characteristics of the both absorption and desorption columns of the pilot plant and Figure 3.4 shows process flow diagram for the gas absorption/desorption unit.

Table 3.8: Characteristics of absorber and stripper

	Absorber	Stripper
Column type	packed	packed
Column internal diameter(mm)	80	80
Effective packing height(m)	1.5	1.5
Packing type	Raschig rings	Raschig rings
Nominal packing size (mm)	8	8

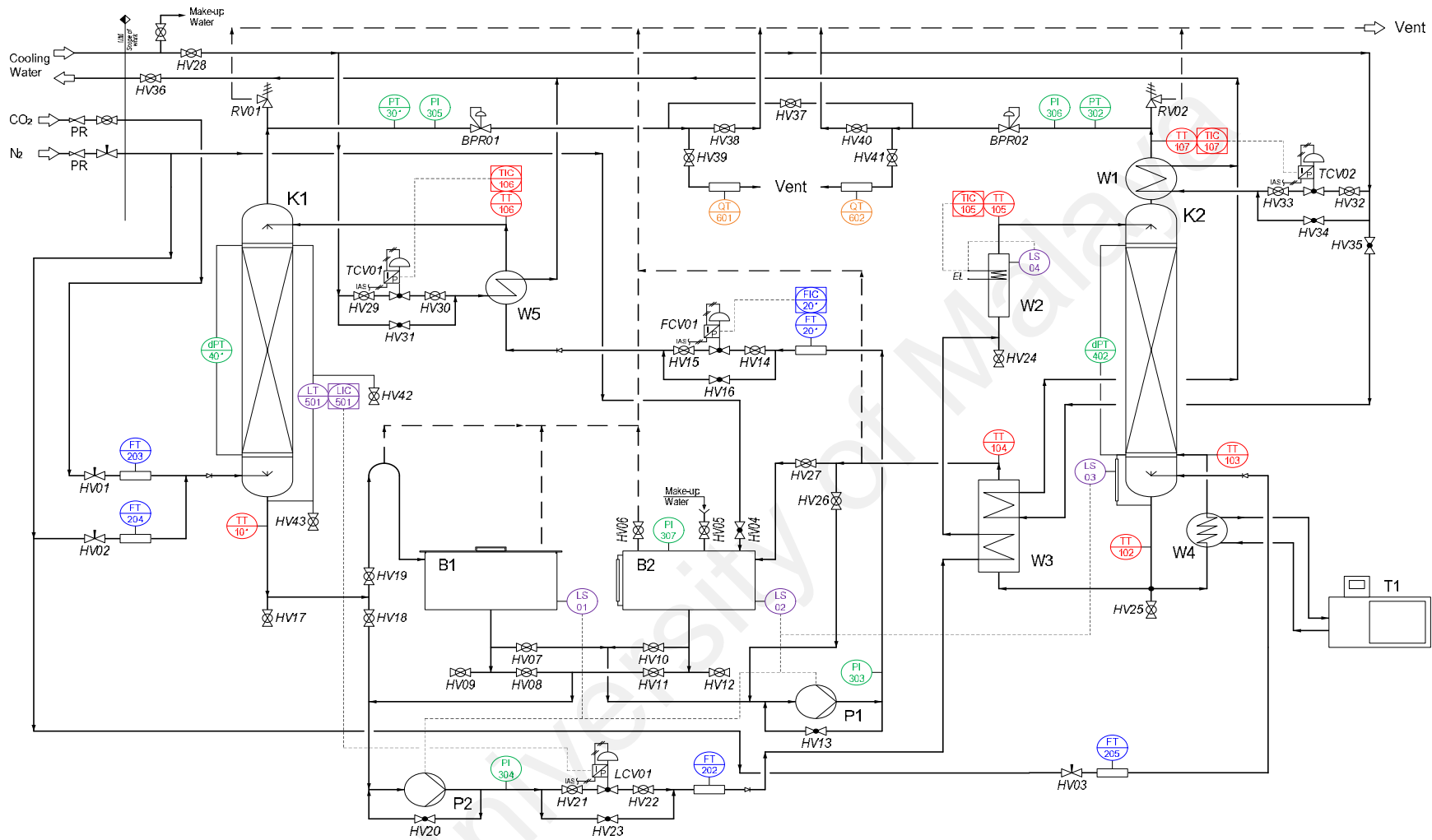


Figure3.4: Absorption-desorption unit

3.3.2.1 Assembly of pilot scale absorption/desorption unit

(a) *Sump Tanks (B1 & B2)*

Tanks with level sight tube (B1 rectangular, B2 cylindrical)

Capacity: 50 L

Material: stainless steel

Low level switch for protection of centrifugal pumps from dry run

(b) *Circulation Pumps (P1 & P2)*

Magnetic drive sealless centrifugal pumps

Maximum delivery: 60 liter per minute (L/min)

Maximum head: 5.6 m

Output power: 65 W

Material: polypropylene (PP)

Maximum flow rate in the system: 4 L/min

(c) *Absorption / Desorption Columns (K1 & K2)*

Packed columns filled with Raschig rings

Diameter: 80 mm

Effective packing height: 1.5 m

Material: borosilicate glass and stainless steel

Packing: 8 mm glass Raschig rings

(d) *Condenser (W1)*

Water cooled coiled condenser

Exchange area: 0.2 m²

Material: stainless steel

(e) *Liquid Preheater (W2)*

Temperature controlled heater with safety level switch

Heating element: immersion cartridge heaters

Heating power: 4 kW

Material: stainless steel

(f) Heat Exchanger (W3)

Coiled heat exchanger

Exchange area: 0.2 m² with feed liquid, 0.2 m² with cooling water

Material: stainless steel

(g) Heat Exchanger (W4)

Shell and tube heat exchanger

Exchange area: 0.45 m²

Tube count: 253

Material: stainless steel

(h) Heat Exchanger (W5)

Shell and tube heat exchanger

Exchange area: 0.3 m²

Tube count: 127

Material: stainless steel

(i) Digital Heating Circulator (T1)

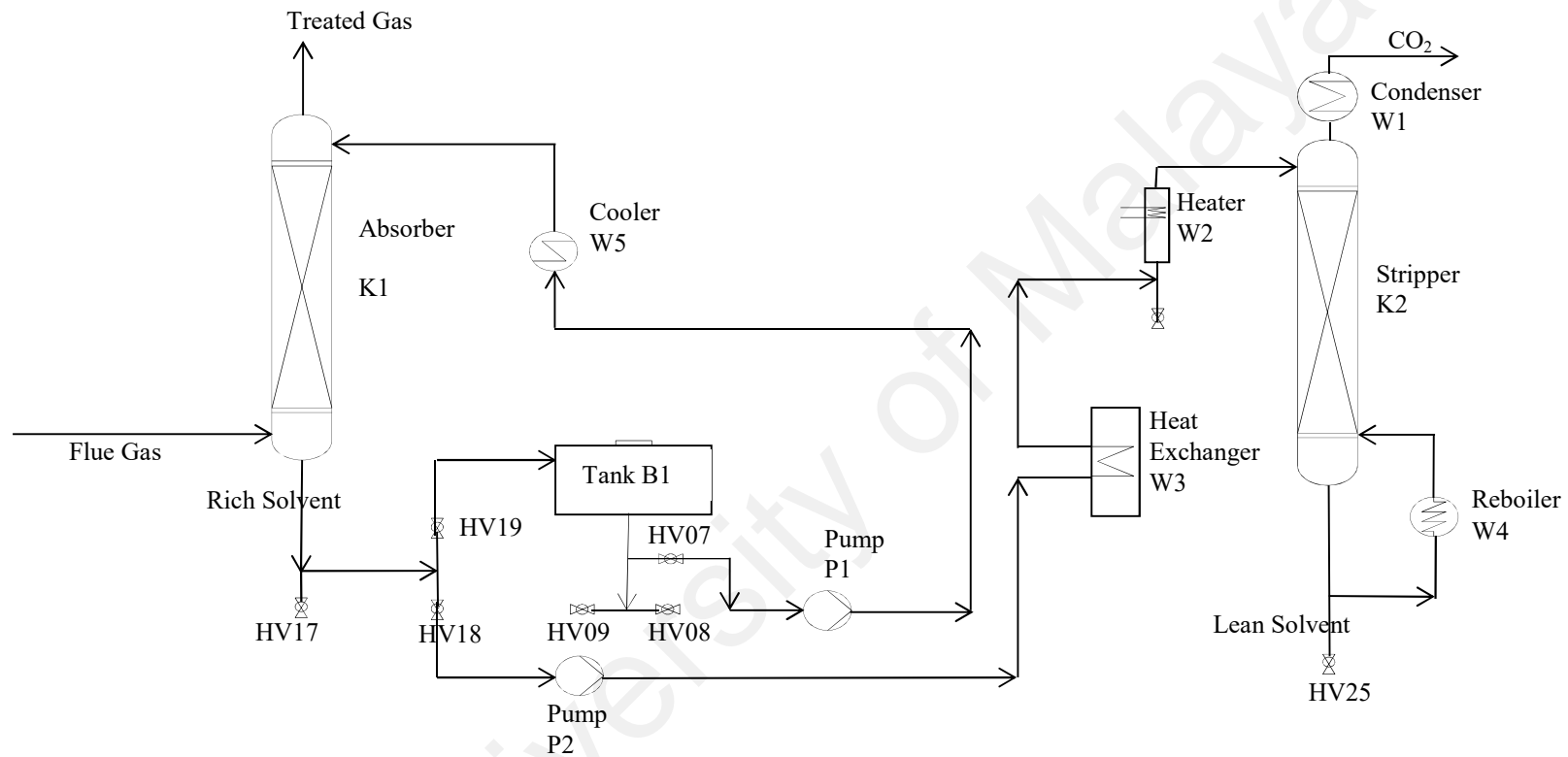
Microprocessor PID controller

Range: up to 150°C

Heater: 1500 W

Bath Capacity: 10-L

The simple schematic and pictures of unit BP 51 for post-combustion CO₂ capture are shown in Figure 3.5.



a

Figure 3.5: a) simple schematic of the CO₂ absorption/desorption pilot scale unit in

University of Malaya



b

c

Figure 3.5 (Continued): b and c) Pictures of the CO₂ absorption/desorption pilot scale unit in University of Malaya

3.3.3 Solution preparation

In this experimental work, CO₂ absorption/desorption process utilized three types of solvents including 10 wt% MEA aqueous solution, 10 wt% glycerol aqueous solution and the mixture of 10 wt% MEA-10 wt% glycerol aqueous solution. These concentrations were selected based on simulation results in section 3.2.

50 liters of each aqueous solution was prepared based on volume concentrations using the distilled water. Then the solution was poured in the tank (B1) and mixed thoroughly through the circulation of aqueous solution between the tank and the absorber column.

The water used in this experimental work was provided by a Water Still W4L favorit

water purification system. This system provides, distilled water produced through a power input by a chromium plated heater housed in a horizontal glass boiler.

3.3.4 Operation

Fourteen experimental runs were performed in the absorption/desorption unit at 5 different gas flow rates (1.4, 1.7, 2.9, 3.3 and 3.9 L/min) using MEA aqueous solution, glycerol aqueous solution and the mixture of MEA-glycerol aqueous solution. The solvent was fed into the absorption column with the temperature of approximately 29.4°C and 0.7 L/min flow rate. The gas mixture with the composition of 15 v% CO₂ and 85 v% N₂ was entered into the absorber. Gas entering the absorber (K1) is counter-currently contacted with the aqueous solvent. CO₂ is absorbed into the aqueous solvent to form a rich solvent. The rich solvent is then sent through a heat exchanger (W3). In the stripper (K2), heat is provided in the reboiler (W4) in the form of increasing the temperature by oil bath (T1). The liberated CO₂ and the hot, lean solvent leave the stripper from the top and bottom of column.

Liquid samples were collected in the absorber outlet stream (rich solvent) and also in the stripper outlet stream (lean solvent) to check for CO₂ loading. The stripper feed was not sampled because both, the absorber outlet stream and the stripper feed have the same composition. The CO₂ absorption/desorption system was kept at steady state conditions for almost five minutes before liquid samplings. After each sampling, the new CO₂ absorption process was attempted by changing the gas flow rate. In addition to the liquid sampling, instantaneous online measurements such as temperatures, flow rates, and liquid levels were recorded using the software.

3.3.5 Experimental Procedure

First of all, the quantity of solvent was monitored in tank B1 and both pilot plant and computer was turned on for recording online data. In the next step, valves HV7, HV18 and HV25 were made open and switched on both pump 1 and pump 2. When the steady flow was coming from top of K1 and K2, the heater was turned on. Then, adjusted the valves HV7 and HV25 slowly till the level of solution in absorber (K1) and desorber (K2) become stable. Later on, HV28 valve was made open and switched on the cooling water pump. The feed gas was allowed to enter absorber and as the gas bubbles were passed through the solution in the absorber, the flow was adjusted by HV7 and HV25 to keep the level of solution inside the columns (K1 and K2). The steady state conditions in both columns were kept for 5 minutes and the data was recorded using online software. The rich solvent was collected from HV17 valve and lean solvent from HV25. The gas flow rate was increased and again repeated the same procedure and the necessary data was recorded online.

The standard precipitation-titration method is used to determine the CO₂ loadings in the collected samples from absorber and stripper. The experimental conditions of CO₂ absorption process and operating parameters are shown in Tables 3.9 and 3.10, respectively.

Table 3.9: Experimental conditions for the CO₂ absorption in packed column

Operating parameter	Gas	Amine solution	Mixed solvent	Glycerol solution
Temperature (°C)	30	29.4	29.4	29.4
Pressure (barg)	0.11	0.11	0.11	0.11
	Vol frac.	Mass frac.	Mass frac.	Mass frac.
H ₂ O	-	0.9	0.8	0.9
CO ₂	0.15	-	-	-
MEA	-	0.1	0.1	-
N ₂	0.85	-	-	-
Glycerol	-	-	0.1	0.1

Table 3.10: Operating parameters of absorption/desorption unit

Parameter	value
Pressure of pump 1 (barg)	0.5
Pressure of pump 2 (barg)	0.3
Temperature of inlet solvent to absorber (°C)	29.4
Absorber pressure (barg)	0.1
Stripper pressure (barg)	0.1

3.3.6 Solvent titration

Titration was used for two purposes; to determine the concentration/alkalinity of the solution and amount of CO₂ loading, which is commonly used method (Stephanie Anne Freeman, 2011; Hilliard, 2008; T. Wang, 2013).

3.3.6.1 Amine titration

To investigate the amine concentration, a 3 g sample was taken from the prepared solution and diluted with 60 ml distilled water before titration using a 250 ml beaker. To prepare the auto-titrator, the dosing probe was placed in the probe holder and lowered into an empty waste beaker then manually 60 ml of sulfuric acid (H₂SO₄) solution was withdrawn from the titrant to clean the line. The beaker was then placed on the stirrer plate and a small magnetic stirrer was put into it for proper mixing during titration. After settling the beaker, the auto-titrator probe was washed with distilled water, cleaned with tissue paper and then was inserted into the beaker. The probe sensor was fully submerged in the solution, but kept well above from the magnetic stirrer so that it should not damage the probe. A method, which was formulated before starting the actual sample titration based on some trials, was used. Stop conditions were programmed, in the method and other options like pH, number of endpoints (Eps) were left off. Total alkalinity test was performed by using 0.1 M/0.2 N H₂SO₄. Once titration stopped, the volume at last endpoint was used to calculate the total alkalinity.

3.3.6.2 Mixed MEA-glycerol titration

To investigate the alkalinity of the solution, a 3 g sample was taken from the prepared mixed MEA-glycerol solution and was diluted with 60 ml distilled water before titration using a 250 ml beaker and the procedure in section 3.3.6.1 was repeated.

Figure 3.6 is provided as an example, which is showing the titration path of MEA-glycerol blend against sulfuric acid with respect to time. Equation 3.16 was used in calculations of total alkalinity.

$$\text{Total Alkalinity (mol/kg-solution)} = (V_{\text{H}_2\text{SO}_4} \times 0.2) / \text{Sample (g)} \quad (3.16)$$

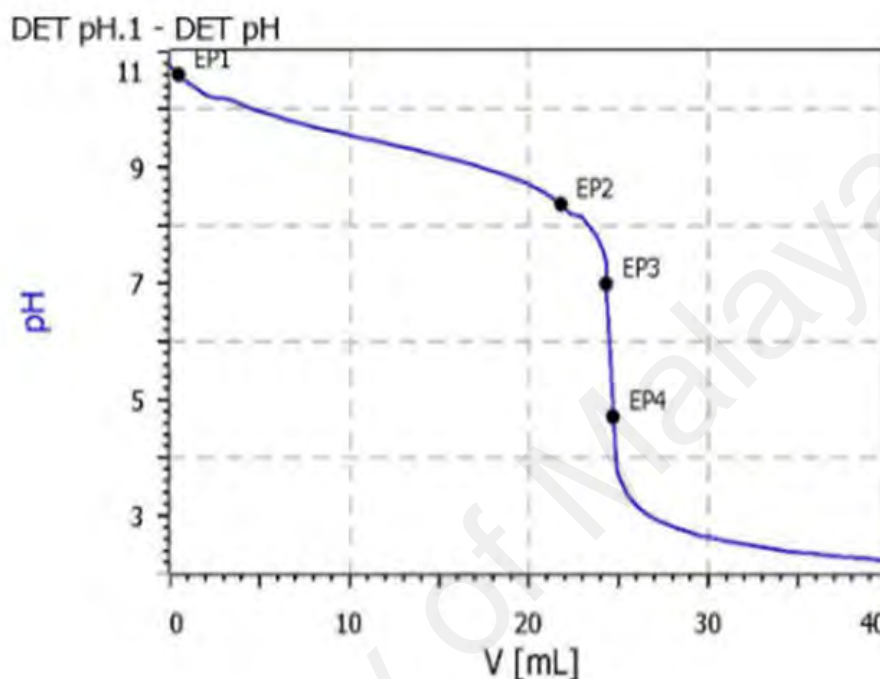


Figure 3.6: Typical titration graph for the determination of total alkalinity of mixed MEA-glycerol solution

3.3.7 CO₂ loading analysis

Solutions were loaded with CO₂ by sparging the mixture of 15 vol% CO₂-85 vol% N₂ through the solutions inside the absorption column. The procedure is similar as described in the section 3.3.4. The CO₂-N₂ gas mixture provided by Linde, special gases centre (Malaysia) passed through the inlet tube at the bottom of the absorber. The distributor dispersed the gas into the solution and the solution absorbs CO₂ when flowing down the absorber. Samples were collected from the bottom of absorber as rich solvent and bottom of desorber as lean solvent. Once the samples were collected during the experiment and CO₂ was loaded in the solution, they were titrated for CO₂ loading verification. For each CO₂ loading, two samples of 2 g were taken, and were mixed with

50 ml of BaCl₂ (0.3 M) and 50 ml NaOH (0.1 M) in a 250 ml Erlenmeyer flask. The mixture was heated and kept at the boiling point for 5 minutes to enhance the barium carbonate (BaCO₃) formation, and then cooled to ambient temperature and filtered by using 0.45 μm pore size filters with the help of vacuum and washed with distilled water. The membrane, covered by BaCO₃, was transferred to a 250 ml beaker. 50-55 ml distilled water was used to wash the crystals and transferred to the beaker to make sure that all precipitated BaCO₃ particles were collected into the beaker. 0.1 N HCl was added to dissolve the BaCO₃. Meanwhile, the weight of HCl was monitored precisely. The samples were heated until 100 °C for at least 5 minutes in the oven to ensure that all the CO₂ are released. Hot acidified samples were cooled to room temperature and then titrated with 0.1 M NaOH in a titrator. In parallel, a blank sample of 0.1 M NaOH and 0.1 N HCl was also titrated. Endpoint method was used for the titration and last endpoint volume was used for calculations. All titration tasks were performed using a titrator (785 DMP Titrino). Equations 3.17 and 3.18 present chemistry of the analysis for the reaction of BaCl₂ with NaOH and BaCO₃ with HCl, respectively:



The following set of equations 3.19-3.23 were used for the calculation of CO₂ loading.

$$n_{CO_2-sample} = \frac{V_{HCl} \times N_{HCl} - V_{NaOH} \times N_{NaOH}}{2} \quad (3.19)$$

$$n_{CO_2-blank} = \frac{V_{HCl} \times N_{HCl} - V_{NaOH} \times N_{NaOH}}{2} \quad (3.20)$$

$$n_{CO_2} = n_{CO_2-sample} - n_{CO_2-blank} \quad (3.21)$$

$$n_{solvent} = C_{solvent} \times m_{sample} \quad (3.22)$$

$$\alpha_{CO_2} = \frac{n_{CO_2}}{n_{solvent}} \quad (3.23)$$

Where V_{HCl} is the volume of HCl solution added to dissolve $BaCO_3$, mL. V_{NaOH} is the volume of NaOH solution used for titration, ml. n_{CO_2} is the number of moles CO_2 /kg solution, $C_{solvent}$ is the alkalinity of the solvent, m_{sample} is mass of the sample, α_{CO_2} is the CO_2 loading/mol alkalinity.

3.4 Validation of simulation study with experimental work

The design, development, and enhancement of a CO_2 absorption/desorption technology tend to be expensive and time consuming. Therefore, suitable model should be developed to reduce the cost and time of process development.

Understanding the CO_2 absorption/desorption process using aqueous mixture of MEA and glycerol and solvent behavior, as well as predicting CO_2 removal capacity of the solvent at different operation conditions by developing a model are necessary to develop and scale up the process to industrial scale. Therefore, simulation study of a pilot scale CO_2 absorption/desorption unit at the University of Malaya was carried out using Aspen Plus (v7.3). The rich CO_2 loading and temperature profiles in the absorber and lean CO_2 loading profiles in stripper were investigated by changing the gas flow rates in the experiment.

3.4.1 Simulation using a rate-based model

CO_2 -MEA-glycerol system was simulated using a rate-based model and simulation results were validated using experimental data of pilot scale columns. CO_2 -MEA-glycerol system is an electrolyte system in which the liquid phase non-ideality must be accounted. ENRTL-RK is adopted as thermodynamic property in the simulations as it is an extended asymmetric ENRTL model for mixed electrolyte systems (Zhao et al., 2013). All chemical reactions, equilibrium constants, kinetic parameters for the

reactions and also Henry's constants have been discussed completely in section 3.2.3 and are employed for this model.

3.4.1.1 Absorber simulation

The simulation is based on a rigorous rate-based model, which was implemented in the process simulator Aspen Plus v7.3. All experimental data used to validate the simulation of CO₂ absorption using MEA-glycerol solution are presented in Tables 3.11 and 3.12. Characteristics of absorption column are specified in Table 3.13. The absorber simulation flowsheet is illustrated in Figure 3.7. Both the absorber and stripper were modelled using RadFrac packed column and twenty stages were used to represent the packing. The number of twenty was chosen based on the simulations in section 3.2. Table 3.14 shows physical characteristics of Raschig rings used in experimental setup for absorber column.

Table 3.11: Experimental conditions for the CO₂ absorption in packed column

Operating parameter	Gas	MEA-Glycerol solution
Temperature (°C)	30	29.4
Pressure (barg)	0.11	0.11
	Vol frac.	Mass frac.
H ₂ O	-	0.8
CO ₂	0.15	-
MEA	-	0.1
N ₂	0.85	-
glycerol	-	0.1

Table 3.12: Actual operating conditions performed

Run	solvent	CO ₂ (v%)	Solvent flow rate (L/min)	Gas flow rate (L/min)
1	MEA-glycerol	15	0.7	1.4
2	MEA-glycerol	15	0.7	1.7
3	MEA-glycerol	15	0.7	2.9
4	MEA-glycerol	15	0.7	3.3
5	MEA-glycerol	15	0.7	3.9

Table 3.13: Characteristics of absorption column

Parameter	Absorber
Column type	Packed
Column internal diameter(mm)	80
Effective packing height(m)	1.5
Packing type	Raschig rings
Nominal packing size (mm)	8

Table 3.14: Physical characteristics of Raschig rings (Oguz et al., 1983)

Material	Size (mm)	Geometric surface area (cm^2/cm^3)	Void fraction (cm^3/cm^3)	Packing factor (cm^{-1})
glass	8	4.61	0.76	10.50

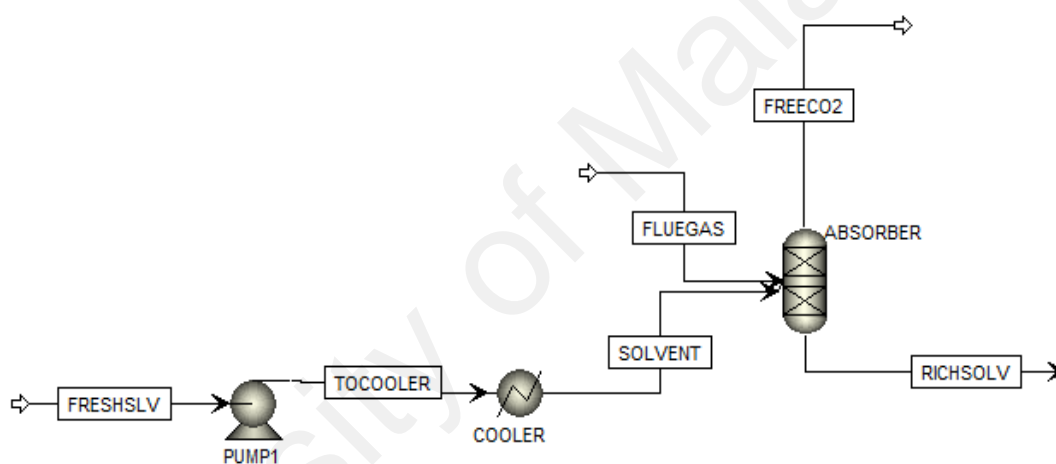


Figure 3.7: Process flow diagram of the absorption process

3.4.1.2 Stripper simulation

The stripper simulation flowsheet is shown in Figure 3.8. The 1st stage and 20th stage in stripper indicate condenser and reboiler, respectively. Table 3.15 and 3.16 present characteristics of desorption column and Raschig rings used in the experimental setup, respectively. Operating conditions in simulation study are the same as experimental setup which are shown in Table 3.17.

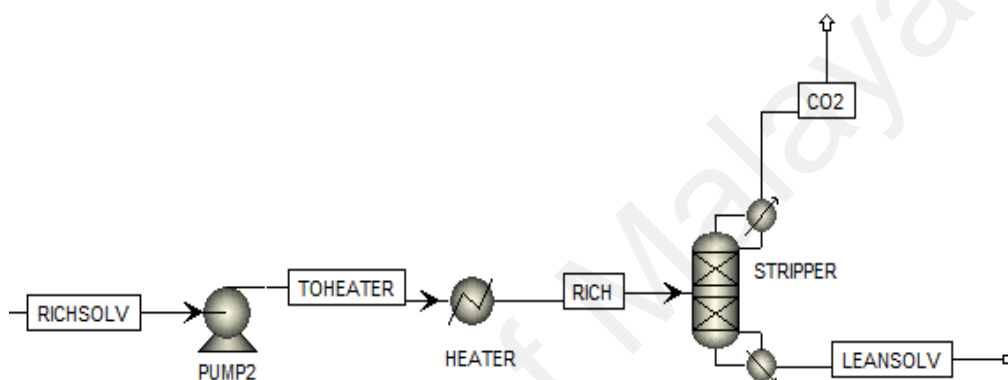


Figure 3.8: Process flow diagram of the desorption process

Table 3.15: Characteristics of desorption column

Parameter	Stripper
Column type	Packed
Column internal diameter(mm)	80
Effective packing height(m)	1.5
Packing type	Raschig rings
Nominal packing size (mm)	8

Table 3.16: Physical characteristics of Raschig rings (Oguz et al., 1983)

Material	Size (mm)	Geometric surface area (cm ² /cm ³)	Void fraction (cm ³ /cm ³)	Packing factor (cm ⁻¹)
glass	8	4.61	0.76	10.50

Table 3.17: Operating conditions in both experimental and simulation study

Parameter	Experimental work	Simulation study
Pressure for pump 1 (barg)	0.5	0.5
Absorber pressure (barg)	0.1	0.1
Pressure for pump 2 (barg)	0.3	0.3
Inlet solvent temperature to absorber (°C)	29.4	29.4
Stripper pressure (barg)	0.1	0.1

CHAPTER 4: RESULTS AND DISCUSSION

4.1 Simulation of CO₂ absorption process using MEA, glycerol and MEA-glycerol aqueous solutions

4.1.1 Validation of rate-based modeling

The modeling of the absorption column was validated using the experimental data obtained from the University of Texas at Austin (Dugas, 2006).

Equation 4.1 presents the average absolute deviation percent (%AAD) and used to calculate the deviation between the experimental and simulated data. The calculated errors are presented in Table 4.1.

$$\%AAD = \frac{100}{N} \sum_i^N \frac{|Y_i^{sim} - Y_i^{Exp}|}{Y_i^{Exp}} \quad (4.1)$$

where N is the number of process variables; and Y_{Exp} and Y_{sim} are the experimental and simulated data of the component i, respectively. The percentage of CO₂ removal is a key parameter for determining the efficiency of a CO₂ operation unit. This parameter is calculated using equation 4.2:

$$\% CO_2 removal = 1 - \left(\frac{\text{molar flowrate}_{CO_2 \text{ in outlet gas from absorber}}}{\text{molar flowrate}_{CO_2 \text{ in flue gas}}} \right) \quad (4.2)$$

4.1.1.1 Base case simulation (CO₂-MEA)

The comparison of experimental and simulation results for CO₂-MEA system are presented in Table 4.1. Figures 4.1-4.3 describe the liquid temperature profiles along the absorption column for the CO₂-MEA system; these profiles were validated using the experimental data of Dugas (Dugas, 2006). Figure 4.1 shows the comparison of mixed and counter-current flow models. Several models for mass transfer coefficient correlations and interfacial area are incorporated in the rate-based model. The correlations proposed by Onda et al. (Onda et al., 1968) and Bravo and Fair (Bravo & Fair, 1982) were employed and temperature profiles were compared in Figure 4.2.

Figure 4.3 describes the comparison of three film-resistance methods (Discrxn–Filmrxn, Filmrxn–Filmrxn, and Discrxn–Film) for liquid and vapor phases.

University of Malaya

Table 4.1: Comparison of experimental and simulation data for absorber and stripper

	Lean loading (mol CO ₂ /mol MEA)		Rich loading (mol CO ₂ /mol MEA)				CO ₂ removal%			
	Experimental (Dugas, 2006)	Simulation (this study)	Experimental (Dugas, 2006)	Simulation (this study)	AAD%	Simulation (Ying Zhang et al., 2009)	Experimental (Dugas, 2006)	Simulation (this study)	AAD%	Simulation (Ying Zhang et al., 2009)
Absorber	0.281	0.281	0.539	0.492	8.72	0.480	69	66.4	3.768	68
Stripper	0.286	0.284	-	-	-	-	-	-	-	-

The presence of temperature bulge in the absorber, Figures 4.1-4.3, may be explained by the fact that liquid absorbs CO₂ when flowing down the absorber; this process generates reaction heat and increases the liquid temperature. Temperature reduction at the bottom of the absorber is caused by cold gas, which enters from the bottom of the absorber and comes in contact with hot liquid flowing downwards. Heat of absorption from the hot liquid by the cold gas decreases the liquid temperature; thus, the temperature bulge appears at the top of the column. In summary, temperature increases when the amount of heat used is less than the heat relieved from the absorption reaction. Figures 4.1-4.3 show the temperature bulge located near the top of the absorption column.

Based on Figure 4.1 the profile obtained using the counter-current flow model is unstable therefore the mixed flow model was considered for the simulations. However, the countercurrent flow model yields precise results for packing because in this model, the bulk properties for each phase are the average of the inlet and outlet properties but in the mixed flow model, the bulk properties for each phase should be the same as the passing conditions for the phase leaving that stage (Ying Zhang et al., 2009; Aspen Technology, 2011). The estimated absorber temperatures are higher than the experimental temperatures; the discrepancy in the results could be due to the fact that heat loss is not considered in the simulation.

Since, mass transfer coefficients and interfacial area for the IMTP random packing (number 40) are predicted with the Onda et al., 1968 (Onda et al., 1968; Ying Zhang et al., 2009), Figure 4.2 shows that the profile obtained using the model of Onda et al. (Onda, et al., 1968) is close the experimental profile.

The profiles obtained from filmrxn method for both liquid and gas phases (Figure 4.3) are closer to the experimental data than the two other methods. Furthermore,

temperature profiles calculated from Discrxn–Filmrxn and Discrxn–Film methods overlap each other.

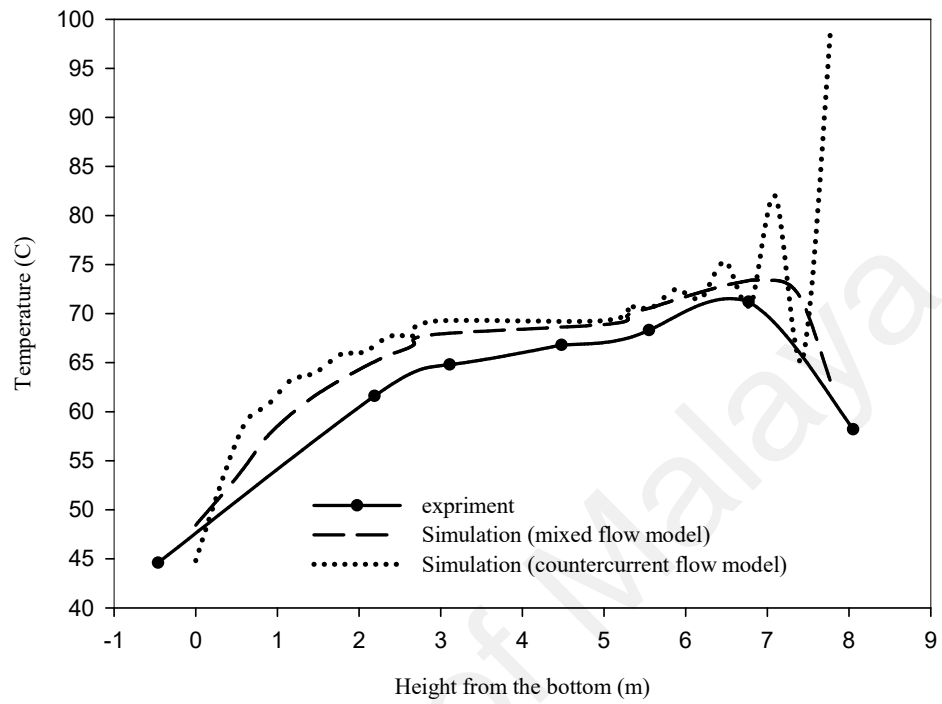


Figure 4.1: Liquid temperature profile for the absorber

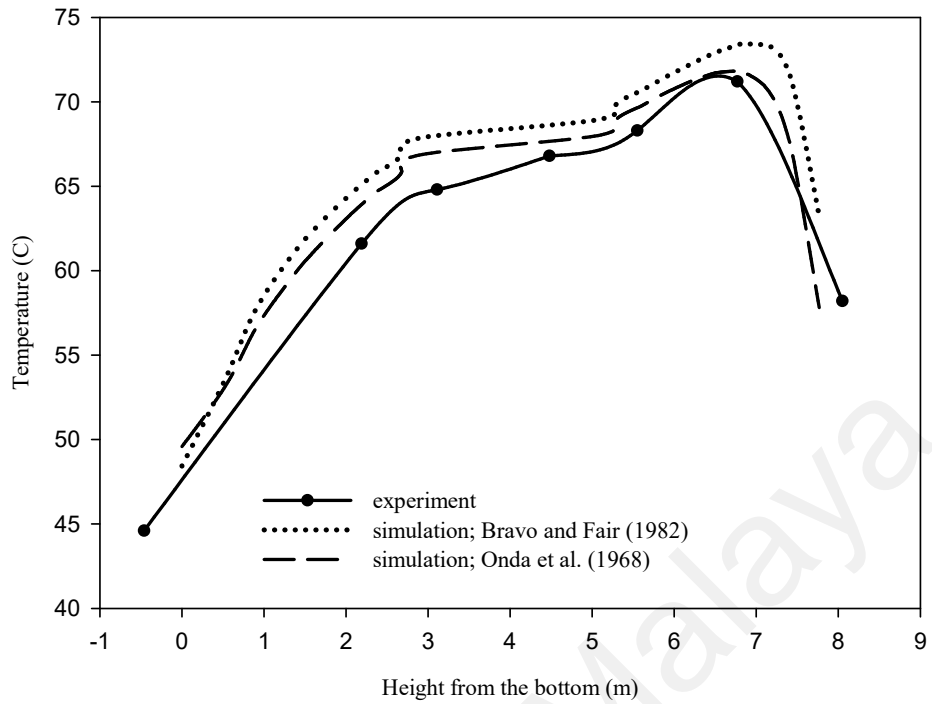


Figure 4.2: Temperature profiles for the liquid phase in the CO₂-MEA system with the mixed flow model

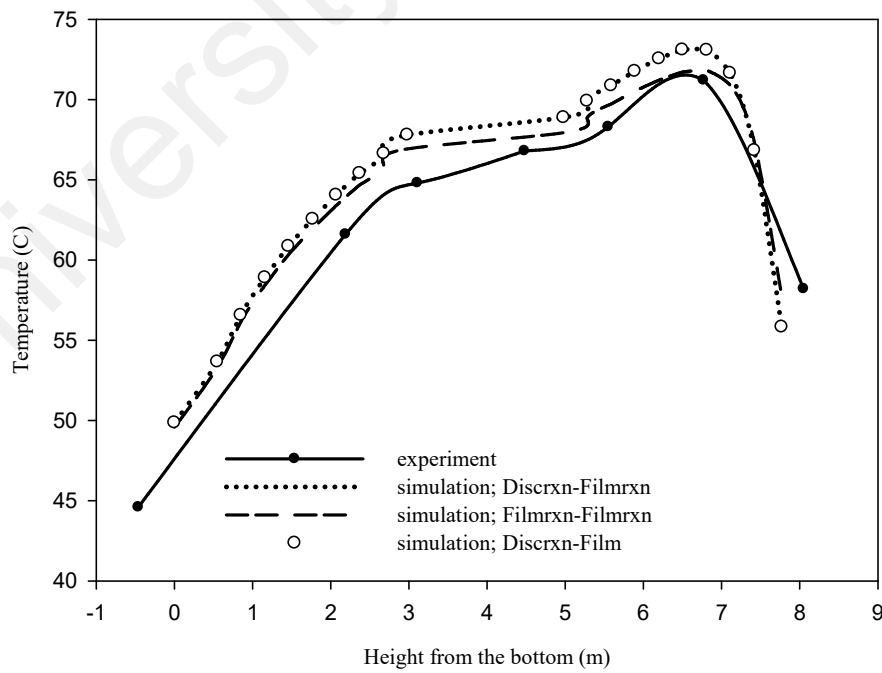


Figure 4.3: Temperature profiles for the liquid phase in the CO₂-MEA system with different film resistances

Figure 4.4 shows the comparison of temperature profiles between experimental and simulation data for the stripper. Some experimental data, for example reboiler heat duty cannot be interpreted through stripper simulation because in the experimental conditions there is heat loss for the reboiler but in the simulation the heat loss is neglected and the reboiler heat duty in the simulation study is lower than the experimental work. Therefore, in the first part of study, most of the discussion is based on the results obtained in the absorption column.

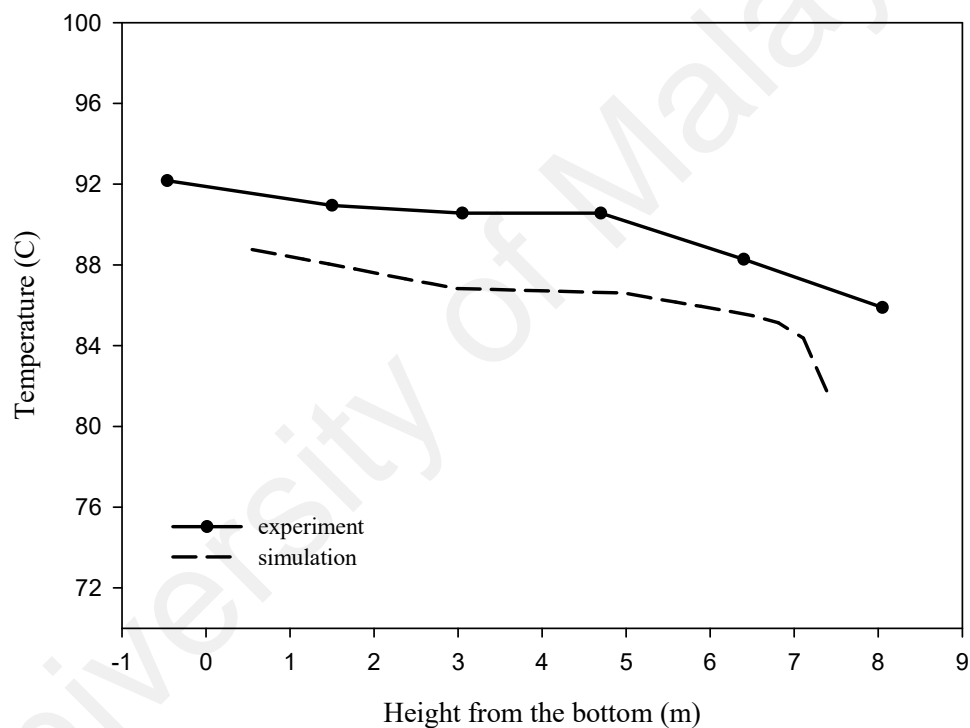


Figure 4.4: Temperature distribution along the stripper

4.1.1.2 Glycerol solvent (CO₂-glycerol)

Figures 4.5 and 4.6 indicate the CO₂ mole fractions in liquid and vapor phases, respectively, along the absorber for different glycerol concentrations in water. The amount of CO₂ absorbed decreases with increasing glycerol concentration. CO₂ absorption is reduced when the glycerol concentration is increased to 60–90 wt%, and

the profiles are close to each other within 2–10 wt% and 40–60 wt% glycerol. The absorption is enhanced within the range of 10–40 wt%. As such, the amount of water in physical solvents is important for CO₂ absorption efficiency. The increase in glycerol concentration is correlated with viscosity, which can be reduced by adding water. In summary, the amount of CO₂ absorbed decreases in high glycerol concentrations with decreasing amount of water. Hence, 10–40 wt% is the most suitable glycerol concentration for CO₂ absorption.

Comparison of the results obtained from Figure 4.6 shows that the amount of CO₂ in the outlet gas from the absorber decreases with decreasing glycerol concentration within the range of 10–40 wt%. In this concentration range, 10 wt% glycerol exhibits the lowest CO₂ concentration in the vapor phase.

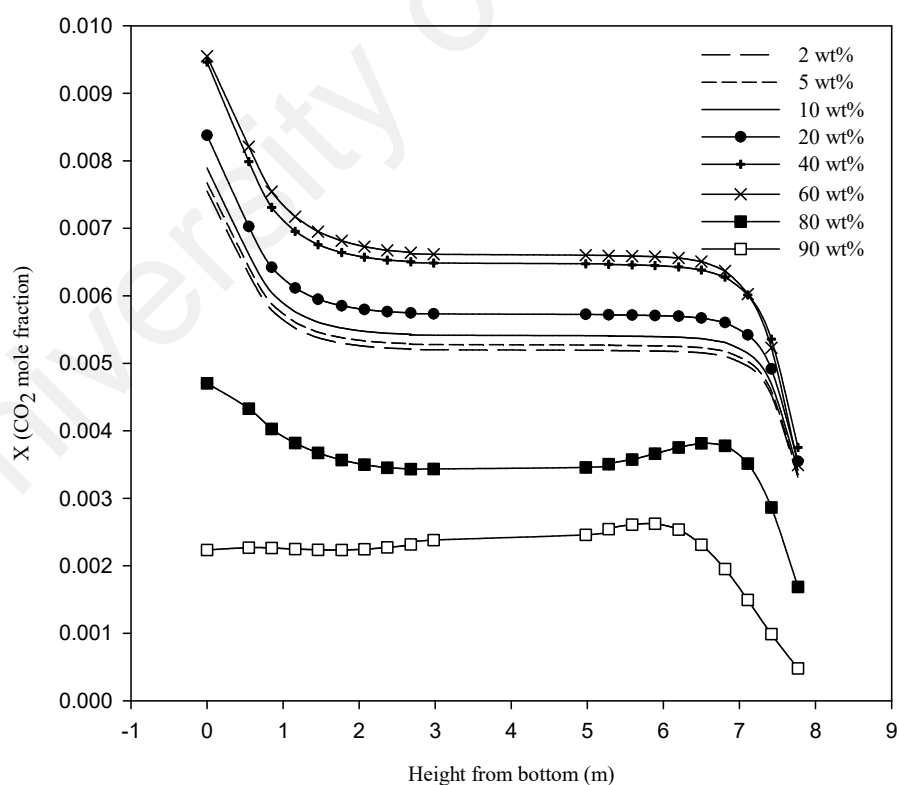


Figure 4.5: CO₂ concentration in the liquid phase along the absorption column for glycerol solvent

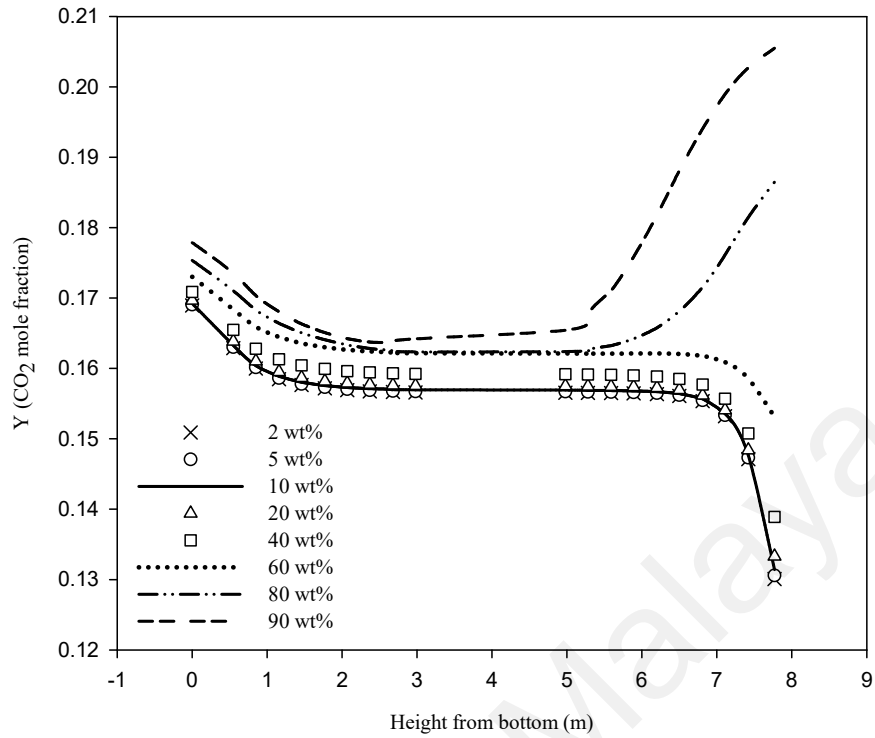


Figure 4.6: CO₂ concentration in the vapor phase along the absorption column for glycerol solvent

As shown in Figure 4.7, when the glycerol concentration increases in the solution, CO₂ removal efficiency decreases.

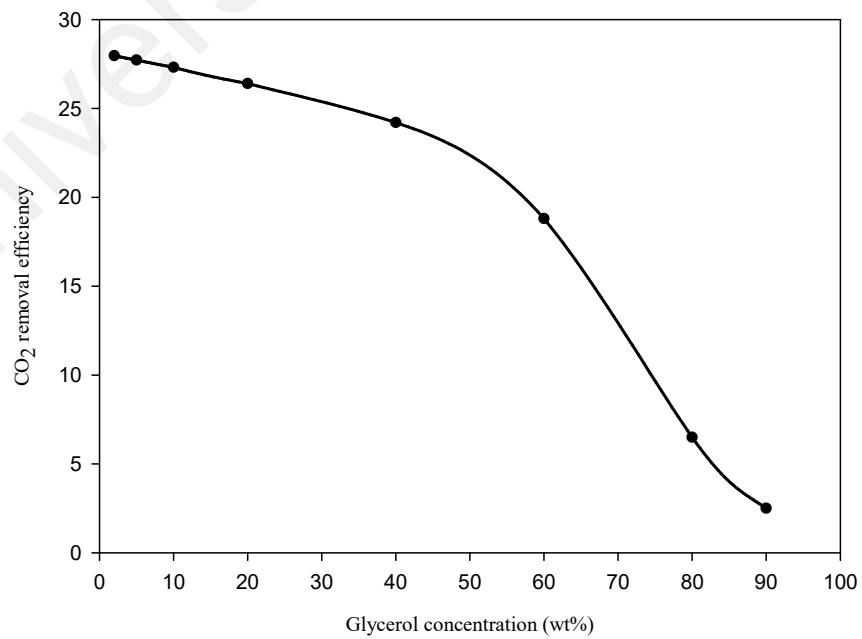


Figure 4.7: CO₂ removal efficiency for different glycerol concentrations in water

Figure 4.8 indicates the H₂O mole fraction in the vapor phase along the absorber for different glycerol concentrations in water. The amount of water vapor in the outlet gas from the absorber decreases with increasing glycerol concentration in the solution. Based on Figures 4.5-4.8, the optimal glycerol concentration in CO₂ capture is 10 wt%.

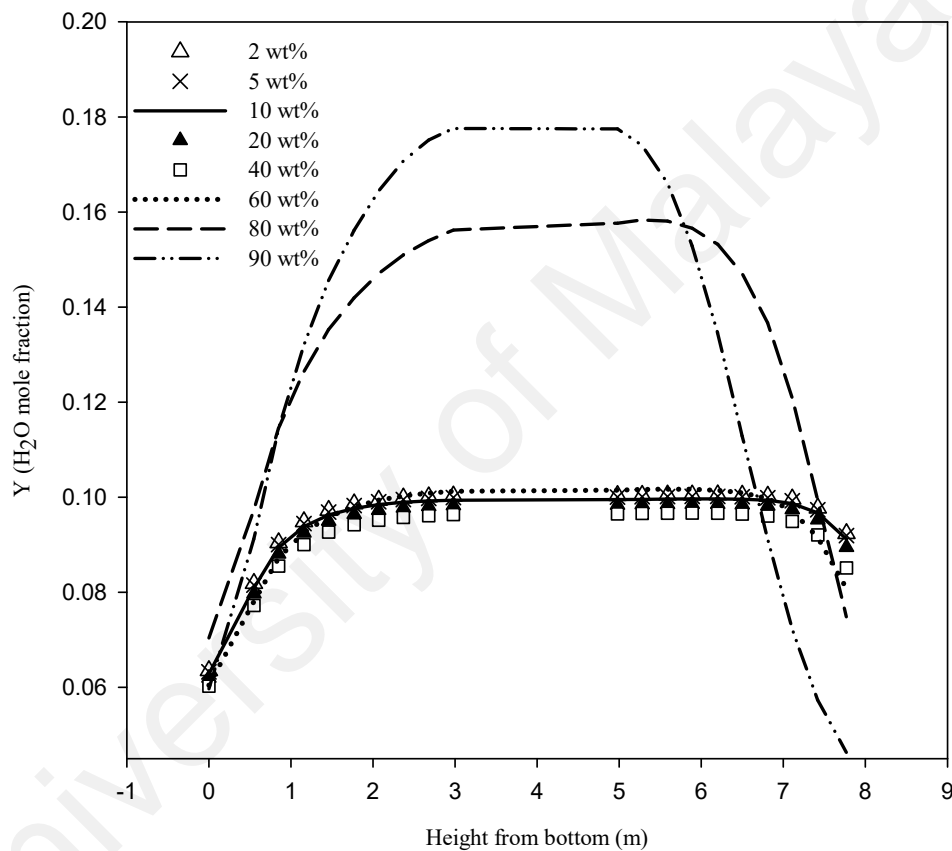


Figure 4.8: H₂O mole fraction in the vapor phase along the absorber for different glycerol concentrations in water

Figure 4.9 describes the liquid temperature profile along the absorption column for various glycerol concentrations in water. A very broad temperature bulge occurs, and the temperature rapidly changes at the top and bottom of the absorber with increasing glycerol concentration.

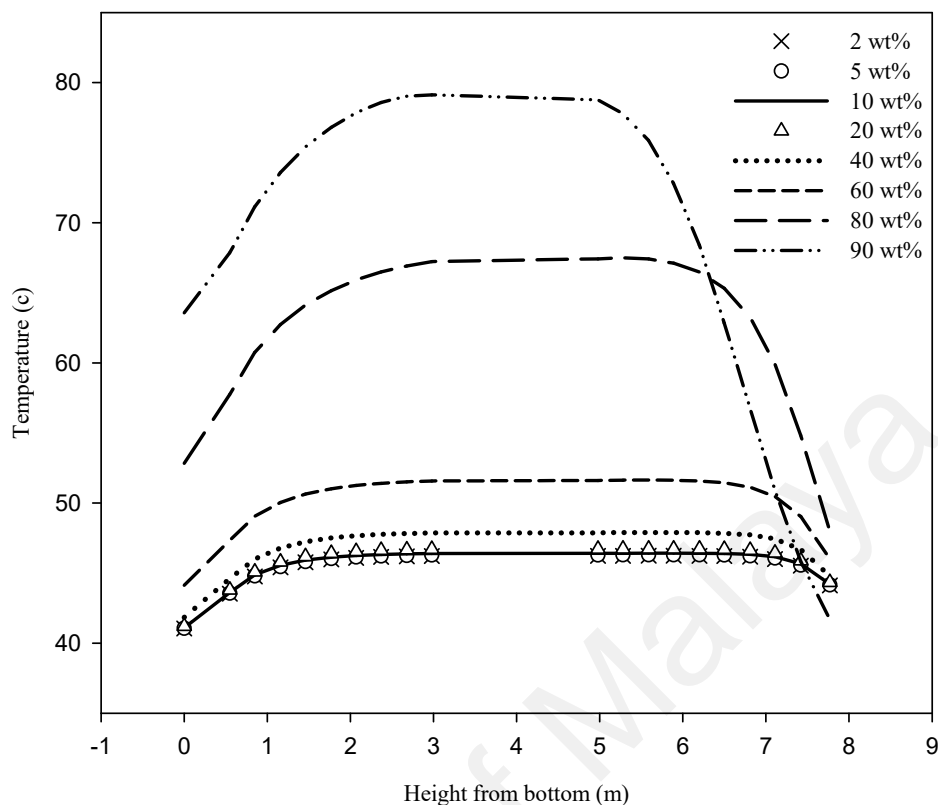


Figure 4.9: Liquid temperature profiles along the absorber for different glycerol concentrations in water

4.1.1.3 Glycerol promoter in MEA process (CO₂-glycerol-MEA)

Figure 4.10 shows that the temperature profiles significantly differ between MEA and glycerol processes. Furthermore, the reaction of CO₂ with MEA causes a temperature bulge in the absorber; this temperature bulge influences the absorption rate. Thus, the temperature bulge increases with increasing MEA concentration in the mixed solvent. As predicted, the temperature profile for 10 wt% MEA solution at the bottom of the column is close to that obtained from 10 wt% MEA–10 wt% glycerol solution. However, the bulge for 10 wt% glycerol–10 wt% MEA solution is higher than that for 10 wt% MEA.

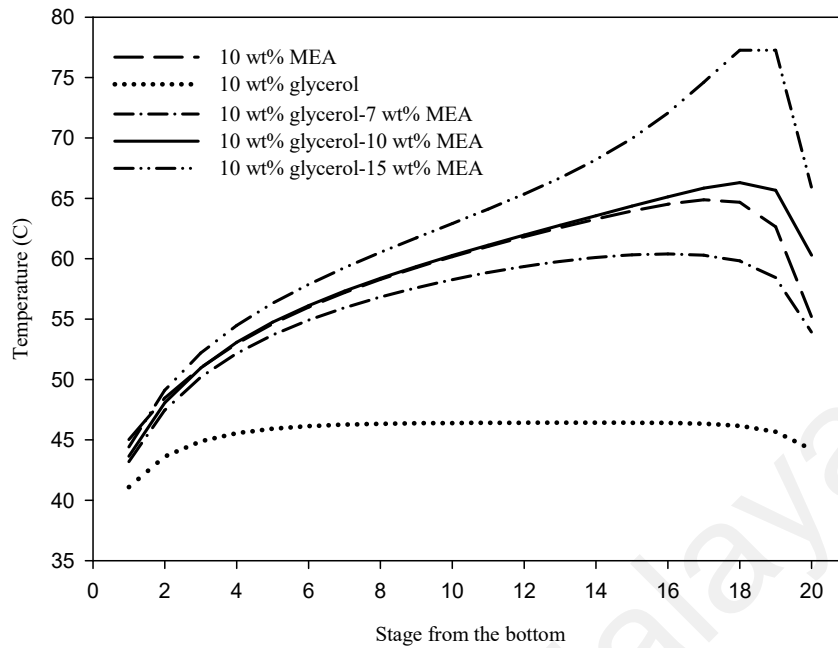


Figure 4.10: Liquid temperature profiles along absorber for MEA, glycerol, and glycerol–MEA solutions

Figure 4.11 shows the comparison among the five profiles of the liquid CO_2 mole fractions along the absorption column for MEA and glycerol solutions and their mixtures. The CO_2 mole fraction in the liquid phase for MEA solution is higher than that in glycerol solution; upon addition of glycerol to MEA, the liquid CO_2 mole fraction increases compared with the glycerol profile. The profile obtained from 10 wt% glycerol–7 wt% MEA is lower than that from the 10 wt% MEA profile; by contrast, 10 wt% glycerol–10 wt% MEA profile is located higher than the MEA profile. Moreover, the use of 15 wt% MEA in MEA–glycerol significantly increases the liquid CO_2 mole fraction at the bottom of the column.

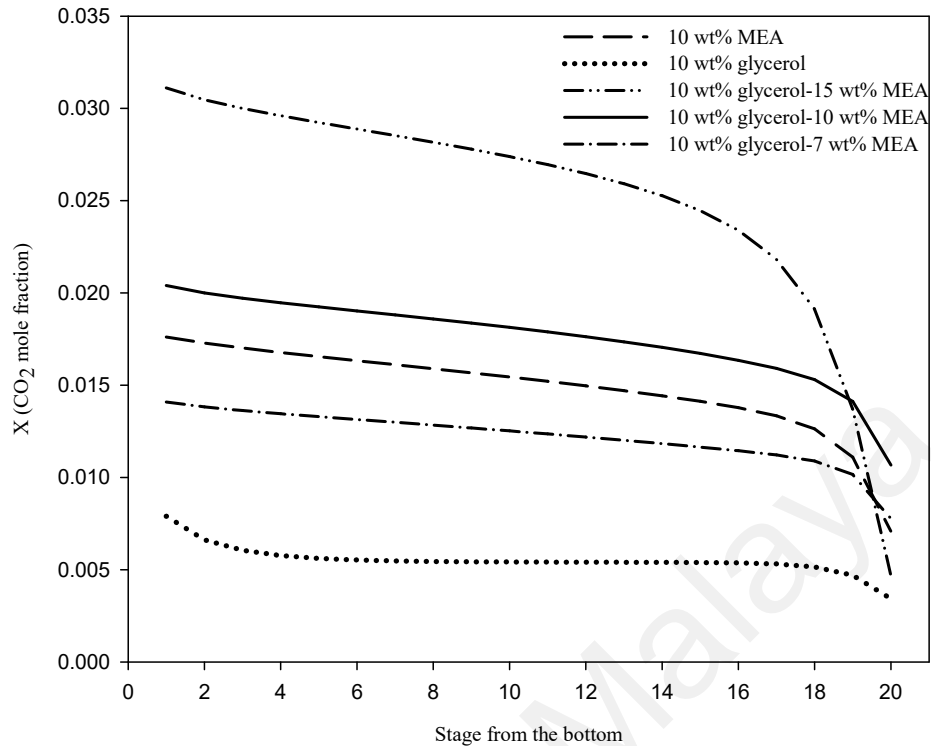


Figure 4.11: Comparison of CO₂ mole fractions in the liquid phase along the absorber for MEA, glycerol, and their mixtures

Figures 4.12 and 4.13 show the comparison of CO₂ and H₂O mole fractions in the vapor phase along the absorption column, respectively. As shown in Figure 4.12, under the same operating conditions for MEA and glycerol processes, the amount of CO₂ in the outlet gas from the absorption column for MEA is less than that for glycerol. By contrast, the H₂O amount is higher than that obtained from the glycerol profile (Figure 4.13). With increasing MEA concentration in the mixture, H₂O mole fraction in vapor phase increases. The profiles obtained for CO₂ composition show that the amount of CO₂ in the outlet gas from the absorber decreases with increasing MEA concentration in the mixture of MEA–glycerol.

The addition of 7 wt% MEA to the glycerol solution decreases the CO₂ concentration in the outlet gas from the absorber, but 10 wt% MEA solution alone can absorb more CO₂.

The CO₂ concentration in the outlet gas for 10 wt% glycerol-15 wt% MEA solution is less than that of 10 wt% MEA solution.

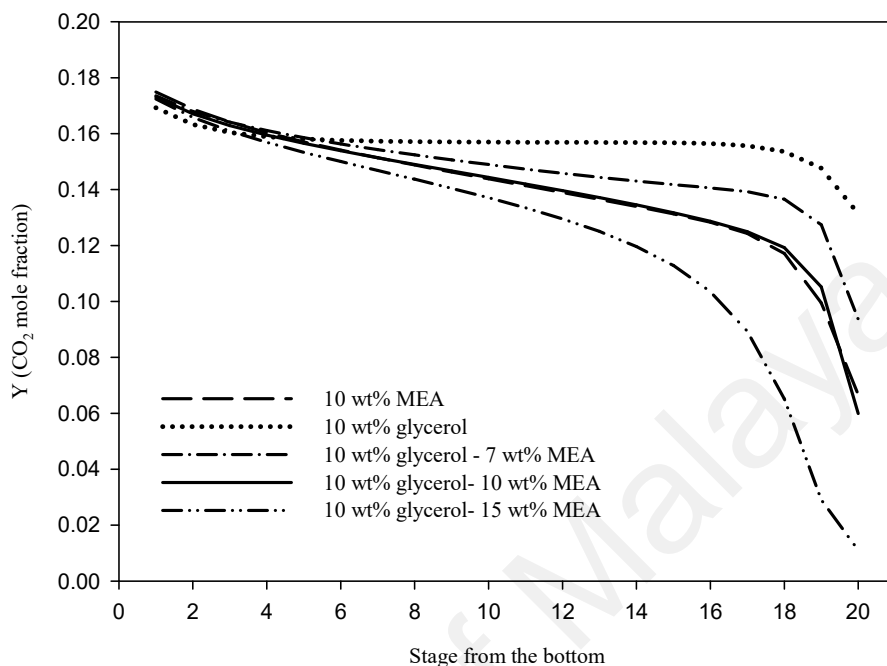


Figure 4.12: Comparison of CO₂ mole fractions in the vapor phase along the absorber

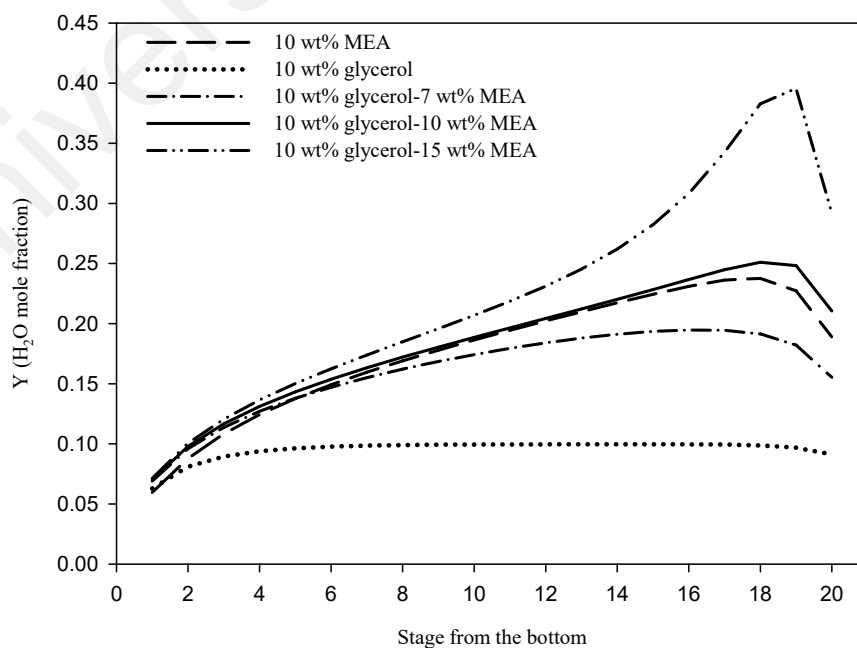


Figure 4.13: Comparison of H₂O mole fractions in the vapor phase along the absorber

The optimal concentration for the mixed solvent is 10 wt% glycerol–10 wt% MEA. Despite that 10 wt% glycerol–15 wt% MEA shows high CO₂ absorption, the energy requirements of this system for solvent regeneration are higher than those of 10 wt% glycerol–10 wt% MEA. Hence, the use of 10 wt% MEA solution is considered more economical.

Amine concentration must be selected carefully considering solution viscosity and operating condition. In industrial applications, the circulation rate decreases with increasing amine concentration, thereby reducing the operating cost.

Figure 4.14 depicts the comparison of the apparent CO₂ mole fraction (XAPP) in CO₂ rich stream to the stripper (RICH-IN stream in Figure 3.2). Notably, the CO₂ mole fraction in rich stream to the stripper for 10 wt% glycerol solution is 0.008. The amount of CO₂ absorbed increases from 0.008 for 10 wt% glycerol solution to 0.014, 0.020, and 0.031 for 7 wt%, 10 wt%, and 15 wt% MEA mixed with glycerol, respectively.

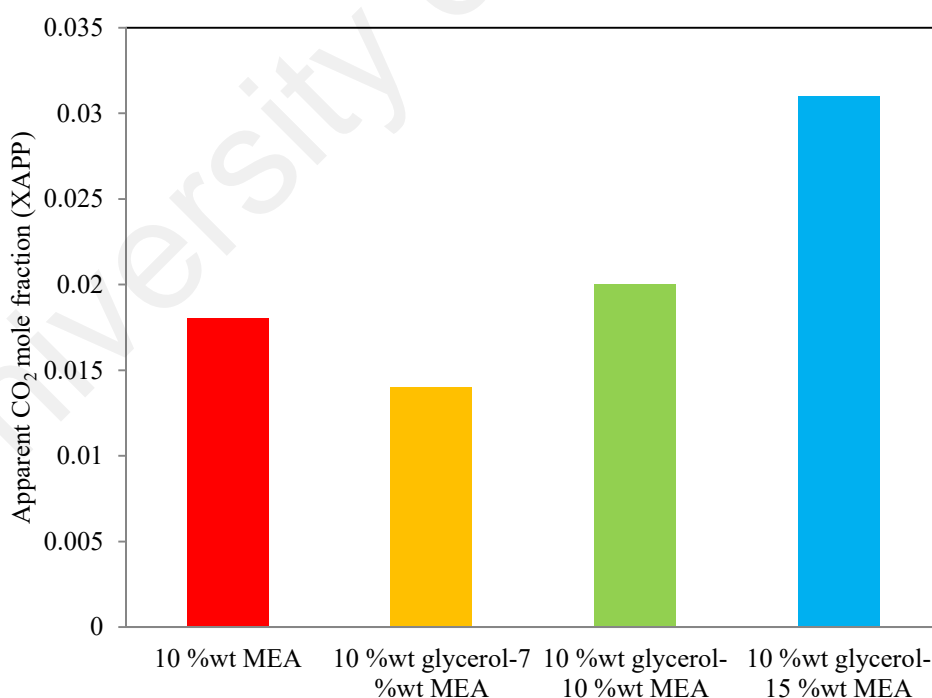


Figure 4.14: Comparison of apparent CO₂ mole fractions in rich stream to the stripper

Figure 4.15 compares XAPP along the stripper in mixtures of glycerol and MEA of different concentrations. CO₂ desorption starts from stage 2 as CO₂ mole fraction reduces toward the bottom of the stripper, and lean solvent exits from stage 20.

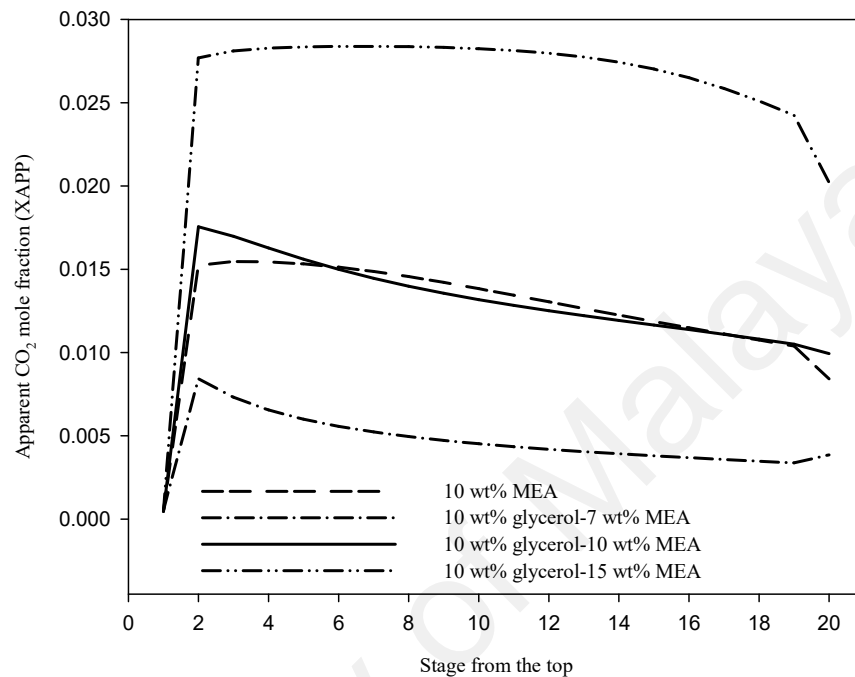


Figure 4.15: Comparison of apparent CO₂ mole fraction along the stripper

As shown in Figure 4.16, in the same concentration of MEA and glycerol, the amount of CO₂ removed for MEA is considerably higher than that in glycerol. CO₂ removal efficiency for 10 %wt glycerol aqueous solution is 27.31% but, CO₂ removal percentage increases when MEA is mixed with glycerol. The CO₂ removal efficiency increases steadily with increasing MEA concentration. Comparison of the results shows that the amounts of CO₂ removed slightly differ between the mixtures of 10 wt%, 5 wt%, and 2 wt% glycerol with 10 wt% MEA solutions and 10 wt%, 5 wt%, and 2 wt% glycerol with 7 wt% MEA solutions.

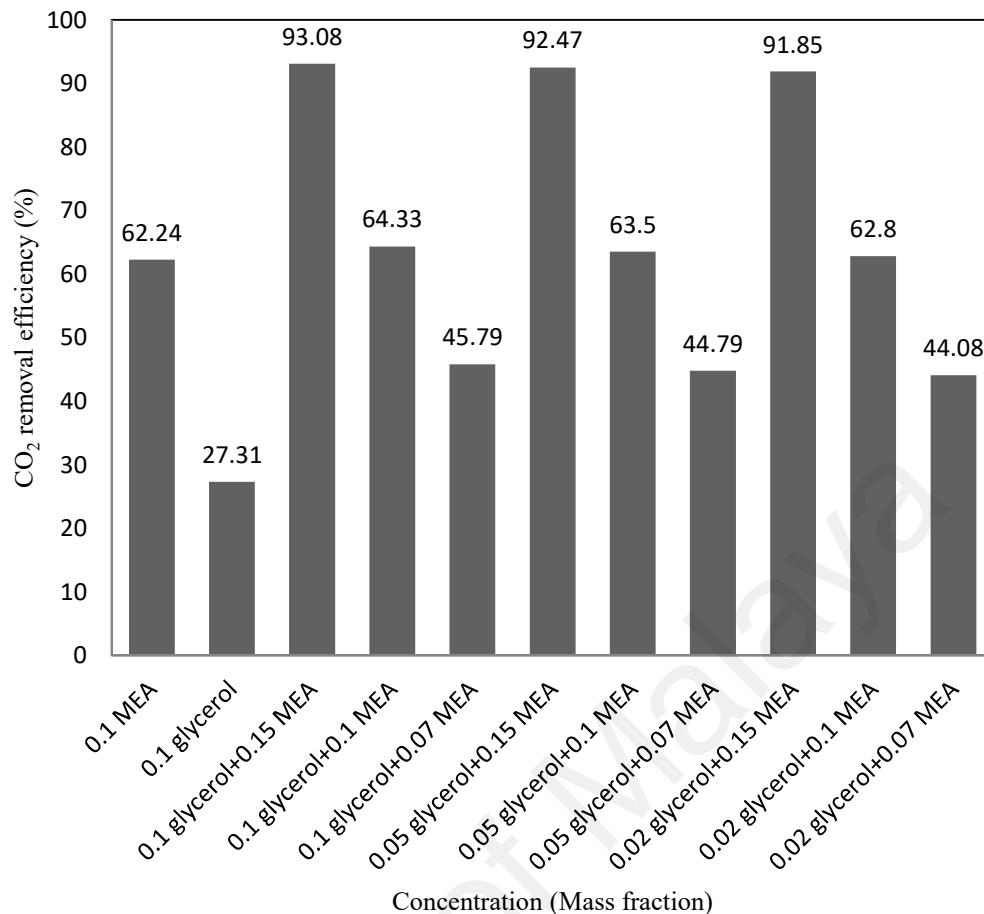


Figure 4.16: Comparison of CO₂ removal percentage for various concentrations of MEA/ glycerol solution

Figure 4.17 illustrates the amount of CO₂ loading along the absorber. In the experiment, this loading is based on the absorber height in three points (rich, middle, and lean loading) (Dugas, 2006). The absorber CO₂ loading computed from 10 wt% glycerol is lower than that from 10 wt% MEA; however, the CO₂ loading increases with the addition of MEA in the mixture of MEA-glycerol.

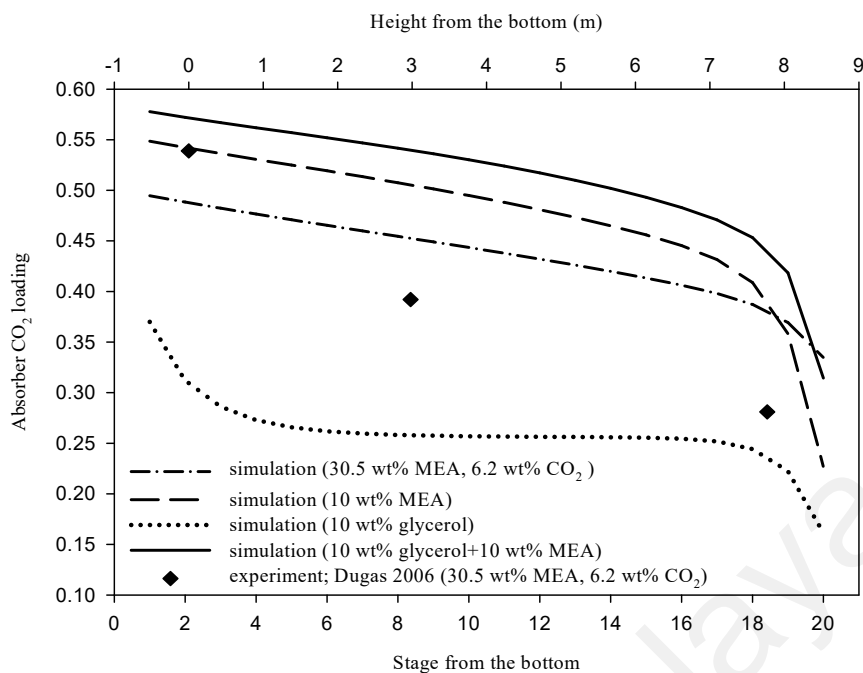


Figure 4.17: CO₂ loading along the absorption column

Figure 4.18 depicts the comparison of reboiler heat duty for simulations in the present study under the same operating conditions. Under the same concentrations of solvents, the reboiler heat duty for the mixture of MEA–glycerol is higher than that for MEA and glycerol alone because of higher amount of CO₂ absorbed. The obtained results from this part of study are summarized in Table 4.2.

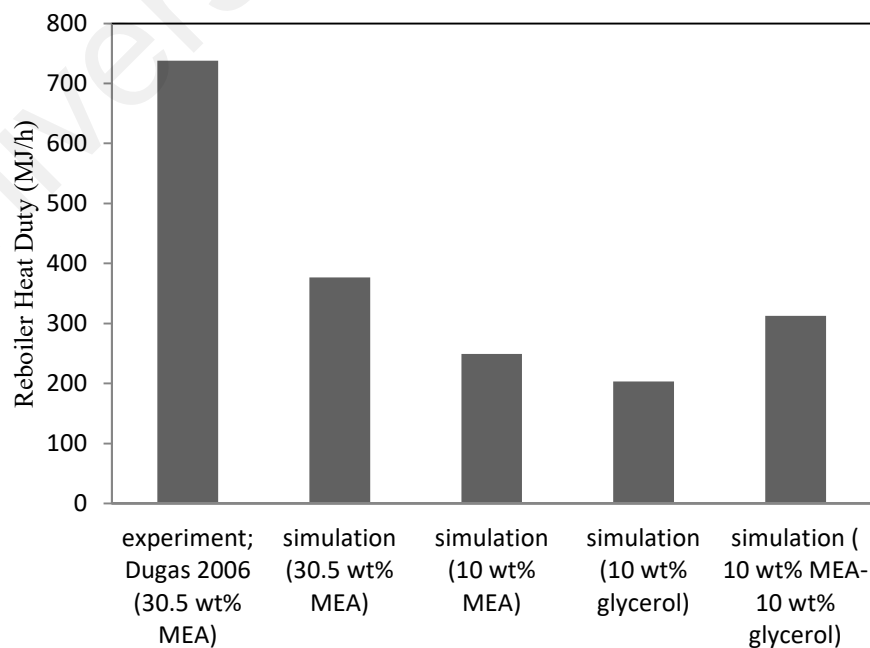


Figure 4.18: Comparison of reboiler heat duty between the present simulation results

Table 4.2: Summary of the obtained results for CO₂-MEA, CO₂-MEA-glycerol and CO₂-glycerol systems

	Simulation (10 wt% MEA-10 wt% glycerol)	Simulation (10 wt% MEA)	Simulation (10 wt% glycerol)	Simulation (30.5 wt% MEA)	Experiment; Dugas (Dugas, 2006)(30.5 wt% MEA)
CO ₂ removal efficiency (%)	64.33	62.24	27.31	66.4	69
Absorber lean loading (mol CO ₂ /mol alkalinity)	-	-	-	0.281	0.281
Absorber rich loading (mol CO ₂ / mol alkalinity)	0.571	0.562	0.381	0.492	0.539
Reboiler Heat Duty(MJ/h)	312.5	249.25	203.15	376.82	738
Stripper lean loading (mol CO ₂ / mol alkalinity)	0.278	0.25	trace	0.284	0.286

Figure 4.19 shows the comparison of the temperature profile along the absorber height between the experimental data reported by Dugas (Dugas, 2006) and the simulation results for 10 wt% glycerol–10 wt% MEA solution. The simulation results are plotted in two mixed flow and counter-current flow models. By comparing these profiles, both mixed flow model and experimental profiles exhibit a temperature bulge, located close to the top of the column. However, in the profile calculated from the counter-current flow model, the temperature bulge is located near the bottom of the absorption column.

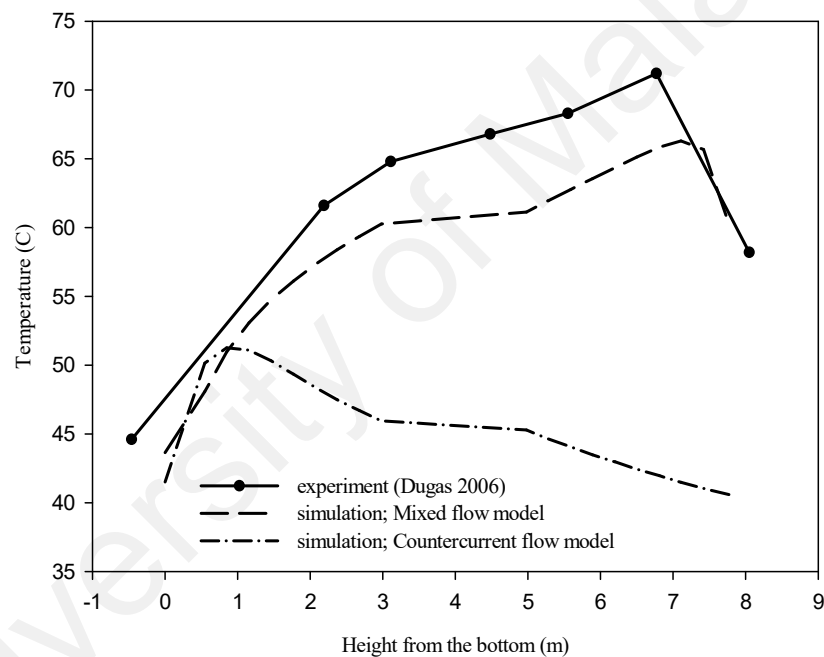


Figure 4.19: Comparison of temperature profile between MEA solution and glycerol–MEA solution along the absorption column

4.1.2 The Comparison of ENRTL-RK and ELECNRTL thermodynamic models

Comparison of the results obtained from Figures 4.20 and 4.21 shows that the profiles of temperature and CO₂ loading in the absorber are influenced by varying the thermodynamic model. The temperature of the absorption column using ENRTL-RK thermodynamic model is higher than that of ELECNRTL (Figure 4.20); this result can be explained by the fact that the reaction heat of CO₂ with MEA is high and thus

increases the CO₂ reaction rate. An increase in the CO₂ reaction rate leads to an increase in the amount of CO₂ absorbed; therefore, the CO₂ loading along absorber determined using ENRTL-RK thermodynamic model is larger than that derived using ELECNRTL (Figure 4.21). Thus, ENRTL-RK model is an improved version of ELECNRTL.

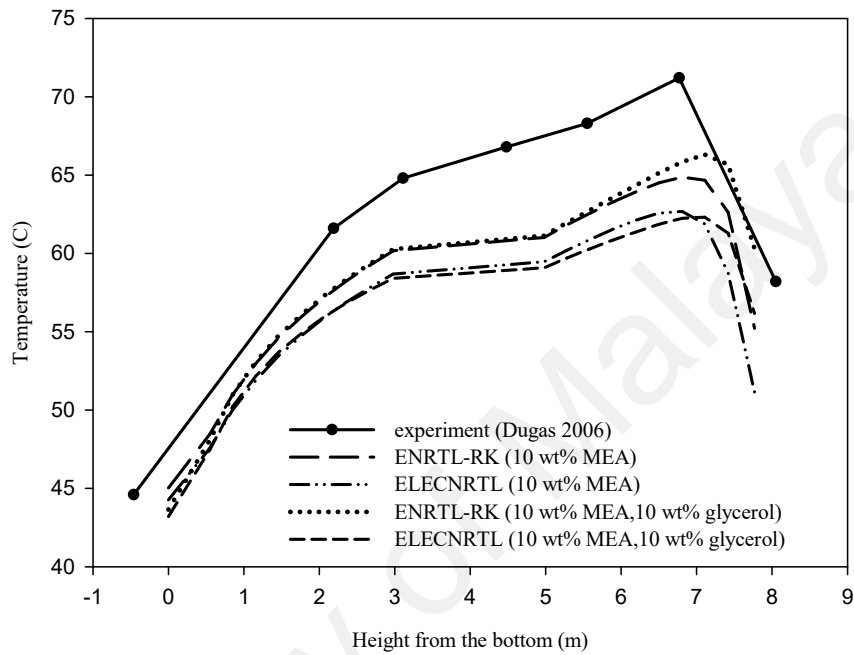


Figure 4.20: Temperature profile along the absorber

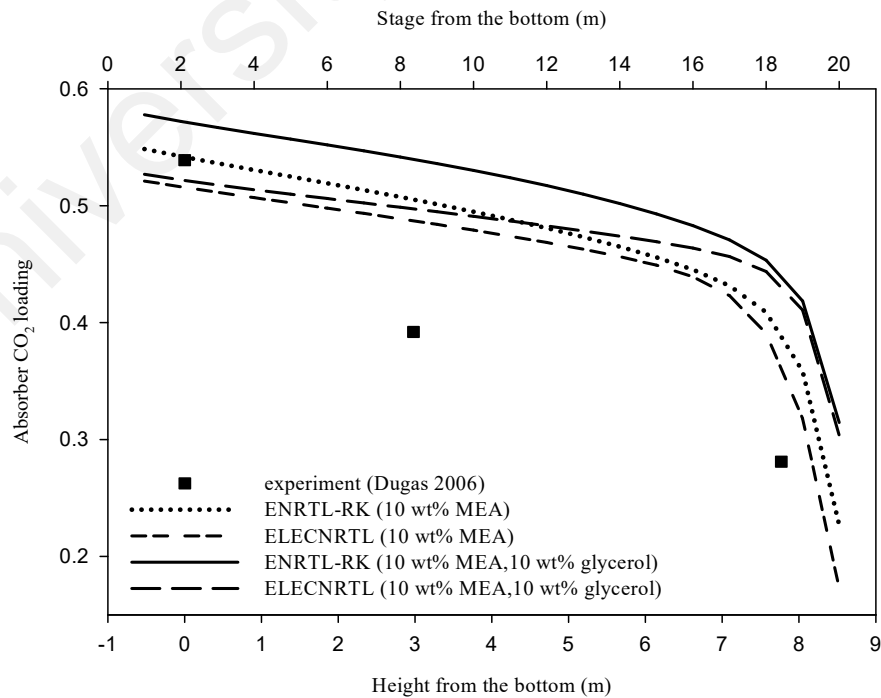


Figure 4.21: CO₂ loading profile along the absorber

4.2 Experimental study of CO₂ absorption in a packed column

Fourteen experimental runs were carried out with various liquid to gas (L/G) flow ratios in the pilot-scale absorber and stripper columns. The CO₂ concentration in the liquid phase was evaluated only at the outlet stream of the absorber and stripper columns by collecting the samples during the experiment. Table 4.3 illustrates the performance of both absorber and stripper columns. Based on this experimental study, hybrid solution MEA-glycerol shows a better CO₂ absorption over aqueous MEA solution. Sample from stripper lean CO₂ loading in run No. 4 was not taken due to some problems.

As can be seen from Table 4.3, rich CO₂ loadings in the absorption column for glycerol solution are less than MEA solution. Furthermore, rich CO₂ loadings for the mixture of MEA-glycerol aqueous solution (runs No. 5-9) are more than MEA aqueous solution and glycerol aqueous solution at the same gas flow rates. According to the results, glycerol can be used as promoter with MEA solvent to enhance the CO₂ absorption capacity.

Table 4.3: Operating conditions used in this experimental study with 0.7 L/min solvent flow rate and CO₂ (15 v%)-N₂ (85 v%) gas mixture

Run	Solvent	Gas flow rate (L/min)	Absorber rich stream CO ₂ loading	Stripper lean stream CO ₂ loading
1	MEA	1.4	0.0365	0.0344
2	MEA	1.7	0.0456	0.0341
3	MEA	2.9	0.0675	0.0312
4	MEA	3.3	0.126	-
5	Mixed	1.4	0.0519	0.0402
6	Mixed	1.7	0.0561	0.0389
7	Mixed	2.9	0.0759	0.0351
8	Mixed	3.3	0.1446	0.0303
9	Mixed	3.9	0.1596	0.0296
10	Glycerol	1.4	0.018	0.011
11	Glycerol	1.7	0.021	0.019
12	Glycerol	2.9	0.0508	0.0409
13	Glycerol	3.3	0.087	0.039
14	Glycerol	3.9	0.098	0.0325

Figure 4.22 shows the influence of gas flow rate on rich stream CO₂ loadings between MEA solution, glycerol solution and mixed MEA-glycerol solution in the absorption/desorption unit with 15 vol % CO₂ feed composition. Based on this Figure, an increase of the gas flow rate increases the amount of CO₂, which is moved between the phases thus, the CO₂ rich loading increases. The rich loading for the mixed MEA-glycerol solution is clearly higher than that for MEA solution. On the other hand, rich CO₂ loading for glycerol solution is lower than those for MEA and mixed solution in the same operating conditions. A lower rich CO₂ loading for the glycerol solution means that the capacity of this physical solvent for CO₂ absorption is less than MEA solution in the same operating conditions. The reaction 4.3 describes the CO₂ absorption by MEA.



Based on the reaction two mole of MEA absorbs one mole of CO₂ (Kingma, 2016). As a result, MEA has a maximum loading of 0.5 mol CO₂/mol MEA (Witzøe, 2015). On the other hand, the glycerol-rich phase dissolves CO₂ at mole fractions up to 0.13 in temperature ranges of 40°C-200 °C and pressures up to 350 bar (Medina-Gonzalez et al., 2013; Mirzaei et al., 2015). The CO₂ solubility in glycerol is higher than that of CO₂ in water (Medina-Gonzalez et al., 2013; Mirzaei et al., 2015). The addition of 5 wt% and 10 wt% glycerol improves the CO₂ solubility of MEA at pressures below 10 bar whereas, the solubility of CO₂ reduces at 15 wt% and 20 wt% glycerol concentrations (Shamiri et al., 2016). By comparing the absorber rich loadings for MEA solvent and MEA-glycerol solvent in Table 4.3 and Figure 4.22, higher loadings are shown for the MEA-glycerol solvent.

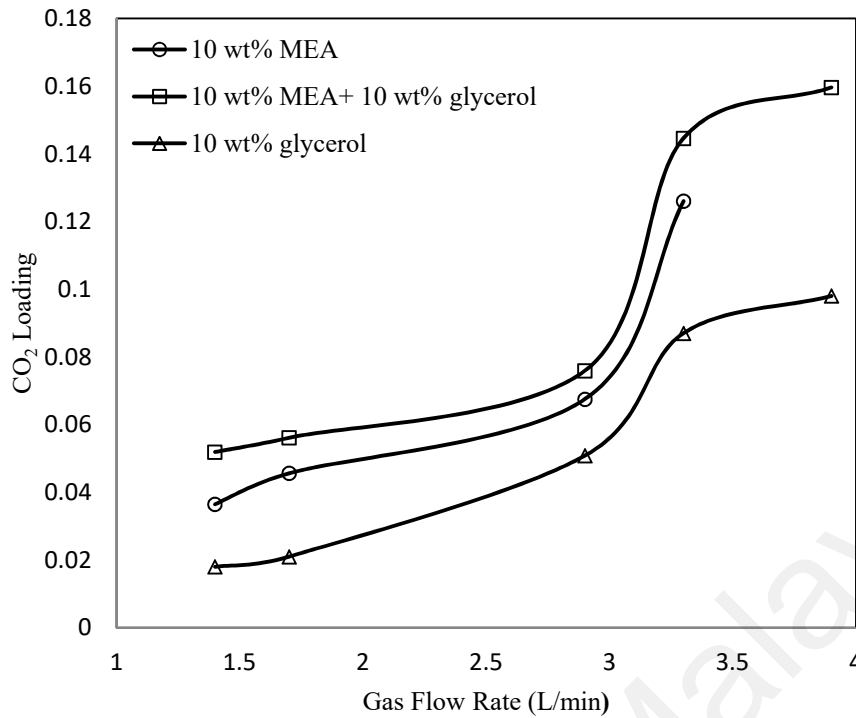


Figure 4.22: CO₂ loading in rich solvents. Experiments with a) aqueous MEA solution b) aqueous mixture of MEA-glycerol solution and c) aqueous glycerol solution

Figures 4.23-4.25 show the CO₂ loading of rich and lean solvent as a function of gas flow rate. As expected, the lean loadings profiles are lower than those of rich loadings because of solvent regeneration and releasing of CO₂ in the desorption column. In this set of experiments, the solvent flow rate is kept constant, while the gas flow rate is varied. Therefore, the difference of CO₂ loadings between the rich and lean solvents increases. By increasing the gas flow rate, the contact time of the phases rises and thus the rich loading increases. The rich loading can significantly affect the absorber outlet temperature.

For measuring CO₂ loadings of both rich and lean streams, the samples are collected from the bottom of columns. During regeneration, the stripper column was heated to 100 °C and the heat exchanger (W4) could increase the temperature to 110 °C. As shown in Figure 4.24, only three samples were used to plot the CO₂ loading profile of lean stream and due to some operational problems the sample 4 was not collected.

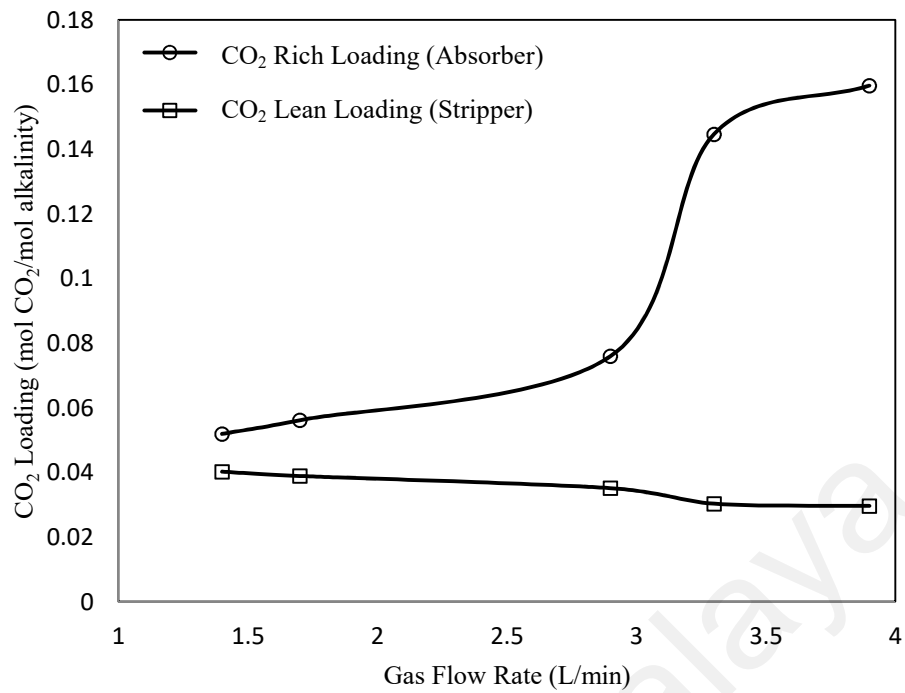


Figure 4.23: A comparison of CO₂ loading in the outlet streams of absorber and stripper columns. Experiment with the mixture of 10 wt% MEA-10 wt% glycerol aqueous solution

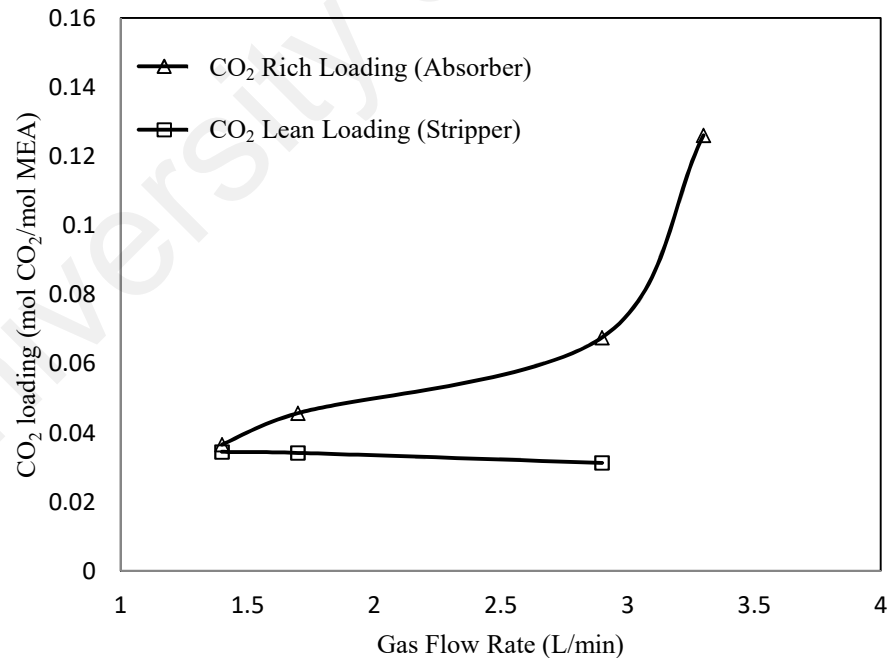


Figure 4.24: A comparison of CO₂ loading in the outlet streams of absorber and stripper columns. Experiment with 10 wt% MEA aqueous solution

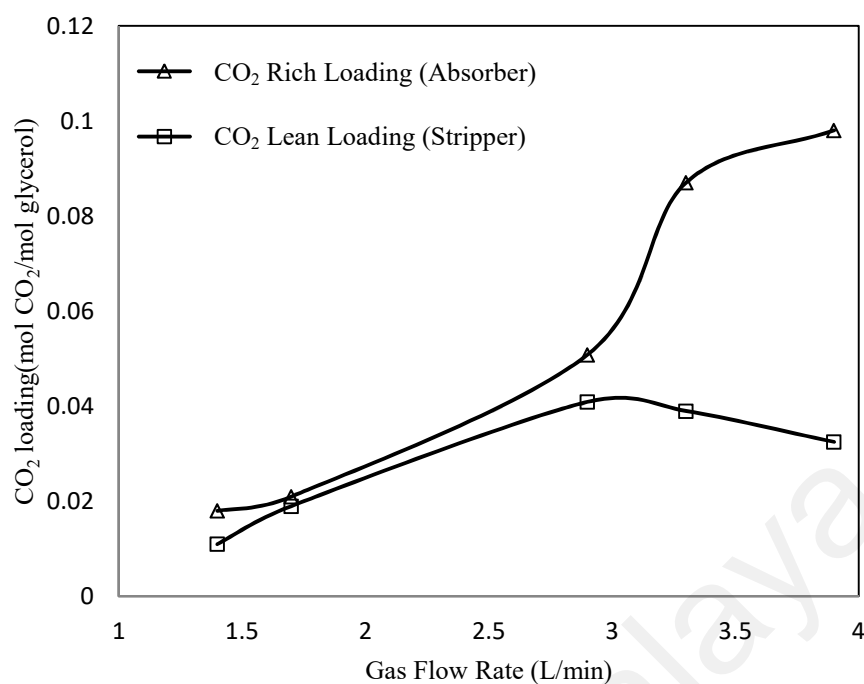


Figure 4.25: A comparison of CO₂ loading in the outlet streams of absorber and stripper columns. Experiment with 10 wt% glycerol aqueous solution

Figures 4.26-4.28 illustrate dependence of the outlet liquid temperature of absorber on rich CO₂ loading. There is visible relationship between rich CO₂ loading and temperature which confirms the fact that temperature increases with increasing of CO₂ loading. With the increase of CO₂ loading from 0.0365 to 0.126 mol CO₂/mol MEA, temperature increased from 30°C to 31.8°C. On the other hand, temperature increase for CO₂ loadings 0.0519-0.1596 mol CO₂/mol alkalinity is 32.01°C-32.75°C but, in the case of glycerol solvent when the CO₂ loading increases from 0.018 to 0.098 mol CO₂/mol glycerol temperature rises from 29.85°C to 30.81°C.

In this experimental study, solvent is counter-currently contacted by the gas comprising CO₂ in the absorber column. The liquid absorbs CO₂ when the solvent is MEA solution and MEA-glycerol solution. Due to chemical absorption, process generates reaction heat and the liquid temperature increases. Temperature changes for CO₂ loadings obtained from glycerol solvent is very less because there is no reaction for this system and CO₂ dissolves into the glycerol solution.

Comparison of rich stream temperature profiles based on gas flow rates is shown in Figure 4.29. This figure shows that by increasing the gas flow rate the temperature of rich loading rises. Because as mentioned, an increase in the gas flow rate leads to higher CO₂ absorption and higher temperatures.

The adding of glycerol to MEA promotes the amount of CO₂ absorbed. Therefore, the temperature increase for the MEA-glycerol solvent is more and temperature profile is located upper than MEA and glycerol profiles. 1.4 L/min gas flow rate has rich loading temperature of 30°C by using MEA solvent. While, this gas flow rate shows rich loading temperatures of 32.01°C and 29.85°C for MEA-glycerol solvent and glycerol solvent, respectively.

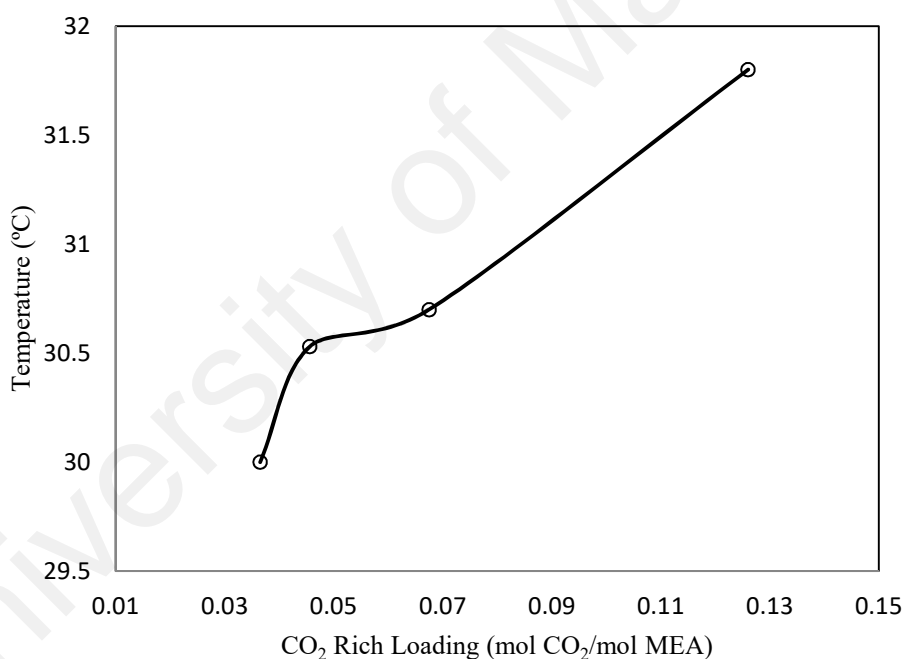


Figure 4.26: Temperature profile of absorber outlet stream at different CO₂ loadings. Experiment with 10 wt% MEA aqueous solution

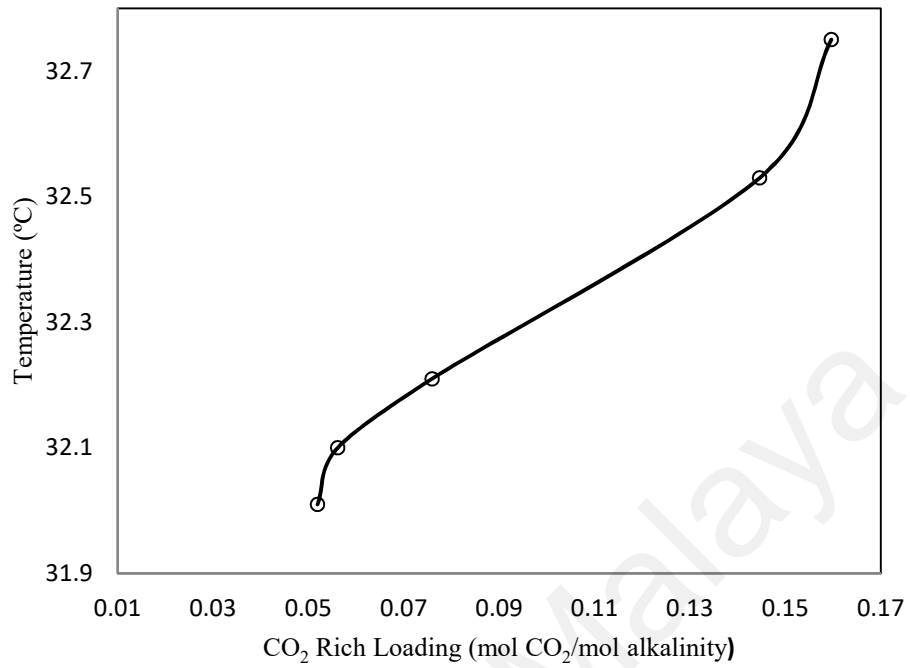


Figure 4.27: Temperature profile of absorber outlet stream at different CO₂ loadings. Experiment with the mixture of 10 wt% MEA -10 wt% glycerol aqueous solution

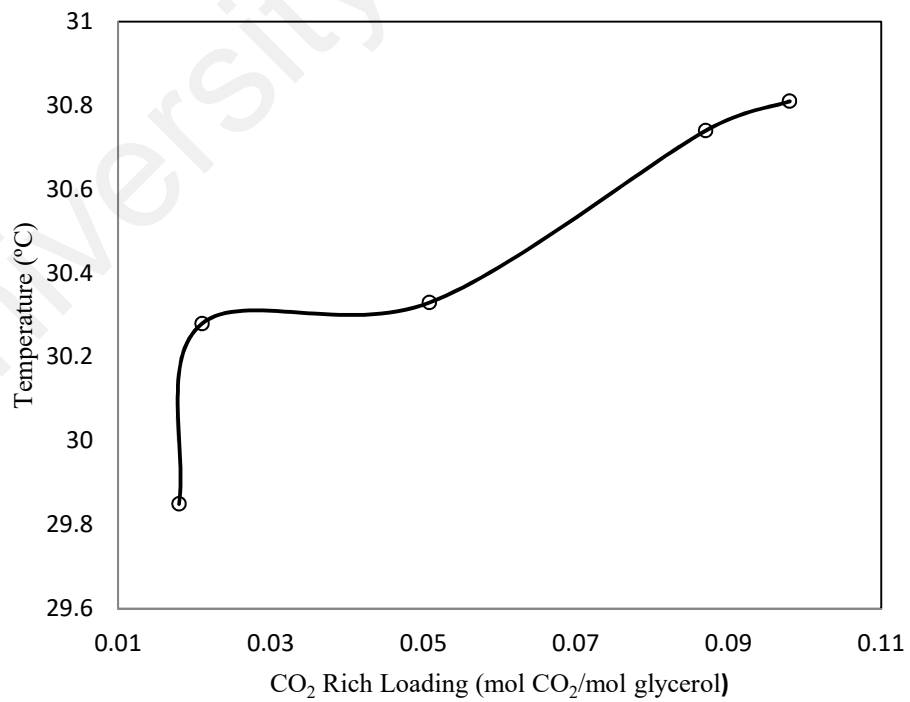


Figure 4.28: Temperature profile of absorber outlet stream at different CO₂ loadings. Experiment with 10 wt% glycerol aqueous solution

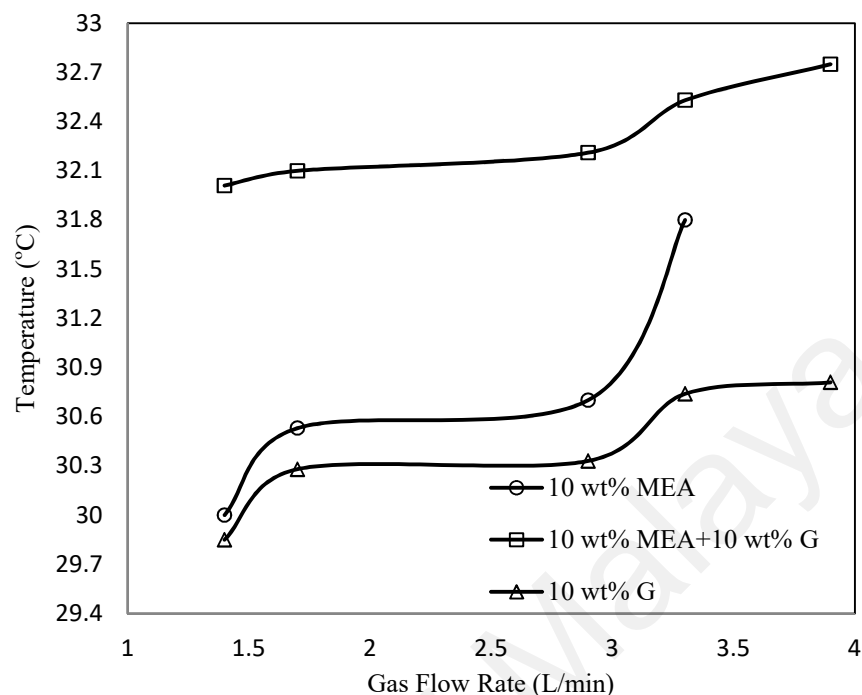


Figure 4.29: A comparison of temperature profiles of absorber outlet stream at different gas flow rates. Experiments with a) aqueous MEA solution b) aqueous mixture of MEA-glycerol solution c) aqueous glycerol solution

Figure 4.30 estimates the pH values of different CO₂ loadings. As can be seen from this figure the aqueous mixture of MEA-glycerol solvent has less pH compared to aqueous MEA solution. It means that MEA-glycerol is more favoured to achieve a CO₂ loading higher than that of the MEA system. As a result, more CO₂ can be absorbed into MEA-glycerol solution than a MEA solution at the same gas flow rates. Thus, we can conclude that the glycerol can increase the CO₂ absorption capacity of the MEA as primary amine. Glycerol is neutral to litmus and as shown in the figure, pH values for all samples collected from CO₂ absorption process using glycerol solution is between 7.5- 8.5.

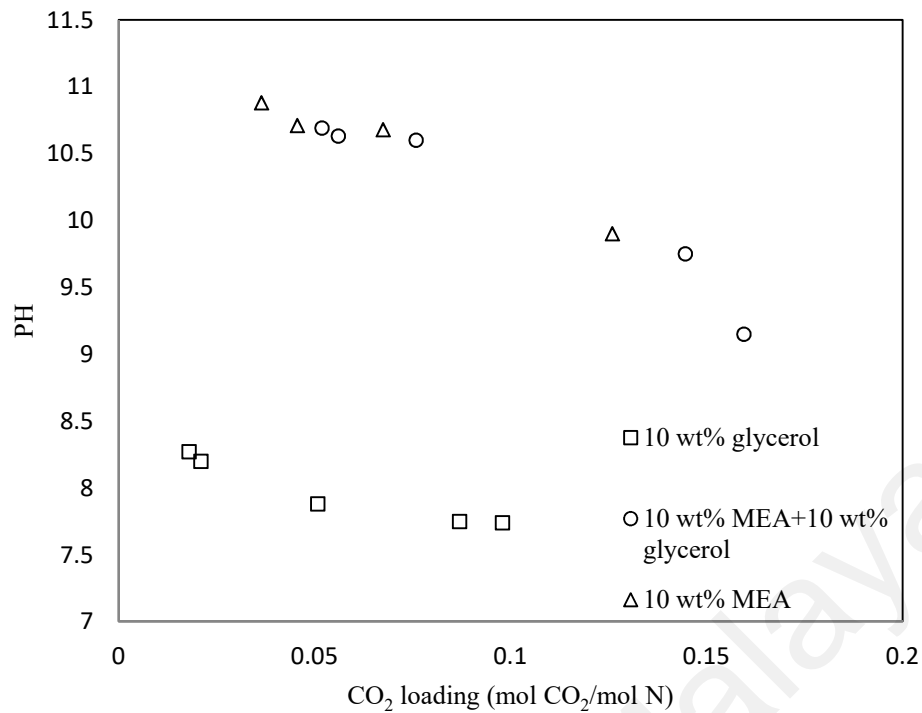


Figure 4.30: pH Profile at various CO₂ loadings and same gas flow rates of MEA, MEA-glycerol, and glycerol solutions

N: MEA (mol CO₂/ mol MEA); alkalinity (mol CO₂/ mol alkalinity) for the mixture of MEA-glycerol; glycerol (mol CO₂/mol glycerol)

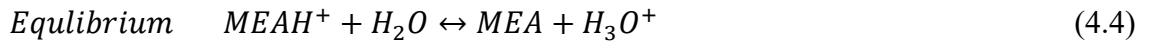
4.3 Validation of simulation study with experimental work

4.3.1 Absorber simulation

Aspen simulations were performed for CO₂ absorption process using MEA-glycerol solution in the rate-based model and the comparisons between simulation results and experimental data of absorption/desorption unit were presented. %AAD also was calculated using the equation 4.1. The liquid temperature and CO₂ loading in the rich solvent (outlet stream from absorber) and CO₂ loading in the lean solvent (outlet stream from stripper) are presented based on different gas flow rates.

In Aspen Plus rate-based simulations, pack rating is used to define the column diameter and packing height, and the packing parameters are used to calculate mass transfer rates and other parameters like the pressure drop. Aspen Plus has been provided with packing specifications from several vendors. However, glass raschig rings are not defined

among different vendors; therefore user type with packing size 8 mm, surface area 4.61 cm²/cm³ and void fraction 0.76 is defined as replacements during the absorber simulations. The absorber performance is modeled by a combination of equilibrium and kinetic reactions. These reactions were described in chapter 3, completely:



As noted before, glycerol solvent does not chemically react when absorbing the CO₂. Instead, the CO₂ dissolves into the glycerol solvent.

Mass transfer coefficients and the interfacial area for the packing are calculated by Aspen Plus using the correlation of Bravo and Fair (Bravo & Fair, 1982). The heat transfer correlation is taken from Chilton and Colburn (Chilton & Colburn, 1934). The correlation of Onda et al. (Onda et al., 1968) cannot be used to calculate the mass transfer coefficients and the interfacial area because of convergence problems in Aspen Plus. Bravo and Fair (1982) correlation predicts mass transfer coefficients and interfacial area for random packing. They used the same expressions as the Onda correlation for the mass transfer coefficients, but the modified Reynolds number used in calculating the liquid phase mass transfer coefficient is based on the effective surface area, rather than wetted surface area (Aspen Technology, 2011).

Table 4.4 shows the comparison of rich CO₂ loadings between experimental and simulation study. In the experimental study the CO₂ loadings were measured based on standard precipitation-titration method which was mentioned in section 3.3.7 and CO₂ loadings in simulation study were calculated based on equation 3.13. As shown in the table, the solvent flow rate is kept constant, while gas flow rate increases between 1.4 L/min to 3.9 L/min. An increase of the gas flow rate increases the amount of CO₂, which is moved between the phases and rich CO₂ loading increases. Average absolute deviation percentage (AAD %) for all gas flow rates are less than 10%. The highest deviation percentage was calculated 9.22% for 2.9 L/min gas flow rate, whilst the lowest deviation percentage obtained 0.36% for 1.7 L/min gas flow rate. The advantage of adding glycerol to the MEA is that glycerol promotes the amount of CO₂ absorption capacity for MEA-glycerol solution. The comparison of experimental result between MEA process and MEA-glycerol process was presented in Table 4.3.

Table 4.4: CO₂ loadings in outlet stream from absorber for CO₂-MEA-glycerol system with 0.7 L/min solvent flow rate and CO₂ (15 v%)-N₂ (85 v%) gas mixture

Rich loading (mol CO ₂ /mol alkalinity)			
Gas flow rate (L/min)	Experimental	Simulation	AAD%
1.4	0.0519	0.0528	1.73
1.7	0.0561	0.0559	0.36
2.9	0.0759	0.0689	9.22
3.3	0.1446	0.148	2.35
3.9	0.1596	0.1634	2.38

Figure 4.31 shows the CO₂ loading of rich solvent as a function of L/G ratio. Both experimental results and simulation study show increasing the CO₂ loading with decreasing the L/G-ratio. This plot confirms that the prediction of the simulation model fits well with experimental data. In this experiments, the gas flow rate increases, while the solvent flow rate is maintained stable. Accordingly, the ratio of the two volume flow rates, L/G ratio, is changed. By increasing the gas flow rate in quantities 1.4, 1.7, 2.9, 3.3 and 3.9 L/min, L/G ratio decreases to 0.5, 0.41, 0.24, 0.21 and 0.18.

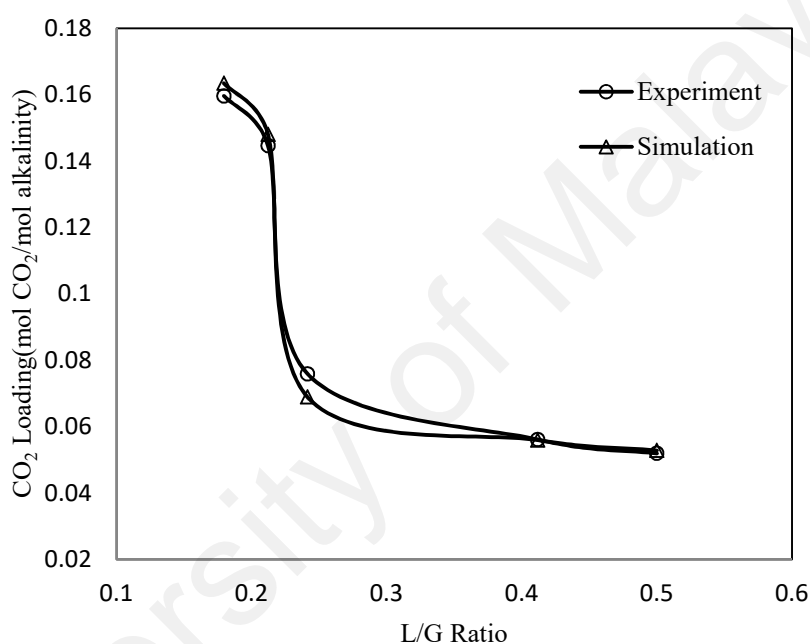
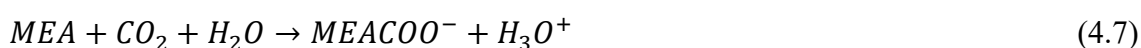


Figure 4.31: Dependence of the rich CO₂ loading on L/G ratio

Figure 4.32 shows the liquid temperature profiles along the absorber column for mixture of MEA-glycerol aqueous solution. Absorber column consists of 20 stages where the feed gas enters in the bottom; stage 20, as “Gas-only” and the lean solvent enters in the top, stage 1, as “Liquid-only”.

The CO₂-MEA reaction is exothermic. Since this reaction produces energy, the temperature in the absorber column rises. Reaction 4.7 is one of the most important reactions which takes place in the absorber column, representing the reaction between MEA and CO₂ forming carbamate (MEACOO⁻).



As can be seen from the Figure 4.32, high gas flow rates change the temperatures in the absorption column to the upper values. With an increasing of gas flow rate, the released heat of CO₂ absorption increases which causes a rise in the absorber temperature. The heat of CO₂ reaction with MEA produces a temperature bulge in the column.

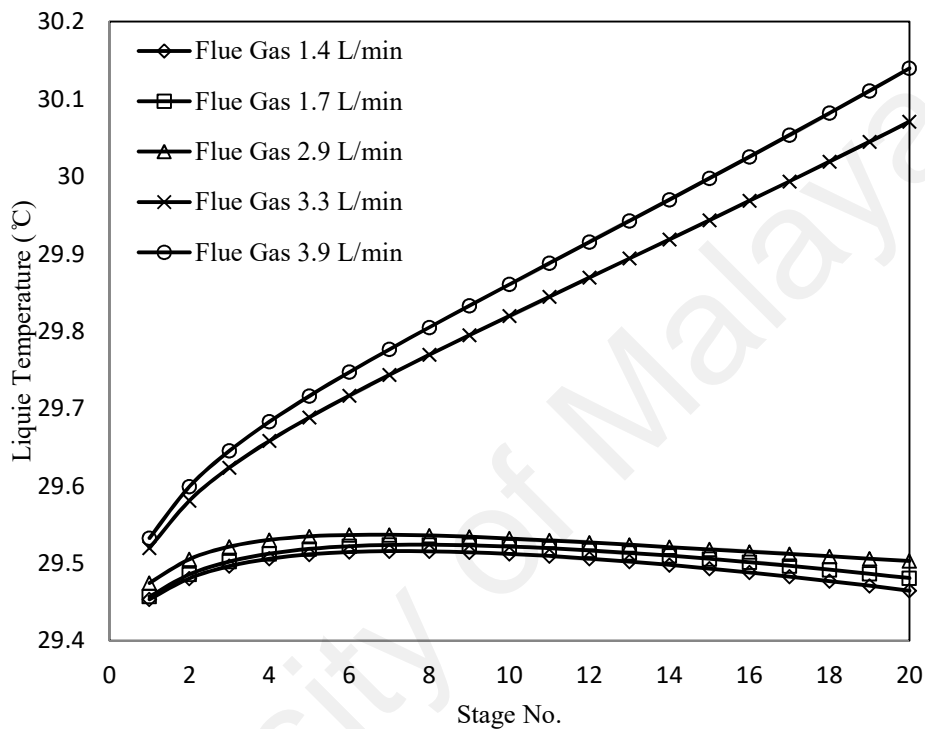


Figure 4.32: liquid temperature profiles along the absorber height for different gas flow rates

Figure 4.33 shows that gas flow rates of 1.4, 1.7 and 2.9 L/min has a temperature bulge at the top of the absorption column. This temperature change at the top of the absorber confirms the reaction of CO₂ with solvent and generation of reaction heat. When there is insufficient solvent relative to the inlet CO₂, the greatest absorption will occur at the top of the column, giving the temperature bulge there.

Temperature reduction at the lower part of the absorber is caused by heat transfer from the liquid to the gas. By increasing the gas flow rate to 3.3 L/min and 3.9 L/min temperature bulge broadens along the stages of absorber (d,e). This means the heat

released from the CO₂ absorption reaction is more than the heat consumed for heating of gas stream. Therefore, the temperature increases along the absorber.

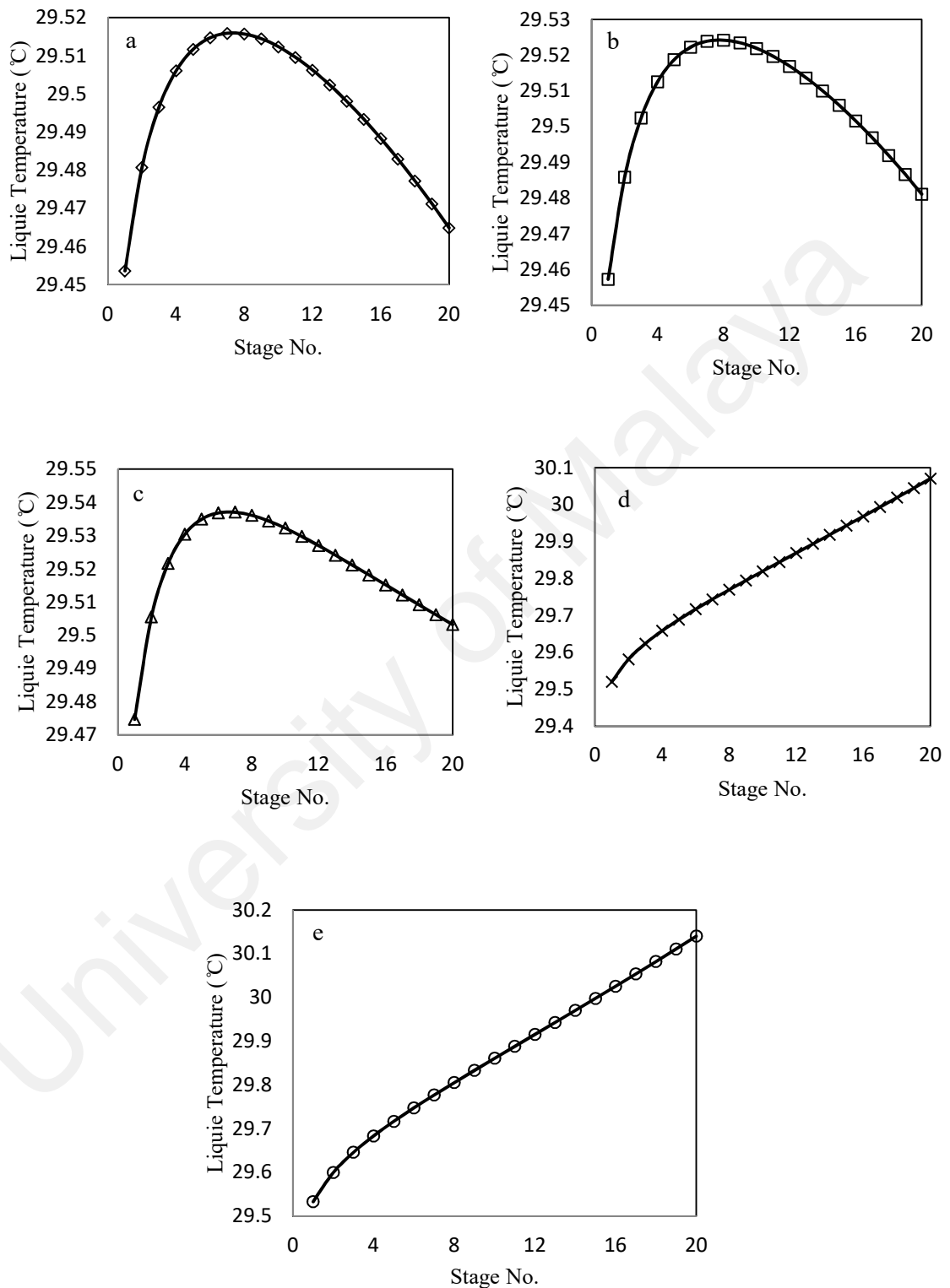


Figure 4.33: liquid temperature profiles along the absorber height for gas flow rates with a)1.4 L/min b)1.7 L/min c)2.9 L/min d)3.3 L/min e)3.9 L/min

Table 4.5 shows the comparison of temperature in the outlet stream of absorber between experiment and simulation studies. In the experimental work, there were not temperature sensors during the absorption column and temperature was measured only in the outlet liquid stream. By increasing the gas flow rate from 1.4 L/min to 3.9 L/min calculated temperature increases from 29.46°C to 30.14°C. Average absolute deviation percentage less than 10% confirms that the simulations fit well with the experimental values for all gas flow rates.

Table 4.5: Rich stream temperature for CO₂-MEA- glycerol system

Gas flow rate (L/min)	Temperature (°C)		
	Experimental	Simulation	AAD%
1.4	32.01	29.46	7.96
1.7	32.1	29.48	8.16
2.9	32.21	29.50	9.96
3.3	32.53	30.07	7.56
3.9	32.75	30.14	7.97

Figures 4.34 and 4.35 indicate liquid CO₂ mole fraction and CO₂ loadings along the absorption column for different gas flow rates, respectively. As mentioned, the absorber has two feeds; the CO₂-N₂ gas mixture which enters at the bottom of column (stage 20) and flows upwards. The MEA-glycerol solvent is fed at the top (stage 1), flowing down the column and contacting the gas phase. During contact between the liquid and the gas phase, the CO₂ enters the liquid phase due to a concentration gradient. MEA drives the

CO₂ into the liquid phase due to a fast reaction and enhances the absorption rate. CO₂ also dissolves in glycerol solvent with no reaction.

As shown in Figures 4.34 and 4.35, stages 1 and 20 have the lowest and the highest liquid CO₂ mole fraction and CO₂ loadings, respectively. Clearly, the amount of liquid CO₂ absorption and CO₂ loading increases towards bottom half of the absorber. When the solvent enters the column from the top, the CO₂ absorption occurs and the CO₂ is transferred to the liquid phase. Since, this liquid phase following down the absorber, the amount of absorbed CO₂ increases on the stages towards the bottom of column.

The packings provide contact area for mass transfer. The liquid phase forms a film around the packing, increasing the contact area between the gas and liquid phases. The rich solvent leaves the column in stage 20 and has the highest CO₂ loading.

As can be seen from Figures 4.34 and 4.35 by increasing the gas flow rate from 1.4 L/min to 3.9 L/min, the amount of CO₂ rises and the location of reaction along the column is transferred to the bottom stages thus the CO₂ absorption increases because of the higher driving force and less amount of CO₂ can transfer to the upper stages. It should be noted that both chemical and physical absorption occur on the stages. CO₂ dissolves in the glycerol and flows down the column. When gas flow rate rises more amount of CO₂ can dissolve in the glycerol.

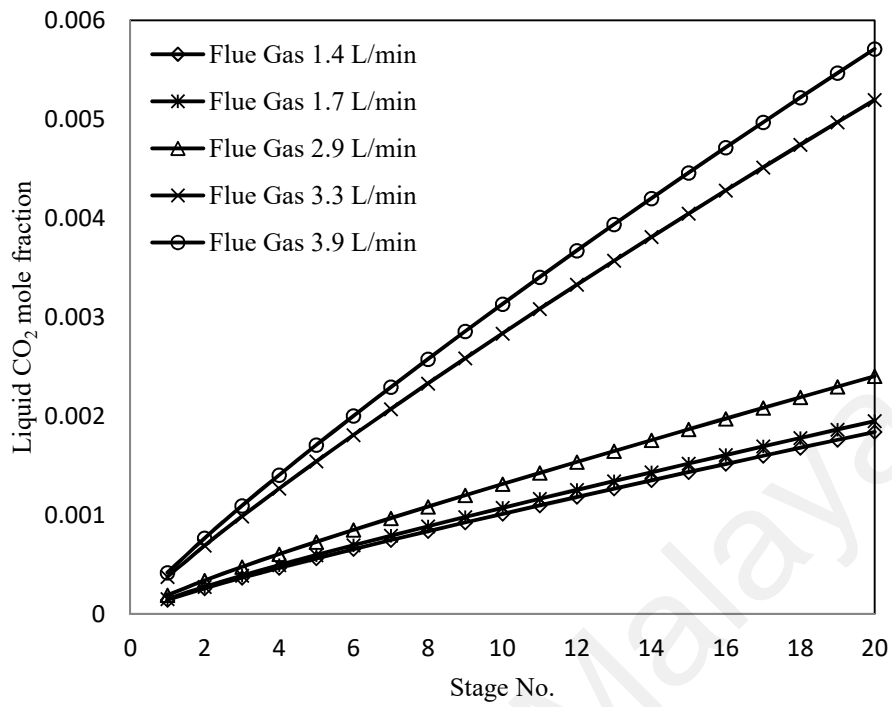


Figure 4.34: CO₂ mole fraction profiles in liquid phase along the absorber height for CO₂-MEA-glycerol system

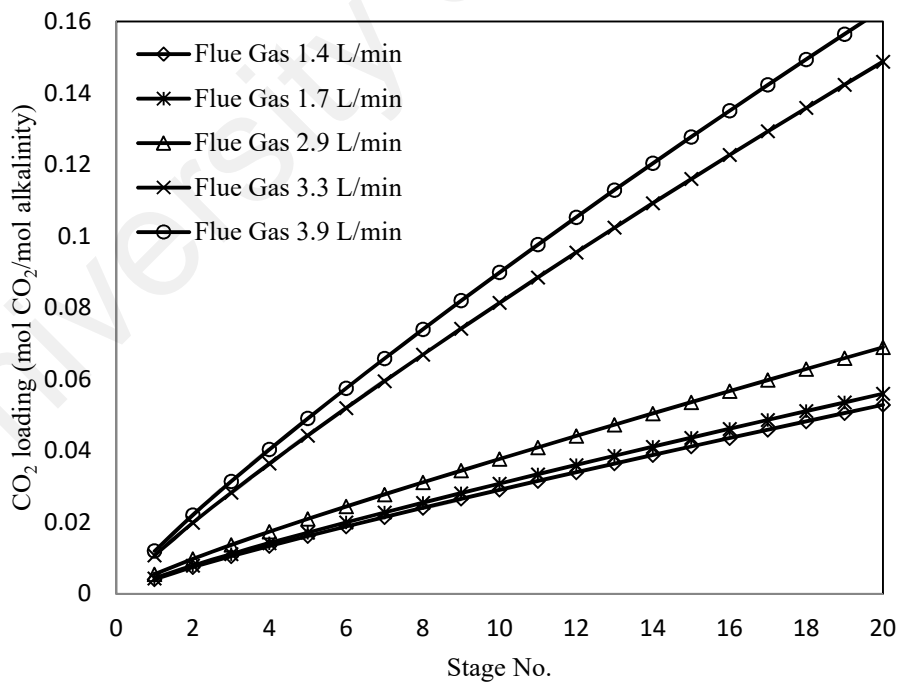


Figure 4.35: CO₂ loading profiles along the absorber height for CO₂-MEA-glycerol system

4.3.2 Stripper simulation

The stripper column was simulated similar to the absorber column. The pressure, temperature, flow rate and composition of the stripper feed were introduced into the model (Figure 3.8). The column was simulated using a RadFrac column consisting of 20 stages, with partial-vapor condenser (stage 1) and a kettle reboiler at the bottom (stage 20).

For stripper the packing type specified in Aspen Plus differs from the packing type used in the experiments. This was done because convergence problems of stripper. The Aspen model was run with ceramic raschig packings 10 mm. It has $4.72 \text{ cm}^2/\text{cm}^3$ surface area which is almost similar to glass raschig packings 8 mm with $4.61 \text{ cm}^2/\text{cm}^3$ surface area. The choice of using ceramic raschig packings 10 mm as replacement was based on a trial-and-error approach. Different packings with surface area near $4.61 \text{ cm}^2/\text{cm}^3$ was tested in the simulations and ceramic raschig packings 10 mm gave the best convergence. The stripper performance was modeled by a combination of equilibrium and kinetic reactions. The correlation of Onda et al. (Onda et al., 1968) is used in Aspen Plus as mass transfer coefficient method and interfacial area method. Heat transfer coefficients are calculated by Aspen Plus using the correlation of Chilton and Colburn (Chilton & Colburn, 1934).

Since only the chemical solvent (MEA) is the thermally stripped, this is the only phase which was regenerated at high temperature but, regeneration of the physical solvent (glycerol) was achieved by removal of the pressure. Due to this limitation of operations, the regeneration of MEA-glycerol solvent was done at $100 \text{ }^\circ\text{C}$ and 0.1 barg . Therefore, there is no energy required to regenerate the glycerol as physical solvent (Kingma, 2016).

Table 4.6 shows the comparison of experimental and simulation result for lean CO_2 loadings at different gas flow rates. In the experimental study the CO_2 loadings were

measured based on standard precipitation-titration method which was mentioned in section 3.3.7 and CO₂ loadings in simulation study were calculated based on equation 3.13. The deviation percentage between the simulated and experimental lean loadings was calculated from equation 4-1. As shown in the table, by increasing the gas flow rate from 1.4 L/min to 3.9 L/min, lean loading decreases from 0.0367 to 0.0318 mol CO₂/mol alkalinity. This result means an increase of the reboiler heat duty. Deviation percentage between experimental and simulated lean loadings was calculated less than 10% for all gas flow rates. The lowest and highest calculated deviation percentages were 1.42% and 9.90% for the gas flow rates with 2.9 L/min and 3.3 L/min, respectively.

Figure 4.36 confirms the increasing of reboiler heat duty by increasing the gas flow rate in the simulation study. The investigation of this figure shows that reboiler heat duty is a function of rich loading. When the gas flow rate increases from 1.4 L/min to 3.9 L/min, the amount of CO₂ absorption rises in the absorber column, this leads to increase the rich loading and more CO₂ has to be stripped in the desorber column thus, the reboiler heat duty rises from 98.14 to 305.46 MJ/h.

Table 4.6: CO₂ loadings in outlet stream from stripper for CO₂-MEA-glycerol system with 0.7 L/min solvent flow rate and CO₂ (15 v%)-N₂ (85 v%) gas mixture

Lean loading (mol CO ₂ /mol alkalinity)			
Gas flow rate (L/min)	Experimental	Simulation	AAD%
1.4	0.0402	0.0367	8.70
1.7	0.0389	0.0366	5.91
2.9	0.0351	0.0356	1.42
3.3	0.0303	0.0333	9.90
3.9	0.0296	0.0318	7.43

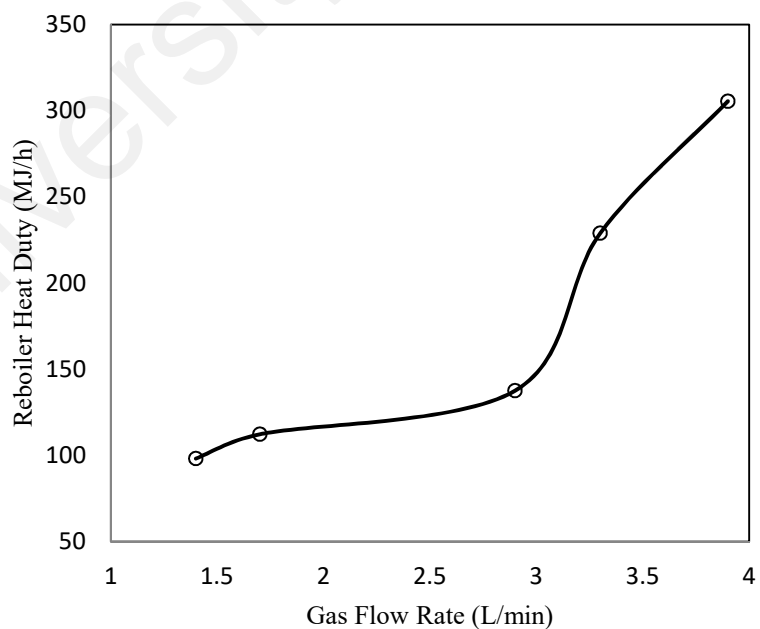
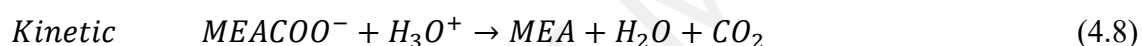


Figure 4.36: Dependence of the gas flow rate on reboiler heat duty

Figure 4.37 shows CO₂ mole fraction in liquid phase along the stages 2-19 in the stripper. Solvent regeneration occurs when the rich solvent from the absorber is entered to the stage number 2 as the feed of stripper. Regenerated solvent is discharged from stage number 20 while it has the low CO₂ loadings. In Aspen model, the equilibrium reactions only were defined for condenser (stage1) and reboiler (stage 20). These equilibrium reactions (3.1-3.5) were clarified in chapter 3, completely.

The combination of equilibrium and kinetic reactions were defined for stage 2-19. Since, the rich stream is entered to stage 2 it has the most CO₂ mole fraction in the column. CO₂ desorption occurs along the stages of desorber, where the chemical reaction of MEA+CO₂ is reversed by the addition of heat. Carbamate reversion (reaction 4.8) takes place in the desorber column and the CO₂ is liberated.



The CO₂ rich solvent is heated before entering the stripper column to decrease the solubility of CO₂ in solvent. The stripper removes CO₂ by increasing the temperature of the solution. The heat produced can drive the mass transfer from the liquid to the gas phase and the released CO₂ flows upwards the column. Therefore, liquid CO₂ mole fraction decreases toward the bottom of column. The heat of CO₂ desorption for physical solvent (glycerol) is only a fraction of that for chemical solvent (MEA). Therefore, heat requirements are usually much less for glycerol than for MEA (Burr & Lyddon, 2008). As noted before, the pressure removal can be a suitable method for regeneration of glycerol. Because of this, the desorber column operated in 0.1 barg as operating pressure.

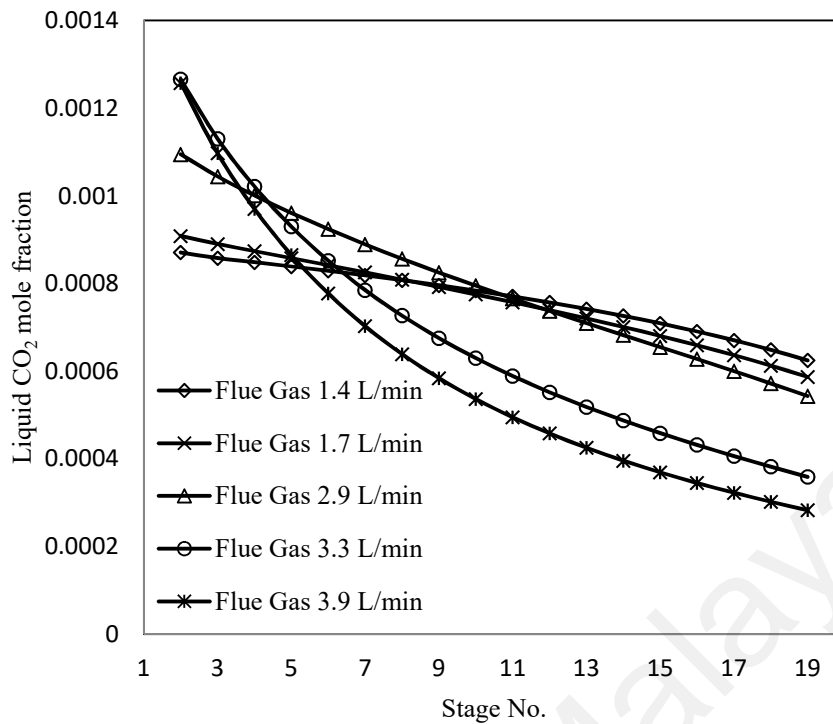


Figure 4.37: CO₂ mole fraction profile in liquid phase along the stripper height at different gas flow rates

Figure 4.38 shows the CO₂ loading of the lean solvent as a function of the L/G ratio. In this experimental study, the gas flow rate increases in quantities 1.4, 1.7, 2.9, 3.3 and 3.9 L/min, while the solvent flow rate is kept constant, 0.7 L/min. Accordingly, the ratio of the two volume flow rates, L/G ratio, decreases to 0.5, 0.41, 0.24, 0.21 and 0.18. In Figure 4.38 both experimental results and simulation study show decreasing the CO₂ loading with decreasing the L/G-ratio. This figure confirms that by increasing the gas flow rate the lean loading decreases. Therefore, reboiler heat duty increases (Figure 4.36).

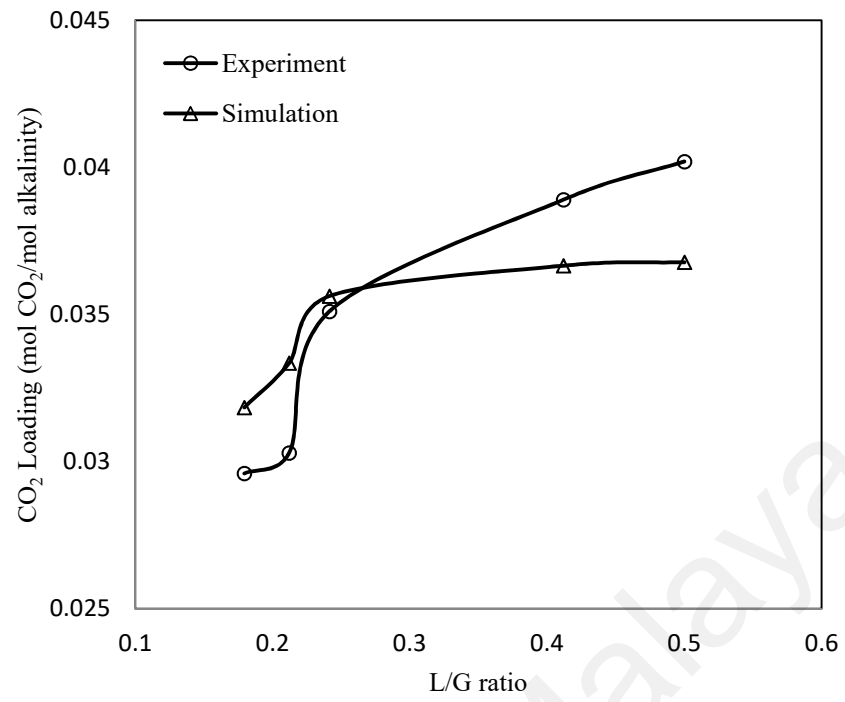


Figure 4.38: Dependence of the lean CO₂ loading on L/G ratio

University of Malaya

CHAPTER 5: CONCLUSIONS AND RECOMMENDATIONS

5.1 Conclusions

1. Simulation of CO₂ absorption process using MEA, glycerol and MEA-glycerol aqueous solutions.

- (a) The amount of CO₂ in the outlet gas from the absorber decreased with the decrease in glycerol concentration within the range of 10–40 wt %.
- (b) The optimal glycerol concentration in CO₂ absorption was obtained 10 wt %.
- (c) The optimal concentration for the mixed solvent was obtained 10 wt% glycerol–10 wt% MEA.
- (d) The CO₂ removal efficiency increased from 62.24% for 10 wt% MEA solution to 64.33% for 10 wt% MEA–10 wt% glycerol solution.

2. Experimental study of CO₂ absorption in a packed column.

- (a) CO₂ rich loading increased by increasing the gas flow rate from 1.4 to 3.9 L/min.
- (b) CO₂ rich loading at 1.4 L/min gas flow rate increased from 0.0365 mol CO₂/mol MEA to 0.0519 mol CO₂/mol alkalinity for MEA-glycerol system.
- (c) CO₂ rich loading at 3.3 L/min gas flow rate increased from 0.126 mol CO₂/mol MEA to 0.1446 mol CO₂/mol alkalinity for MEA-glycerol system.
- (d) Hybrid MEA-glycerol solution showed a better CO₂ absorption performance at specified gas flow rates compared to MEA system.

3. Validation of simulation study with experimental work.

- (a) Rich CO₂ loading increased from 0.0528 to 0.1634 mol CO₂/mol alkalinity by increasing the gas flow rate from 1.4 to 3.9 L/min.
- (b) Reboiler heat duty increased from 98.14 to 305.46 MJ/h in the range of 1.4 to 3.9 L/min gas flow rates.

5.2 Recommendations

Employing the temperature sensors along the columns is effective in investigating the temperature profiles along the absorber and stripper. CO₂ absorption with 30 wt% MEA and different glycerol concentrations can be tested because this concentration is employed industrially. In the pilot plant, the installation of pH meter in the outlet streams from absorber and stripper may be useful in measuring acidity of both rich and lean CO₂ loadings. CO₂ absorption mechanism by glycerol can be studied in more detail, to explore that it is either physical or due to the reactions between glycerol and CO₂. More studies on the desorber performance should be carried out by simulation, as well as defining new or other reactions for glycerol and CO₂. Moreover, data regression can be set optimum binary interaction parameters for the simulation model. An attempt should also be made to connect the absorber and desorber to test the performance of the simulation model as a whole.

REFERENCES

- Aaron, D., & Tsouris, C. (2005). Separation of CO₂ from flue gas: A review. *Separation Science and Technology*, 40(1-3), 321-348.
- Aboudheir, A., Tontiwachwuthikul, P., Chakma, A., & Idem, R. (2003). Kinetics of reactive absorption of carbon dioxide in high CO₂-loaded, concentrated aqueous monoethanolamine solutions. *Chem. Eng. Sci.*, 58(23), 5195-5210.
- Adhikari, S., Fernando, S. D., & Haryanto, A. (2008). Hydrogen production from glycerin by steam reforming over nickel catalysts. *Renewable Energy*, 33(5), 1097-1100.
- Afkhamipour, M., & Mofarahi, M. (2013a). Comparison of rate-based and equilibrium-stage models of a packed column for post-combustion CO₂ capture using 2-amino-2-methyl-1-propanol (AMP) solution. *Int. J. Greenh. Gas Control*, 15, 186-199.
- Afkhamipour, M., & Mofarahi, M. (2013b). Comparison of rate-based and equilibrium-stage models of a packed column for post-combustion CO₂ capture using 2-amino-2-methyl-1-propanol (AMP) solution. *International Journal of Greenhouse Gas Control*, 15, 186-199.
- Ahmad, A., Jawad, Z., Low, S., & Zein, S. (2014). A cellulose acetate/multi-walled carbon nanotube mixed matrix membrane for CO₂/N₂ separation. *Journal of Membrane Science*, 451, 55-66.
- Ahmady, A., Hashim, M. A., & Kheireddine Aroua, M. (2011). Absorption of carbon dioxide in the aqueous mixtures of methyldiethanolamine with three types of imidazolium-based ionic liquids. *Fluid Phase Equilibria*, 309(1), 76-82.
- Al-Baghli, N. A., Pruess, S. A., Yesavage, V. F., & Selim, M. S. (2001). A rate-based model for the design of gas absorbers for the removal of CO₂ and H₂S using aqueous solutions of MEA and DEA. *Fluid Phase Equilibria*, 185(1), 31-43.
- Alatiqi, I., Sabri, M. F., Bouhamra, W., & Alper, E. (1994). Steady-state rate-based modelling for CO₂/amine absorption—desorption systems. *Gas Separation & Purification*, 8(1), 3-11.
- Alper, E. (1990). Reaction mechanism and kinetics of aqueous solutions of 2-amino-2-methyl-1-propanol and carbon dioxide. *Ind. Eng. Chem. Res.*, 29(8), 1725-1728.

- Al-Saleh, Y., Vidican, G., Natarajan, L., & Theeyattuparampil, V. (2012). Carbon capture, utilisation and storage scenarios for the Gulf Cooperation Council region: a Delphi-based foresight study. *Futures*, 44(1), 105-115.
- Anderson, C., Harkin, T., Ho, M., Mumford, K., Qader, A., Stevens, G., & Hooper, B. (2013). Developments in the CO₂CRC UNO MK3 process: a multi-component solvent process for large scale CO₂ capture. *Energy Procedia*, 37, 225-232.
- Araújo, O. d. Q. F., & de Medeiros, J. L. (2017). Carbon capture and storage technologies: present scenario and drivers of innovation. *Current Opinion in Chemical Engineering*, 17, 22-34.
- Aroon, M. A., Ismail, A. F., & Matsuura, T. (2013). Beta-cyclodextrin functionalized MWCNT: A potential nano-membrane material for mixed matrix gas separation membranes development. *Separation and Purification Technology*, 115, 39-50.
- Aroonwilas, A., Chakma, A., Tontiwachwuthikul, P., & Veawab, A. (2003). Mathematical modelling of mass-transfer and hydrodynamics in CO₂ absorbers packed with structured packings. *Chemical Engineering Science*, 58(17), 4037-4053.
- Aroonwilas, A., & Tontiwachwuthikul, P. (1997). Mass transfer studies of high performance structured packing for CO₂ separation processes. *Energy conversion and management*, 38, S75-S80.
- Aroonwilas, A., & Tontiwachwuthikul, P. (2000). Mechanistic model for prediction of structured packing mass transfer performance in CO₂ absorption with chemical reactions. *Chemical Engineering Science*, 55(18), 3651-3663.
- Aschenbrenner, O., & Styring, P. (2010). Comparative study of solvent properties for carbon dioxide absorption. *Energy Environ. Sci.*, 3(8), 1106-1113.
- Aspen Technology, Aspen Plus Help File (2011). *Burlington, MA, USA*.
- Aspen Technology (2001a). Aspen Plus Reference Manual, Aspen Physical Property System, Physical Property Data 11.1, Cambridge, USA.
- Aspen Technology (2001b). Aspen Plus Reference Manual, Aspen Physical Property System, Physical Property Methods and Models 11.1.
- Aspen Technology (2010). Aspen physical property system, physical property methods.

- Austgen, D. M., Rochelle, G. T., & Chen, C. C. (1991). Model of vapor-liquid equilibria for aqueous acid gas-alkanolamine systems. 2. Representation of hydrogen sulfide and carbon dioxide solubility in aqueous MDEA and carbon dioxide solubility in aqueous mixtures of MDEA with MEA or DEA. *Ind. Eng. Chem. Res.*, 30(3), 543-555.
- Austgen, D. M., Rochelle, G. T., Peng, X., & Chen, C. C. (1989). Model of vapor-liquid equilibria for aqueous acid gas-alkanolamine systems using the electrolyte-NRTL equation. *Ind. Eng. Chem. Res.*, 28(7), 1060-1073.
- Babamohammadi, S., Shamiri, A., & Aroua, M. K. (2015). A review of CO₂ capture by absorption in ionic liquid-based solvents. *Reviews in Chemical Engineering*, 31(4), 383-412.
- Baker, M. Inc. Environmental Health & Safety. *MSDS Number G4774, USA*.
- Baltus, R. E., Culbertson, B. H., Dai, S., Luo, H., & DePaoli, D. W. (2004). Low-pressure solubility of carbon dioxide in room-temperature ionic liquids measured with a quartz crystal microbalance. *J. Phys. Chem. B*, 108, 721-727.
- Barry, B., & Lili, L. (2008). A comparison of physical solvents for acid gas removal. *Bryan Research & Engineering, Inc., Bryan, Texas, U.S.A.*
- Bastani, D., Esmacili, N., & Asadollahi, M. (2013). Polymeric mixed matrix membranes containing zeolites as a filler for gas separation applications: A review. *Journal of Industrial and Engineering Chemistry*, 19(2), 375-393.
- Billet, R., & Schultes, M. (1993). Predicting mass transfer in packed columns. *Chem. Eng. Technol*, 16, 1-9.
- Blanchard, L. A., Hancu, D., Beckman, E. J., & Brennecke, J. F. (1999). Green processing using ionic liquids and CO₂. *NATURE*, 399(6731), 28-29.
- Bohloul, M., Peyghambarzadeh, S., Lee, A., & Vatani, A. (2014). Experimental and analytical study of solubility of carbon dioxide in aqueous solutions of potassium carbonate. *International Journal of Greenhouse Gas Control*, 29, 169-175.
- Bolles, W., & Fair, J. (1982). Improved Mass-Transfer Model Enhances Packed-Column Design. *Chem. Eng.*, 89(14), 109-116.
- Bravo, J. L., & Fair, J. R. (1982). Generalized correlation for mass transfer in packed distillation columns. *Ind. Eng. Chem. Process Des. Dev.*, 21(1), 162-170.

- Bravo, J. L., Patwardhan, A. A., & Edgar, T. F. (1992). Influence of effective interfacial areas in the operation and control of packed distillation columns. *Ind. Eng. Chem. Res.*, 31(2), 604-608.
- Bravo, J. L., Rocha, J. A., & Fair, J. R. (1985). Mass transfer in gauze packings. *Hydrocarbon Processing*, 64(1), 91-95.
- Burr, B., & Lyddon, L. (2008). *A comparison of physical solvents for acid gas removal*. Paper presented at the 87th Annual Gas Processors Association Convention, Grapevine, TX, March.
- Cammenga, H. K., Schulze, F. W., & Theuerl, W. (1977). Vapor pressure and evaporation coefficient of glycerol. *J. Chem. Eng. Data*, 22(2), 131-134.
- Chen, H., Kovvali, A., Majumdar, S., & Sirkar, K. (1999). Selective CO₂ separation from CO₂-N₂ mixtures by immobilized carbonate-glycerol membranes. *Ind. Eng. Chem. Res.*, 38(9), 3489-3498.
- Chen, X., Closmann, F., & Rochelle, G. T. (2011). Accurate screening of amines by the wetted wall column. *Energy Procedia*, 4, 101-108.
- Chen, X., & Rochelle, G. T. (2011). Aqueous piperazine derivatives for CO₂ capture: Accurate screening by a wetted wall column. *Chemical Engineering Research and Design*, 89(9), 1693-1710.
- Chi, Z., Pyle, D., Wen, Z., Frear, C., & Chen, S. (2007). A laboratory study of producing docosahexaenoic acid from biodiesel-waste glycerol by microalgal fermentation. *Process Biochemistry*, 42(11), 1537-1545.
- Chilton, T. H., & Colburn, A. P. (1934). Mass transfer (absorption) coefficients prediction from data on heat transfer and fluid friction. *Ind. Eng. Chem.*, 26(11), 1183-1187.
- Choi, W.-J., Seo, J.-B., Jang, S.-Y., Jung, J.-H., & Oh, K.-J. (2009). Removal characteristics of CO₂ using aqueous MEA/AMP solutions in the absorption and regeneration process. *Journal of Environmental Sciences*, 21(7), 907-913.
- Chou, C.-T., & Chen, C.-Y. (2004). Carbon dioxide recovery by vacuum swing adsorption. *Separation and Purification Technology*, 39(1), 51-65.
- Comstock, C. S., & Dodge, B. F. (1937). Rate of carbon dioxide absorption by carbonate solutions in a packed tower. *Industrial & Engineering Chemistry*, 29(5), 520-529.

- Cullinane, J. T., & Rochelle, G. T. (2004). Carbon dioxide absorption with aqueous potassium carbonate promoted by piperazine. *Chemical Engineering Science*, 59(17), 3619-3630.
- Cullinane, J. T., & Rochelle, G. T. (2005). Thermodynamics of aqueous potassium carbonate, piperazine, and carbon dioxide. *Fluid Phase Equilibria*, 227(2), 197-213.
- Dang, H., & Rochelle, G. T. (2001). CO₂ absorption rate and solubility in MEA/PZ/water. *Prepared for presentation at the First National Conference on Carbon Sequestration, Washington, May 14–17.*
- Darde, V., Thomsen, K., van Well, W. J. M., & Stenby, E. H. (2009). Chilled ammonia process for CO₂ capture. *Energy Procedia*, 1(1), 1035-1042.
- Davidson, R. (2007). Post-combustion carbon capture from coal fired plants – solvent scrubbing. *IEA Clean Coal Centre.*
- Davison, J., Freund, P., & Smith, A. (2001). Putting carbon back into the ground. *IEA Greenhouse Gas R & D Programme.*
- Deng, L., Kim, T.-J., & Hägg, M.-B. (2009). Facilitated transport of CO₂ in novel PVAm/PVA blend membrane. *Journal of Membrane Science*, 340(1), 154-163.
- Docherty, K. M., Dixon, J. K., & Kulpa Jr., C. F. (2006). Biodegradability of imidazolium and pyridinium ionic liquids by an activated sludge microbial community. *Biodegradation*, 18(4), 481-493.
- Drage, T. C., Smith, K. M., Pevida, C., Arenillas, A., & Snape, C. E. (2009). *Development of adsorbent technologies for post-combustion CO₂ capture.* Paper presented at the Proceedings of the 9th International Conference on Greenhouse Gas Control Technologies (GHGT-9), 16–20 November 2008, Washington DC, USA.
- Dugas, R. E. (2006). Pilot plant study of carbon dioxide capture by aqueous monoethanolamine. *MSE Thesis, University of Texas at Austin.*
- Dugas, R. E. (2007). Rate and Equilibrium Measurements of MEA/Piperazine. *Methods*, 2, 2.
- Dugas, R. E. (2009). Carbon dioxide absorption, desorption, and diffusion in aqueous piperazine and monoethanolamine. *PhD Thesis, University of Texas at Austin.*

- Endo, K., Nguyen, Q. S., Kentish, S. E., & Stevens, G. W. (2011). The effect of boric acid on the vapour liquid equilibrium of aqueous potassium carbonate. *Fluid Phase Equilibria*, 309(2), 109-113.
- Espinal, L., Poster, D. L., Wong-Ng, W., Allen, A. J., & Green, M. L. (2013). Measurement, standards, and data needs for CO₂ capture materials: a critical review. *Environ. Sci. Technol.*, 47(21), 11960-11975.
- Faramarzi, L., Kontogeorgis, G. M., Michelsen, M. L., Thomsen, K., & Stenby, E. H. (2010). Absorber model for CO₂ capture by monoethanolamine. *Industrial & engineering chemistry research*, 49(8), 3751-3759.
- Favre, E. (2007). Carbon dioxide recovery from post-combustion processes: Can gas permeation membranes compete with absorption? *Journal of Membrane Science*, 294(1), 50-59.
- Feng, Z., Cheng-Gang, F., You-Ting, W., Yuan-Tao, W., Ai-Min, L., & Zhi-Bing, Z. (2010). Absorption of CO₂ in the aqueous solutions of functionalized ionic liquids and MDEA. *Chemical Engineering Journal*, 160(2), 691-697.
- Figuerola, J. D., Fout, T., Plasynski, S., McIlvried, H., & Srivastava, R. D. (2008). Advances in CO₂ capture technology—the US Department of Energy's Carbon Sequestration Program. *International Journal of Greenhouse Gas Control*, 2(1), 9-20.
- Fosbøl, P. L., Maribo-Mogensen, B., & Thomsen, K. (2013). Solids modelling and capture simulation of piperazine in potassium solvents. *Energy Procedia*, 37, 844-859.
- Freeman, S. A. (2011). Thermal degradation and oxidation of aqueous piperazine for carbon dioxide capture. *Thesis, The University of Texas at Austin, Doctor of Philosophy in Chemical Engineering.*
- Freeman, S. A., Dugas, R., Van Wagener, D. H., Nguyen, T., & Rochelle, G. T. (2010). Carbon dioxide capture with concentrated, aqueous piperazine. *International Journal of Greenhouse Gas Control*, 4(2), 119-124.
- Freguia, S. (2002a). Modeling of CO₂ Removal from Flue Gases with Monoethanolamine. *Thesis, The University of Texas at Austin, Master of Science in Engineering.*
- Freguia, S. (2002b). Modeling of CO₂ removal from flue gases with monoethanolamine. *Chemical Engineering*, 9-16.

- Freguia, S., & Rochelle, G. T. (2003). Modeling of CO₂ capture by aqueous monoethanolamine. *AIChE Journal*, 49(7), 1676-1686.
- Galindo, P., Schäffer, A., Brechtel, K., Unterberger, S., & Scheffknecht, G. (2012). Experimental research on the performance of CO₂-loaded solutions of MEA and DEA at regeneration conditions. *Fuel*, 101, 2-8.
- Gomes, V. G., & Yee, K. W. (2002). Pressure swing adsorption for carbon dioxide sequestration from exhaust gases. *Separation and Purification Technology*, 28(2), 161-171.
- Gurkan, B. E., Gohndrone, T. R., McCready, M. J., & Brennecke, J. F. (2013). Reaction kinetics of CO₂ absorption in to phosphonium based anion-functionalized ionic liquids. *Physical Chemistry Chemical Physics*, 15(20), 7796.
- Hanley, B., & Chen, C. C. (2012). New mass-transfer correlations for packed towers. *AIChE Journal*, 58(1), 132-152.
- Hansen, C. M. (2007). *Hansen solubility parameters: a user's handbook*: CRC press.
- Hasib-ur-Rahman, M., Siaj, M., & Larachi, F. (2010). Ionic liquids for CO₂ capture—Development and progress. *Chemical Engineering and Processing: Process Intensification*, 49(4), 313-322.
- Heintz, Y. J., Sehabiague, L., Morsi, B. I., Jones, K. L., & Pennline, H. W. (2008). Novel physical solvents for selective CO₂ capture from fuel gas streams at elevated pressures and temperatures. *Energy & Fuels*, 22(6), 3824-3837.
- Henley, E. J., & Seader, J. D. (1981). *Equilibrium-stage separation operations in chemical engineering*: Wiley.
- Hermann, W., Bosshard, P., Hung, E., Hunt, R., & Simon, A. (2005). An assessment of carbon capture technology and research opportunities. *Physical Adsorption*, 25(11).
- Hikita, H., Asai, S., Ishikawa, H., & Honda, M. (1977). The kinetics of reactions of carbon dioxide with monoethanolamine, diethanolamine and triethanolamine by a rapid mixing method. *Chem. Eng. J.*, 13(1), 7-12.
- Hilliard, M. D. (2008). A predictive thermodynamic model for an aqueous blend of potassium carbonate, piperazine, and monoethanolamine for carbon dioxide capture from flue gas. *Thesis, The University of Texas at Austin, Doctor of Philosophy in Chemical Engineering*.

- Hiwale, R., Hwang, S., & Smith, R. (2012). Model Building Methodology for Multiphase Reaction Systems-Modeling of CO₂ Absorption in Monoethanolamine for Laminar Jet Absorbers and Packing Beds. *Ind. Eng. Chem. Res.*, 51(11), 4328-4346.
- Hsu, Y.-H., Leron, R. B., & Li, M.-H. (2014). Solubility of carbon dioxide in aqueous mixtures of (reline+ monoethanolamine) at T=(313.2 to 353.2) K. *The Journal of Chemical Thermodynamics*, 72, 94-99.
- Huang, H. P., Shi, Y., Li, W., & Chang, S. G. (2001). Dual alkali approaches for the capture and separation of CO₂. *Energy & Fuels*, 15(2), 263-268.
- Huang, J., & Rüther, T. (2009). Why are ionic liquids attractive for CO₂ absorption? An overview. *Australian journal of chemistry*, 62(4), 298-308.
- Idem, R., Wilson, M., Tontiwachwuthikul, P., Chakma, A., Veawab, A., Aroonwilas, A., & Gelowitz, D. (2006). Pilot Plant Studies of the CO₂ Capture Performance of Aqueous MEA and Mixed MEA/MDEA Solvents at the University of Regina CO₂ Capture Technology Development Plant and the Boundary Dam CO₂ Capture Demonstration Plant. *Industrial & engineering chemistry research*, 45(8), 2414-2420.
- Irons, R., Sekkappan, G., Panesar, R., Gibbins, J., & Lucquiaud, M. (2007). CO₂ capture ready plants. *IEA Greenhouse Gas R&D Programme 2007*.
- Jalili, A. H., Mehdizadeh, A., Shokouhi, M., Ahmadi, A. N., Hosseini-Jenab, M., & Fateminassab, F. (2010). Solubility and diffusion of CO₂ and H₂S in the ionic liquid 1-ethyl-3-methylimidazolium ethylsulfate. *The Journal of Chemical Thermodynamics*, 42(10), 1298-1303.
- Jalili, A. H., Mehdizadeh, A., Shokouhi, M., Sakhaeinia, H., & Taghikhani, V. (2010). Solubility of CO₂ in 1-(2-hydroxyethyl)-3-methylimidazolium ionic liquids with different anions. *The Journal of Chemical Thermodynamics*, 42(6), 787-791.
- Jie, G., Jun, Y., Feifei, Z., Xin, C., Ming, T., Wanzhong, K., . . . Jun, L. (2016). Study on Absorption and Regeneration Performance of Novel Hybrid Solutions for CO₂ Capture. *Gas*, 15(15), 15.
- Junaidi, M., Leo, C., Ahmad, A., Kamal, S., & Chew, T. (2014). Carbon dioxide separation using asymmetric polysulfone mixed matrix membranes incorporated with SAPO-34 zeolite. *Fuel Processing Technology*, 118, 125-132.

- Kaithwas, A., Prasad, M., Kulshreshtha, A., & Verma, S. (2012). Industrial wastes derived solid adsorbents for CO₂ capture: A mini review. *Chemical Engineering Research and Design*, 90(10), 1632-1641.
- Karinen, R., & Krause, A. (2006). New biocomponents from glycerol. *Applied Catalysis A: General*, 306, 128-133.
- Karpe, P., & Aichele, C. P. (2013). Amine Modeling for CO₂ Capture: Internals Selection. *Environ. Sci. Technol.*, 47(8), 3926-3932.
- Kasahara, S., Kamio, E., Ishigami, T., & Matsuyama, H. (2012). Effect of water in ionic liquids on CO₂ permeability in amino acid ionic liquid-based facilitated transport membranes. *Journal of Membrane Science*, 415, 168-175.
- Kevin, P. R., James, T. Y., & Henry, W. P. (2004). Aqua ammonia process for simultaneous removal of CO₂, SO₂ and NO_x. *Int. J. Environ. Technol. Manage.*, 4, 89 - 104.
- Khalilpour, R., Mumford, K., Zhai, H., Abbas, A., Stevens, G., & Rubin, E. S. (2015). Membrane-based carbon capture from flue gas: a review. *Journal of Cleaner Production*, 103, 286-300.
- Khan, F., Krishnamoorthi, V., & Mahmud, T. (2011). Modelling reactive absorption of CO₂ in packed columns for post-combustion carbon capture applications. *Chemical Engineering Research and Design*, 89(9), 1600-1608.
- Kim, J. Y., Han, K. W., & Chun, H. W. (2009). CO₂ absorption with low concentration ammonia liquor. *Energy Procedia*, 1(1), 757-762.
- Kim, Y. E., Choi, J. H., Nam, S. C., & Yoon, Y. I. (2012). CO₂ absorption capacity using aqueous potassium carbonate with 2-methylpiperazine and piperazine. *Journal of Industrial and Engineering Chemistry*, 18(1), 105-110.
- Kingma, A. (2016). Understanding the equilibrium behaviour of a novel phase splitting solvent in the presence of high pressure CO₂. Faculty of Geosciences Theses, Utrecht University, The Netherlands.
- Kittel, J., Idem, R., Gelowitz, D., Tontiwachwuthikul, P., Parrain, G., & Bonneau, A. (2009). Corrosion in MEA units for CO₂ capture: Pilot plant studies. *Energy Procedia*, 1(1), 791-797.
- Knuutila, H., Svendsen, H. F., & Anttila, M. (2009). CO₂ capture from coal-fired power plants based on sodium carbonate slurry; a systems feasibility and sensitivity study. *International Journal of Greenhouse Gas Control*, 3(2), 143-151.

- Kohl, A., & Nielsen, R. (1997). Gas purification. 5th ed. Gulf Publishing Company.
- Kothandaraman, A. (2010). Carbon dioxide capture by chemical absorption: a solvent comparison study *PhD Thesis, MIT, USA*.
- Kovvali, A. S., & Sirkar, K. K. (2002). Carbon dioxide separation with novel solvents as liquid membranes. *Ind. Eng. Chem. Res.*, 41(9), 2287-2295.
- Krishnamurthy, R., & Taylor, R. (1986). Absorber simulation and design using a nonequilibrium stage model. *The Canadian Journal of Chemical Engineering*, 64(1), 96-105.
- Kumar, P. S., Hogendoorn, J. A., & Versteeg, G. F. (2003). Kinetics of the reaction of CO₂ with aqueous potassium salt of taurine and glycine. *AIChE Journal*, 49, 203-213.
- Kumelan, J., Tuma, D., Kamps, A. P. r.-S., & Maurer, G. (2010). Solubility of the single gases carbon dioxide and hydrogen in the ionic liquid [bmpy][Tf₂N]. *J. Chem. Eng. Data*, 55, 165–172.
- Kvamsdal, H. M., & Rochelle, G. T. (2008). Effects of the temperature bulge in CO₂ absorption from flue gas by aqueous monoethanolamine. *Industrial & engineering chemistry research*, 47(3), 867-875.
- Lawal, A., Wang, M., Stephenson, P., & Yeung, H. (2009). Dynamic modelling of CO₂ absorption for post combustion capture in coal-fired power plants. *Fuel*, 88(12), 2455-2462.
- Leo, C., Shamiri, A., Aroua, M., Aghamohammadi, N., Aramesh, R., Natarajan, E., . . . Akbari, V. (2016). Correlation and measurement of density and viscosity of aqueous mixtures of glycerol and N-methyldiethanolamine, monoethanolamine, piperazine and ionic liquid. *Journal of Molecular Liquids*, 221, 1155-1161.
- Leoneti, A. B., Aragao-Leoneti, V., & De Oliveira, S. V. W. B. (2012). Glycerol as a by-product of biodiesel production in Brazil: Alternatives for the use of unrefined glycerol. *Renewable Energy*, 45, 138-145.
- Leron, R. B., & Li, M.-H. (2013). Solubility of carbon dioxide in a eutectic mixture of choline chloride and glycerol at moderate pressures. *The Journal of Chemical Thermodynamics*, 57, 131-136.
- Li, J.-R., Ma, Y., McCarthy, M. C., Sculley, J., Yu, J., Jeong, H.-K., . . . Zhou, H.-C. (2011). Carbon dioxide capture-related gas adsorption and separation in metal-organic frameworks. *Coordination Chemistry Reviews*, 255(15), 1791-1823.

- Li, M.-H., & Lai, M.-D. (1995). Solubility and Diffusivity of N₂O and CO₂ in (Monoethanolamine+ N-Methyldiethanolamine+ Water) and in (Monoethanolamine+ 2-Amino-2-methyl-1-propanol+ Water). *Journal of Chemical and Engineering Data*, 40(2), 486-492.
- Li, X., Hou, M., Zhang, Z., Han, B., Yang, G., Wang, X., & Zou, L. (2008). Absorption of CO₂ by ionic liquid/polyethylene glycol mixture and the thermodynamic parameters. *Green Chemistry*, 10(8), 879-884.
- Liu, G., Yu, K., Yuan, X., Liu, C., & Guo, Q. (2006). Simulations of chemical absorption in pilot-scale and industrial-scale packed columns by computational mass transfer. *Chemical Engineering Science*, 61(19), 6511-6529.
- Liu, H., Zhang, Y., Yao, H., Yu, D., Zhao, W., & Bai, X. (2012). Improving mass transfer in gas-liquid by ionic liquids dispersion. *Journal of Dispersion Science and Technology*, 33(12), 1723-1729.
- Liu, Y., Zhang, L., & Watanasiri, S. (1999). Representing vapor-liquid equilibrium for an aqueous MEA-CO₂ system using the electrolyte nonrandom-two-liquid model. *Ind. Eng. Chem. Res.*, 38(5), 2080-2090.
- Lu, J.-G., Lu, C.-T., Chen, Y., Gao, L., Zhao, X., Zhang, H., & Xu, Z.-W. (2014). CO₂ capture by membrane absorption coupling process: Application of ionic liquids. *Applied Energy*, 115, 573-581.
- Lv, B., Guo, B., Zhou, Z., & Jing, G. (2015). Mechanisms of CO₂ Capture into Monoethanolamine Solution with Different CO₂ Loading during the Absorption/Desorption Processes. *Environmental Science & Technology*, 49(17), 10728-10735.
- Mamun, S., Svendsen, H. F., Hoff, K. A., Juliussen, O., & Rubin, E. S. (2005). Selection of new absorbents for carbon dioxide capture. *Elsevier Science Ltd., Oxford*.
- Mandal, B. P., Kundu, M., Padhiyar, N. U., & Bandyopadhyay, S. S. (2004). Physical solubility and diffusivity of N₂O and CO₂ into aqueous solutions of (2-amino-2-methyl-1-propanol+ diethanolamine) and (N-methyldiethanolamine+ diethanolamine). *Journal of Chemical & Engineering Data*, 49(2), 264-270.
- Martin, J. L., Otto, F. D., & Mather, A. E. (1978). Solubility of hydrogen sulfide and carbon dioxide in a diglycolamine solution. *Journal of Chemical and Engineering Data*, 23(2), 163-164.
- Medina-Gonzalez, Y., Tassaing, T., Camy, S., & Condoret, J. S. (2013). Phase equilibrium of the CO₂/glycerol system: Experimental data by in situ FT-IR

spectroscopy and thermodynamic modeling. *The Journal of Supercritical Fluids*, 73, 97-107.

Mirzaei, S., Shamiri, A., & Aroua, M. K. (2015). A review of different solvents, mass transfer, and hydrodynamics for postcombustion CO₂ capture. *Rev Chem Eng*, 31(6), 521-561.

Mores, P., Scenna, N., & Mussati, S. (2011). Post-combustion CO₂ capture process: Equilibrium stage mathematical model of the chemical absorption of CO₂ into monoethanolamine (MEA) aqueous solution. *Chemical Engineering Research and Design*, 89(9), 1587-1599.

Mores, P., Scenna, N., & Mussati, S. (2012). A rate based model of a packed column for CO₂ absorption using aqueous monoethanolamine solution. *International Journal of Greenhouse Gas Control*, 6, 21-36.

Morrison, L. R. (2000). *Glycerol*: Wiley Online Library.

Nafisi, V., & Hägg, M.-B. (2014). Development of dual layer of ZIF-8/PEBAX-2533 mixed matrix membrane for CO₂ capture. *Journal of Membrane Science*, 459, 244-255.

Nagy, T., & Mizsey, P. (2013). Effect of fossil fuels on the parameters of CO₂ capture. *Environ. Sci. Technol.*, 47(15), 8948-8954.

Nik, O. G., Chen, X. Y., & Kaliaguine, S. (2011). Amine-functionalized zeolite FAU/EMT-polyimide mixed matrix membranes for CO₂/CH₄ separation. *Journal of Membrane Science*, 379(1), 468-478.

Oguz, H., Ozturk, s., & Alper. (1983). measurement of effective interfacial area in a packed column absorber by sulfid oxidation method: influence of liquid viscosity. *The University of Ankara, Chemical Engineering, communications*.

Olajire, A. A. (2010). CO₂ capture and separation technologies for end-of-pipe applications- A review. *Energy*, 35, 2610-2628.

Onda, K., Takeuchi, H., & Okumoto, Y. (1968). Mass transfer coefficients between gas and liquid phases in packed columns. *J. Chem. Eng. Jpn.*, 1(1), 56-62.

Onda, K., Takeuchl, H., & Okumoto, Y. (1968). Mass transfer coefficients between gas and liquid phases in packed columns *J Chem. Eng. Jpn.*, 1, 56-62.

- Ostonen, A., Sapei, E., Uusi-Kyyny, P., Klemelä, A., & Alopaeus, V. (2014). Measurements and modeling of CO₂ solubility in 1, 8-diazabicyclo-[5.4. 0]-undec-7-ene—Glycerol solutions. *Fluid Phase Equilibria*, 374, 25-36.
- Padurean, A., Cormos, C.-C., Cormos, A.-M., & Agachi, P.-S. (2011). Multicriterial analysis of post-combustion carbon dioxide capture using alkanolamines. *Int. J. Greenh. Gas Control*, 5(4), 676-685.
- Pagliaro, M., & Rossi, M. (2010). *The future of glycerol*: Royal Society of Chemistry.
- Palmeri, N., Cavallaro, S., & Bart, J. (2008). Carbon dioxide absorption by MEA. *Journal of Thermal Analysis and Calorimetry*, 91(1), 87-91.
- Pandya, J. (1983). Adiabatic gas absorption and stripping with chemical reaction in packed towers. *Chemical Engineering Communications*, 19(4-6), 343-361.
- Park, J.-Y., Yoon, S. J., & Lee, H. (2003). Effect of steric hindrance on carbon dioxide absorption into new amine solutions: thermodynamic and spectroscopic verification through solubility and NMR analysis. *Environ. Sci. Technol.*, 37, 1670-1675.
- Park, S.-B., Shim, C.-S., Lee, H., & Lee, K.-H. (1997). Solubilities of carbon dioxide in the aqueous potassium carbonate and potassium carbonate-poly (ethylene glycol) solutions. *Fluid Phase Equilibria*, 134(1), 141-149.
- Penders-van Elk, N. J., Hamborg, E. S., Huttenhuis, P. J., Fradette, S., Carley, J. A., & Versteeg, G. F. (2013). Kinetics of absorption of carbon dioxide in aqueous amine and carbonate solutions with carbonic anhydrase. *International Journal of Greenhouse Gas Control*, 12, 259-268.
- Perez, E. V., Balkus, K. J., Ferraris, J. P., & Musselman, I. H. (2009). Mixed-matrix membranes containing MOF-5 for gas separations. *Journal of Membrane Science*, 328(1), 165-173.
- Pinsent, B., Pearson, L., & Roughton, F. (1956). The kinetics of combination of carbon dioxide with hydroxide ions. *Transactions of the Faraday Society*, 52, 1512-1520.
- Pinto, A. M., Rodríguez, H., Arce, A., & Soto, A. (2013). Carbon dioxide absorption in the ionic liquid 1-ethylpyridinium ethylsulfate and in its mixtures with another ionic liquid. *International Journal of Greenhouse Gas Control*, 18, 296-304.

- Pires, J., Martins, F., Alvim-Ferraz, M., & Simões, M. (2011). Recent developments on carbon capture and storage: an overview. *Chemical Engineering Research and Design*, 89(9), 1446-1460.
- Plaza, J. M., Van Wagener, D., & Rochelle, G. T. (2010). Modeling CO₂ capture with aqueous monoethanolamine. *International Journal of Greenhouse Gas Control*, 4(2), 161-166.
- Portugal, A., Sousa, J., Magalhães, F., & Mendes, A. (2009). Solubility of carbon dioxide in aqueous solutions of amino acid salts. *Chemical Engineering Science*, 64(9), 1993-2002.
- Puxty, G., Rowland, R., Allport, A., Yang, Q., Bown, M., Burns, R., . . . Attalla, M. (2009). Carbon dioxide postcombustion capture: a novel screening study of the carbon dioxide absorption performance of 76 amines. *Environ. Sci. Technol.*, 43(16), 6427-6433.
- Puxty, G., Rowland, R., & Attalla, M. (2010). Comparison of the rate of CO₂ absorption into aqueous ammonia and monoethanolamine. *Chemical Engineering Science*, 65(2), 915-922.
- Qi, G., Wang, S., Yu, H., Wardhaugh, L., Feron, P., & Chen, C. (2013). Development of a rate-based model for CO₂ absorption using aqueous NH₃ in a packed column. *Int. J. Greenh. Gas Control*, 17, 450-461.
- Rajabi, Z., Moghadassi, A., Hosseini, S., & Mohammadi, M. (2013). Preparation and characterization of polyvinylchloride based mixed matrix membrane filled with multi walled carbon nano tubes for carbon dioxide separation. *Journal of Industrial and Engineering Chemistry*, 19(1), 347-352.
- Ramachandran, N., Aboudheir, A., Idem, R., & Tontiwachwuthikul, P. (2006). Kinetics of the absorption of CO₂ into mixed aqueous loaded solutions of monoethanolamine and methyldiethanolamine. *Ind. Eng. Chem. Res.*, 45, 2608-2616.
- Rao, A. B., & Rubin, E. S. (2002). A technical, economic, and environmental assessment of amine-based CO₂ capture technology for power plant greenhouse gas control. *Environmental Science & Technology*, 36(20), 4467-4475.
- Razi, N., Svendsen, H. F., & Bolland, O. (2013). Validation of mass transfer correlations for CO₂ absorption with MEA using pilot data. *Int. J. Greenh. Gas Control*, 19, 478-491.

- Resnik, K. P., Yeh, J. T., & Pennline, H. W. (2004). Aqua ammonia process for simultaneous removal of CO₂, SO₂ and NO_x. *International Journal of Environmental Technology and Management*, 4(1-2), 89-104.
- Riemer, P., Webster, I., Ormerod, W., & Audus, H. (1994). Results and full fuel cycle study plans from the IEA greenhouse gas research and development programme. *Fuel*, 73(7), 1151-1158.
- Robertson, S. (2002). SIDS Initial Assessment Report For SIAM 14, France.
- Rubin, E. S., Mantripragada, H., Marks, A., Versteeg, P., & Kitchin, J. (2012). The outlook for improved carbon capture technology. *Progress in Energy and Combustion Science*, 38(5), 630-671.
- Rubin, E. S. (2006). Summary of the IPCC special report on carbon dioxide capture and storage.
- Safaei, H. R., Shekouhy, M., Rahmanpur, S., & Shirinfeshan, A. (2012). Glycerol as a biodegradable and reusable promoting medium for the catalyst-free one-pot three component synthesis of 4H-pyrans. *Green Chem.*, 14(6), 1696-1704.
- Saha, A. K., Bandyopadhyay, S. S., & Biswas, A. K. (1995). Kinetics of absorption of CO₂ into aqueous solutions of 2-amino-2-methyl-1-propanol. *Chemical Engineering Science*, 50, 3587-3598.
- Sairi, N. A., Yusoff, R., Alias, Y., & Kheireddine Aroua, M. (2011). Solubilities of CO₂ in aqueous N-methyldiethanolamine and guanidinium trifluoromethanesulfonate ionic liquid systems at elevated pressures. *Fluid Phase Equilibria*, 300(1-2), 89-94.
- Satyapal, S., Filburn, T., Trela, J., & Strange, J. (2001). Performance and properties of a solid amine sorbent for carbon dioxide removal in space life support applications. *Energy & Fuels*, 15(2), 250-255.
- Savage, D., Sartori, G., & Astarita, G. (1984). Amines as rate promoters for carbon dioxide hydrolysis. *Faraday Discussions of the Chemical Society*, 77, 17-31.
- Savage, D. W., Astarita, G., & Joshi, S. (1980). Chemical absorption and desorption of carbon dioxide from hot carbonate solutions. *Chemical Engineering Science*, 35(7), 1513-1522.
- Schilderman, A. M., Raessi, S., & Peters, C. J. (2007). Solubility of carbon dioxide in the ionic liquid 1-ethyl-3-methylimidazolium bis(trifluoromethylsulfonyl)imide. *Fluid Phase Equilibria*, 260(1), 19-22.

- Seader, J. (1989). The rate-based approach for modeling staged separations. *Chemical engineering progress*, 85(10), 41-49.
- Segur, J. B., & Oberstar, H. E. (1951). Viscosity of glycerol and its aqueous solutions. *Ind. Eng. Chem.*, 43(9), 2117-2120.
- Seo, J.-B., Jeon, S.-B., Kim, J.-Y., Lee, G.-W., Jung, J.-H., & Oh, K.-J. (2012). Vaporization reduction characteristics of aqueous ammonia solutions by the addition of ethylene glycol, glycerol and glycine to the CO₂ absorption process. *Journal of Environmental Sciences*, 24(3), 494-498.
- Seo, J. B., Jeon, S. B., Choi, W. J., Kim, J. W., Lee, G. H., & Oh, K. J. (2011). The absorption rate of CO₂/SO₂/NO₂ into a blended aqueous AMP/ammonia solution. *Korean Journal of Chemical Engineering*, 28(1), 170-177.
- Shafeeyan, M. S., Daud, W. M. A. W., & Shamiri, A. (2014). A review of mathematical modeling of fixed-bed columns for carbon dioxide adsorption. *Chemical Engineering Research and Design*, 92(5), 961-988.
- Shafeeyan, M. S., Daud, W. M. A. W., Shamiri, A., & Aghamohammadi, N. (2015). Modeling of Carbon Dioxide Adsorption onto Ammonia-Modified Activated Carbon: Kinetic Analysis and Breakthrough Behavior. *Energy & Fuels*, 29(10), 6565-6577.
- Shahid, S., & Nijmeijer, K. (2014). High pressure gas separation performance of mixed-matrix polymer membranes containing mesoporous Fe (BTC). *Journal of Membrane Science*, 459, 33-44.
- Shamiri, A., Shafeeyan, M., Tee, H., Leo, C., Aroua, M., & Aghamohammadi, N. (2016). Absorption of CO₂ into aqueous mixtures of glycerol and monoethanolamine. *Journal of Natural Gas Science and Engineering*, 35, 605-613.
- Shariati, A., & Peters, C. (2004). High-pressure phase behavior of systems with ionic liquids: II. The binary system carbon dioxide+ 1-ethyl-3-methylimidazolium hexafluorophosphate. *The Journal of Supercritical Fluids*, 29(1), 43-48.
- Shariati, A., & Peters, C. J. (2004). High-pressure phase behavior of systems with ionic liquids. *The Journal of Supercritical Fluids*, 30(2), 139-144.
- Shiflett, M. B., & Yokozeki, A. (2005). Solubilities and diffusivities of carbon dioxide in ionic liquids:[bmim][PF₆] and [bmim][BF₄]. *Ind. Eng. Chem. Res.*, 44, 4453-4464.

- Simon, L. L., Elias, Y., Puxty, G., Artanto, Y., & Hungerbuhler, K. (2011). Rate based modeling and validation of a carbon-dioxide pilot plant absorption column operating on monoethanolamine. *Chemical Engineering Research and Design*, 89(9), 1684-1692.
- Singh, P., Brilman, D. W. F., & Groeneveld, M. J. (2009). Solubility of CO₂ in aqueous solution of newly developed absorbents. *Energy Procedia*, 1(1), 1257-1264.
- Siriwardane, R. V., Shen, M.-S., Fisher, E. P., & Poston, J. A. (2001). Adsorption of CO₂ on molecular sieves and activated carbon. *Energy & Fuels*, 15(2), 279-284.
- Sistla, Y. S., Jain, L., & Khanna, A. (2012). Validation and prediction of solubility parameters of ionic liquids for CO₂ capture. *Separation and Purification Technology*, 97, 51-64.
- Smith, K. H., Anderson, C. J., Tao, W., Endo, K., Mumford, K. A., Kentish, S. E., . . . Stevens, G. W. (2012). Pre-combustion capture of CO₂—results from solvent absorption pilot plant trials using 30 wt% potassium carbonate and boric acid promoted potassium carbonate solvent. *International Journal of Greenhouse Gas Control*, 10(0), 64-73.
- Sønderby, T. L., Carlsen, K. B., Fosbøl, P. L., Kiørboe, L. G., & von Solms, N. (2013). A new pilot absorber for CO₂ capture from flue gases: measuring and modelling capture with MEA solution. *Int. J. Greenh. Gas Control*, 12, 181-192.
- Song, H.-J., Lee, S., Maken, S., Park, J.-J., & Park, J.-W. (2006). Solubilities of carbon dioxide in aqueous solutions of sodium glycinate. *Fluid Phase Equilibria*, 246(1), 1-5.
- Stichlmair, J., Bravo, J. L., & Fair, J. R. (1989). General model for prediction of pressure drop and capacity of countercurrent gas/liquid packed columns. *Gas Separation and Purification*, 3(1), 19-28.
- Sublet, J., Pera-Titus, M., Guilhaume, N., Farrusseng, D., Schrive, L., Chanaud, P., . . . Durecu, S. (2012). Technico-economical assessment of MFI-type zeolite membranes for CO₂ capture from postcombustion flue gases. *AIChE Journal*, 58(10), 3183-3194.
- Takamura, K., Fischer, H., & Morrow, N. R. (2012). Physical properties of aqueous glycerol solutions. *Journal of Petroleum Science and Engineering*, 98, 50-60.
- Tan, L. S., Lau, K. K., Bustam, M. A., & Shariff, A. M. (2012). Removal of high concentration CO₂ from natural gas at elevated pressure via absorption process in packed column. *Journal of Natural Gas Chemistry*, 21(1), 7-10.

- Taylor, R., & Krishna, R. (1993). *Multicomponent mass transfer* (Vol. 2): John Wiley & Sons.
- Thee, H., Nicholas, N. J., Smith, K. H., da Silva, G., Kentish, S. E., & Stevens, G. W. (2014). A kinetic study of CO₂ capture with potassium carbonate solutions promoted with various amino acids: glycine, sarcosine and proline. *International Journal of Greenhouse Gas Control*, 20, 212-222.
- Thee, H., Smith, K. H., da Silva, G., Kentish, S. E., & Stevens, G. W. (2012). Carbon dioxide absorption into unpromoted and borate-catalyzed potassium carbonate solutions. *Chemical Engineering Journal*, 181, 694-701.
- Thee, H., Suryaputradinata, Y. A., Mumford, K. A., Smith, K. H., da Silva, G., Kentish, S. E., & Stevens, G. W. (2012). A kinetic and process modeling study of CO₂ capture with MEA-promoted potassium carbonate solutions. *Chemical Engineering Journal*, 210, 271-279.
- Tobiesen, F. A., Svendsen, H. F., & Juliussen, O. (2007). Experimental validation of a rigorous absorber model for CO₂ postcombustion capture. *AIChE Journal*, 53(4), 846-865.
- Tontiwachwuthikul, P., Meisen, A., & Lim, C. J. (1992). CO₂ absorption by NaOH, monoethanolamine and 2-amino-2-methyl-1-propanol solutions in a packed column. *Chemical Engineering Science*, 47(2), 381-390.
- Wang, M., Lawal, A., Stephenson, P., Sidders, J., & Ramshaw, C. (2011). Post-combustion CO₂ capture with chemical absorption: A state-of-the-art review. *Chemical Engineering Research and Design*, 89(9), 1609-1624.
- Wang, Q., Luo, J., Zhong, Z., & Borgna, A. (2011). CO₂ capture by solid adsorbents and their applications: current status and new trends. *Energy & Environmental Science*, 4(1), 42-55.
- Wang, T. (2013). Degradation of Aqueous 2-Amino-2-methyl-1-propanol for Carbon Dioxide Capture. Faculty of Technology, Telemark University College, Norway.
- Wappel, D., Gronald, G., Kalb, R., & Draxler, J. (2010). Ionic liquids for post-combustion CO₂ absorption. *International Journal of Greenhouse Gas Control*, 4(3), 486-494.
- Weiland, R. H., & Hatcher, N. A. (2011). Post-combustion CO₂ capture with amino-acid salts. *Abu Dhabi, UAE, March 2011*.

- Whitman, W. G. (1923). A Preliminary Experimental Confirmation of The Two-Film Theory of Gas Absorption. *Chemical and Metallurgical Engineering*, 29, 146-148.
- Witzøe, T. (2015). Simulation of Pilot Data with Aspen Plus. *thesis, Norwegian University of Science and Technology, Department of Chemical Engineering*.
- Wolfson, A., Dlugy, C., & Shotland, Y. (2007). Glycerol as a green solvent for high product yields and selectivities. *Environmental Chemistry Letters*, 5(2), 67-71.
- Xiao, J., Li, C.-W., & Li, M.-H. (2000). Kinetics of absorption of carbon dioxide into aqueous solutions of 2-amino-2-methyl-1-propanol+ monoethanolamine. *Chemical Engineering Science*, 55(1), 161-175.
- Xie, H., Zhang, S., & Li, S. (2006). Chitin and chitosan dissolved in ionic liquids as reversible sorbents of CO₂. *Green Chemistry*, 8(7), 630.
- Xue, Z., Zhang, Z., Han, J., Chen, Y., & Mu, T. (2011). Carbon dioxide capture by a dual amino ionic liquid with amino-functionalized imidazolium cation and taurine anion. *International Journal of Greenhouse Gas Control*, 5(4), 628-633.
- Yang, H., Xu, Z., Fan, M., Gupta, R., Slimane, R. B., Bland, A. E., & Wright, I. (2008). Progress in carbon dioxide separation and capture: A review. *Journal of Environmental Sciences*, 20(1), 14-27.
- Yeh, J. T., Resnik, K. P., Rygle, K., & Pennline, H. W. (2005). Semi-batch absorption and regeneration studies for CO₂ capture by aqueous ammonia. *Fuel Processing Technology*, 86(14-15), 1533-1546.
- Zaman, M., & Lee, J. H. (2013). Carbon capture from stationary power generation sources: a review of the current status of the technologies. *Korean J. Chem. Eng.*, 30(8), 1497-1526.
- Zhang, J., Zhang, S., Dong, K., Zhang, Y., Shen, Y., & Lv, X. (2006). Supported absorption of CO₂ by tetrabutylphosphonium amino acid ionic liquids. *Chemistry—A European Journal*, 12(15), 4021-4026.
- Zhang, Q., Turton, R., & Bhattacharyya, D. (2016). Development of Model and Model-Predictive Control of an MEA-Based Postcombustion CO₂ Capture Process. *Ind. Eng. Chem. Res.*, 55(5), 1292-1308.
- Zhang, S., Lu, Y., & Ye, X. (2013). Catalytic behavior of carbonic anhydrase enzyme immobilized onto nonporous silica nanoparticles for enhancing CO₂ absorption

into a carbonate solution. *International Journal of Greenhouse Gas Control*, 13, 17-25.

Zhang, X., Fan, J.-L., & Wei, Y.-M. (2013). Technology roadmap study on carbon capture, utilization and storage in China. *Energy Policy*, 59, 536-550.

Zhang, Y., Chen, H., Chen, C.-C., Plaza, J. M., Dugas, R., & Rochelle, G. T. (2009). Rate-based process modeling study of CO₂ capture with aqueous monoethanolamine solution. *Industrial & engineering chemistry research*, 48(20), 9233-9246.

Zhang, Y., Zhang, S., Lu, X., Zhou, Q., Fan, W., & Zhang, X. (2009). Dual Amino-Functionalised Phosphonium Ionic Liquids for CO₂ Capture. *Chemistry—A European Journal*, 15(12), 3003-3011.

Zhao, J., Song, X., Sun, Z., & Yu, J. (2013). Simulation on thermodynamic state of ammonia carbonation at low temperature and low pressure. *Frontiers of Chemical Science and Engineering*, 7(4), 447-455.

Zhao, X., Smith, K. H., Simioni, M. A., Tao, W., Kentish, S. E., Fei, W., & Stevens, G. W. (2011). Comparison of several packings for CO₂ chemical absorption in a packed column. *International Journal of Greenhouse Gas Control*, 5(5), 1163-1169.

Zhao, Y., Zhang, X., Dong, H., Zhen, Y., Li, G., Zeng, S., & Zhang, S. (2011). Solubilities of gases in novel alcamines ionic liquid 2-[2-hydroxyethyl (methyl) amino] ethanol chloride. *Fluid Phase Equilibria*, 302(1-2), 60-64.

Zhao, Y., Zhang, X., Zhen, Y., Dong, H., Zhao, G., Zeng, S., . . . Zhang, S. (2011). Novel alcamines ionic liquids based solvents: preparation, characterization and applications in carbon dioxide capture. *International Journal of Greenhouse Gas Control*, 5(2), 367-373.

Zhao, Z., Cui, X., Ma, J., & Li, R. (2007). Adsorption of carbon dioxide on alkali-modified zeolite 13X adsorbents. *International Journal of Greenhouse Gas Control*, 1(3), 355-359.

Zhou, S., Chen, X., Nguyen, T., Voice, A. K., & Rochelle, G. T. (2010). Aqueous ethylenediamine for CO₂ capture. *ChemSusChem*, 3(8), 913-918.

Ziaii Fashami, S. (2012). Dynamic modeling, optimization, and control of monoethanolamine scrubbing for CO₂ capture.

LIST OF PUBLICATIONS AND PAPERS PRESENTED

Published articles:

1. **Somayeh Mirzaei**, Ahmad Shamiri and Mohamed Kheireddine Aroua. 'A review of different solvents, mass transfer, and hydrodynamics for post-combustion CO₂ capture', *Rev. Chem. Eng.* **2015**; 31(6):521-561.
2. **Somayeh Mirzaei**, Ahmad Shamiri, Mohamed Kheireddine Aroua. Simulation of Aqueous Blend of Monoethanolamine and Glycerol for Carbon Dioxide Capture from Flue Gas. *Energy and fuels*, **2016**; 30 (11): 9540-9553.

Submitted article:

1. **Somayeh Mirzaei**, Ahmad Shamiri, Mohamed Kheireddine Aroua. CO₂ absorption in aqueous solutions of Glycerol and Monoethanolamine in a pilot-scale packed bed column (submitted to: *Energy and fuels* journal).

Conference papers:

1. **Somayeh Mirzaei**, Ahmad Shamiri and Mohamed Kheireddine Aroua. 'Study of mass transfer and hydrodynamics for post-combustion CO₂ capture', International Conference on Green & Sustainable Chemistry, Berlin, Germany, 3-6 April, **2016**.
2. **Somayeh Mirzaei**, Ahmad Shamiri and Mohamed Kheireddine Aroua. 'Study of different solvents for post-combustion CO₂ capture', International Conference on Green & Sustainable Chemistry, Berlin, Germany, 3-6 April, **2016**.
3. **Somayeh Mirzaei**, Ahmad Shamiri and Mohamed Kheireddine Aroua. 'Simulation of Carbon Dioxide Absorption from Flue Gas by using Aqueous Mixture of Monoethanolamine and Glycerol'. Workshop on CO₂ capture and utilization, Pullman Hotel, Kuala Lumpur, Malaysia, 6-8 February **2017**.

Somayeh Mirzaei, Ahmad Shamiri and Mohamed Kheireddine Aroua*

A review of different solvents, mass transfer, and hydrodynamics for postcombustion CO₂ capture

DOI 10.1515/revce-2014-0045

Received September 29, 2014; accepted May 13, 2015

Abstract: There is a growing environmental concern regarding carbon dioxide (CO₂) emissions from human activities that result in global warming or climate change. To tackle this potential problem, it is crucial to develop CO₂ capture technologies. This paper reviews the current status of postcombustion carbon capture by absorption in packed column using different solvents. The major concerns with the selection of absorbent, such as absorption rate, CO₂ absorption capacity, CO₂ solubility, environmental cost, and toxicity, are discussed. The hydrodynamics and mass-transfer performance of CO₂ absorption in a packed column are reviewed. The determinant factors of CO₂ absorption, including effective interfacial area and mass-transfer coefficients in different contactors, are discussed. Liquid holdup and pressure-drop models are investigated.

Keywords: carbon dioxide absorption; flue gas; hydrodynamics; mass transfer.

1 Introduction

Carbon dioxide (CO₂) removal methods have been extensively applied in different sections of industry, such as natural gas purification and CO₂ capture from flue gas, with extra emphasis on the latter. The operating condition of flue gas is that it discharges at an atmospheric pressure and a partial pressure of approximately 0.15 bar in nitrogen (Aschenbrenner and Styring 2010). Due to international

efforts to reduce greenhouse gas discharges, the capture of CO₂ from flue gas has received increasing attention in recent years (Aschenbrenner and Styring 2010).

Basically, CO₂ absorption occurs in a column and allows direct contact among gas flows comprising CO₂ and liquid solvents. Using the degree of gas-liquid interaction provided with the column interiors, the removal performance of the absorption process can be determined. It is necessary for the column interiors with excellent degrees of gas-liquid contact to effectively remove CO₂ from gas streams. In recent years, different kinds of column internal system have been developed for use in the gas treatment process. Tower packing, including random and structured packing, is the most common system that is used to remove CO₂ from gas streams. Structured packing, with its regular geometric structures, is usually recommended due to its excellent performance with mass transfer in lower pressure drops (Aroonwilas and Tontiwachwuthikul 2000).

Irons et al. (2007) studied three CO₂ capture technologies for power generation and for the improvement of CO₂ from coal-fired power plants, as a necessary factor in controlling for CO₂ in our environment is its capture from flue gas streams. These three technologies are postcombustion capture, precombustion capture, and oxyfuel combustion (Irons et al. 2007, Olajire 2010). Postcombustion capture is mainly used in coal-fueled energy generators, which are air fired. Postcombustion carbon capture is a process that includes the removal of CO₂ from other components of flue gas in the air or generated via the combustion process (Figuerola et al. 2008).

The low level of CO₂ concentration in flue gas (between 4 and 14%, v/v; Pires et al. 2011) illustrates that there should be a huge volume of the gas, which affects the size of the equipment and capital costs. Furthermore, low CO₂ partial pressure and the high temperature of the flue gases in postcombustion capture provide extra challenges in design (Olajire 2010).

Some parameters, such as CO₂ solubility, CO₂ selectivity over N₂, and solvent loss, are very important in selecting a suitable solvent for CO₂ capture. Other parameters, such as toxicity and environmental cost, have to be considered as well, especially when there is solvent degradation and loss caused by evaporation in the process (Aschenbrenner and Styring 2010).

*Corresponding author: Mohamed Kheireddine Aroua, Faculty of Engineering, Chemical Engineering Department, University Malaya, 50603 Kuala Lumpur, Malaysia, e-mail: mk_aroua@um.edu.my
Somayeh Mirzaei: Faculty of Engineering, Chemical Engineering Department, University Malaya, 50603 Kuala Lumpur, Malaysia
Ahmad Shamiri: Faculty of Engineering, Department of Chemical Engineering, University of Malaya, 50603 Kuala Lumpur, Malaysia; and Faculty of Engineering, Technology & Built Environment, Chemical & Petroleum Engineering Department, UCSI University, 56000 Kuala Lumpur, Malaysia

Simulation of Aqueous Blend of Monoethanolamine and Glycerol for Carbon Dioxide Capture from Flue Gas

Somayeh Mirzaei,[†] Ahmad Shamiri,^{§,§} and Mohamed Kheireddine Aroua^{*,†}

[†]Chemical Engineering Department, Faculty of Engineering, University Malaya, 50603 Kuala Lumpur, Malaysia

[‡]Chemical & Petroleum Engineering Department, Faculty of Engineering, Technology & Built Environment, and [§]Process System Engineering Center, Faculty of Engineering, Technology & Built Environment, UCSI University, 56000 Kuala Lumpur, Malaysia

ABSTRACT: This study investigated CO₂ capture from flue gas by using glycerol as solvent. Absorption was simulated using a rate-based model with three cases under similar operating conditions. CO₂ separation was first simulated using ENRTL-RK thermodynamic model with monoethanolamine (MEA) as solvent. CO₂ absorption was then simulated using NRTL-RK thermodynamic model with glycerol solvent, and then an aqueous mixture of MEA/glycerol was also simulated using ENRTL-RK thermodynamic model. Simulation results confirm that glycerol can be used as promoter with MEA solvent to enhance CO₂ capture. The optimal glycerol concentration for CO₂ absorption is 10–40 wt %, in which 10 wt % glycerol exhibits the lowest CO₂ concentration in the outlet gas from the absorber. The CO₂ removal efficiency increases from 62.24% for 10 wt % MEA aqueous solution to 64.33% for the mixture of 10 wt % MEA–10 wt % glycerol aqueous solution. The CO₂ removal efficiency for 10 wt % glycerol aqueous solution is 27.31%.

1. INTRODUCTION

Carbon dioxide (CO₂) is the main greenhouse gas generated through human activities, particularly from combustion of fossil fuels consumed in transportation vehicles, manufacturing industries, and power generation facilities.^{1–3} As such, reducing CO₂ emission has gained increased attention to alleviate global warming issues.⁴ In recent years, solvent-type processes, which are categorized into chemical, physical, and mixed chemical/physical processes, are employed to remove acid gas from fuel gas.¹ In chemical processes, aqueous alkanolamine solutions,⁵ such as monoethanolamine (MEA), are used to separate CO₂ in packed columns.^{6,6} Physical processes, such as Rectisol, Selexol,^{7,8} and Morphosorb, use chilled methanol, mixture of dimethyl ethers of polyethylene glycol, and *n*-formylmorpholine/*n*-acetylmorpholine as solvents, respectively.¹ Sulfolin is another mixed chemical/physical process; this method uses a mixture of sulfolane and aqueous solution of either methyl diethanolamine or diisopropanolamine as solvent.^{1,7} Post-combustion CO₂ capture comprises the following four main stages (Figure 1): CO₂ is first absorbed from flue gas by using solvent in a packed column; rich solvent-containing CO₂ is then heated by reboiler in the stripper column to release CO₂; the released CO₂ is subsequently compressed for transport and storage; and the lean (regenerated) solvent is finally recycled to the absorption column.^{9,10}

An aqueous MEA solution (10–30 wt %) is commonly used as solvent in postcombustion CO₂ capture.^{9,11,12} The CO₂ concentration in flue gas from coal-fired power plants reaches 15%,⁷ and CO₂ partial pressure in the feed gas influences the economy of CO₂ recovery. However, chemical solvents are corrosive, and the equipment used should undergo carbon steel construction, which increases the operating cost. At high pressure levels, physical solvents are more suitable than chemical solvents.¹³ Solvent regeneration in physical absorption is easier and requires less energy than that in chemical

absorption¹⁴ but has low CO₂ selectivity over N₂.¹⁵ Pressure reduction is a simple technique that requires less energy for physical solvent regeneration as compared to steam stripping for chemical solvent regeneration. A mixture of physical and chemical solvents is suitable for single-unit gas separation to reduce energy consumption.^{16–18} Physical absorption is based on CO₂ solubility in the solvent, not on the chemical reaction with the solvent.¹⁹ The following specifications are important for the economic suitability of physical solvents: (1) low vapor pressure for solvent loss prevention; (2) low viscosity; (3) higher selectivity of acid gases as compared to CO, CH₄, and H₂; (4) excellent chemical and thermal stabilities; (5) noncorrosiveness; and (6) eco-friendly behavior.¹ In the present study, glycerol is an eco-friendly solvent introduced in postcombustion CO₂ capture from flue gas. This technique aims to replace/reduce the use of harmful chemical solvents with environment friendly solvents. Glycerol, a physical solvent used for CO₂ capture, is stable, nontoxic, and liquid at low vapor pressure levels.¹⁴ This compound is biodegradable and a byproduct in the biodiesel industry; glycerol is a sweet tasting, colorless, odorless, clear, and viscous liquid. Glycerol exhibits high boiling point (290 °C) and is nonvolatile under atmospheric pressure.²⁰ The viscosity of pure glycerol is high but decreases in glycerol aqueous solution with increasing amount of water and temperature.^{21,22} For example, the viscosity of glycerol solution with 30 wt % water at 20 °C is almost 1.59% of that of pure glycerol.²² Leo et al.²³ investigated density and viscosity of aqueous mixtures of glycerol and *N*-methyl-diethanolamine (MDEA), glycerol and MEA, glycerol and Piperazine (PZ), as well as glycerol and 1-butyl-3-methylimidazolium dicyanamide ([bmim][DCA]) in the

Received: May 22, 2016

Revised: September 14, 2016